Geological Survey of Finland

Bulletin 360

Geology and geochemistry of the metakomatiite-hosted Pahtavaara gold deposit in Sodankylä, northern Finland, with emphasis on hydrothermal alteration

by Esko A. Korkiakoski

Geologian tutkimuskeskus
Espoo 1992

Geological Survey of Finland, Bulletin 360

GEOLOGY AND GEOCHEMISTRY OF THE METAKOMATIITE-HOSTED PAHTAVAARA GOLD DEPOSIT IN SODANKYLÄ, NORTHERN FINLAND, WITH EMPHASIS ON HYDROTHERMAL ALTERATION

by

ESKO A. KORKIAKOSKI

with 39 figures and 12 tables in the text and one appendix

ACADEMIC DISSERTATION

GEOLOGIAN TUTKIMUSKESKUS
ESPOO 1992

Korkiakoski, Esko A. 1992. Geology and geochemistry of the metakomatiite-hosted Pahtavaara gold deposit in Sodankylä, northern Finland, with emphasis on hydrothermal alteration. *Geological Survey of Finland, Bulletin* 360. 96 pages, 39 figures, 12 tables and one appendix.

The early Proterozoic Pahtavaara gold deposit is situated in the eastern part of the Central Lapland Greenstone Belt, within the extensive, predominantly pyroclastic Sattasvaara Komatiite Complex. The present mineral composition of the weakly altered komatiites consists of an amphibole-chlorite assemblage resulting from regional greenschist facies metamorphism. The intensively altered rocks form a subvertically dipping alteration zone about 100 m × 600 m in extent, represented by two heterogenous and intercalated lithological types: (1) biotite schists with talc-carbonate ± pyrite veins and (2) coarse-grained and non-schistose amphibole rocks with associated quartz ± barite veins and pods.

The least altered amphibole-chlorite schists correspond compositionally to Geluk-type basaltic komatiites. The original komatiitic nature of the altered rock types is indicated by (1) the similarity in homogeneous immobile element ratios (Al/Ti) compared to those of less altered type, (2) mineralogical and geochemical gradation between rock types, and (3) similar REE patterns to those of the Sattasvaara komatiites.

In the biotite schists gold is closely associated with magnetite and talc-carbonate veins, in which it is fine-grained and occurs together with pyrite. In amphibole rocks gold is coarse-grained and occurs dominantly in native form towards the margins of the quartz ± barite veins, where it may locally comprise aggregates up to 1 cm in length.

Mass balance calculations have shown that biotite schists have been enriched in K, Fe, CO_2, Au, Ba, S, W, Te, Sr, and Mn, and depleted in Mg, Ca, Co, Si, and Zn, accompanied by a general 10—30 % decrease in volume. Amphibole rocks record a marked increase in volume, with gains in Si, Ca, Au, Na, Ba, Te, S, W, Sr and P, and conversely losses of CO_2, Co, Mg, Fe, and Zn.

The two major altered rock types reflect two stages of hydrothermal alteration, which, on the basis of textural and geochemical evidence, include: (1) biotitization (potassic alteration) and (2) later amphibole overgrowth (calc-silicate alteration). The former has been interpreted to have taken place during or immediately after the peak of regional metamorphism, and during ductile deformation. Its distribution was controlled by a combination of high permeability in the originally pyroclastic komatiites, and NE — SW trending deformation zones. Later amphibole growth was related at least locally to the NNE — trending shearing resulting in the formation of zones of dilation into which hydrothermal fluids were focused under conditions straddling the brittle-ductile transition.

The Early Proterozoic Central Lapland Greenstone Belt is comparable to highly mineralized late Archaean greenstone belts in many respects. The ore forming processes at Pahtavaara were related to wider cratonization processes associated with the Svecokarelian orogeny, and emplacement of extensive granitoid intrusives in connection with the remobilization of Archaean basement.

Key words (GeoRef Thesaurus, AGI): mineral deposits, genesis, gold ores, greenstone belts, komatiite, geochemistry, chemical composition, mineral assemblages, hydrothermal processes, Proterozoic, Pahtavaara, Sodankylä, Lapland, Finland

Esko A. Korkiakoski, Geological Survey of Finland, P.O. BOX 77, SF-96101 Rovaniemi, Finland

ISBN 951-690-455-6
ISSN 0367-522X

Vammala 1992, Vammalan Kirjapaino Oy

CONTENTS

INTRODUCTION

Preface

Gold exploration has increased markedly in Finland during the last few years, reflecting to a large extent the general world wide resurgence of interest in the metal. An important additional factor, however, has been the development of more accurate and rapid analytical techniques by the Geological Survey of Finland (GSF) (e.g. Kontas, 1981), in connection with systematic regional geochemical studies (Bolviken et al., 1986). As a result, a number of Proterozoic Au occurrences have been discovered throughout the country, including those of Kittilä (Härkönen & Keinänen, 1989; Keinänen, 1987; Tamminen, in prep.), Pohjanmaa (Mäkelä et al., 1987), Rantasalmi (Kontoniemi, 1989; Makkonen & Ekdahl, 1988), Kuusamo (Pankka, 1988; Pankka & Vanhanen, 1989; Pankka et al., 1991) and Orivesi (Ollila et al. 1990). Archaean occurrences have also been found in eastern Finland, at Ilomantsi (Nurmi et al., 1988; Nurmi & Ward, 1989; Pekkarinen, 1988).

Prior to these discoveries, only the Haveri Au-Cu deposit NW of Tampere (Mäkelä, 1980) and a minor vein-type Au occurrence at Kivimaa in Tervola (Rouhunkoski & Isokangas, 1974) had been exploited. The former contained 1.5 million metric tonnes of ore with a grade of 2.8 g/t and has been compared with Cyprus-type deposits, whereas the latter ore contained 20,000 metric tonnes of ore with a grade of 5.3 g/t occurred in calcite-quartz vein which according to E. Hanski (pers. comm.) is hosted by intrusions belonging to the Early Proterozoic gabbro-wehrlite association. Of the recent discoveries the only deposit being worked at the time of writing is that at Saattopora near Kittilä (Ketola, 1989; Tamminen, in prep.) which is hosted by albite-rich rock adjacent to silicified and carbonated ultramafic volcanites (now talc-chlorite schists).

In spite of the limited number of detailed geological studies, information related to gold mineralization is increasing rapidly, due to the intense exploration and research undertaken e.g. by geologists at the GSF (Autio, 1989; Björklund, 1991; Nurmi et al., 1991). In addition to the discovery of a number of small gold deposits, integrated exploration methods and sampling strategies have also been developed (Härkönen & Keinänen, 1989; Nurmi et al., 1989).

The Pahtavaara gold deposit (Figs. 1 and 2) situated in the municipality of Sodankylä, ca. 120 km north of the Arctic Circle, is one example currently under study within the early Proterozoic Central Lapland Greenstone Belt (CLGB). It is hosted by metakomatiites which are an important lithological type within a number of Archaean greenstone-associated gold deposits in South Africa, Australia and Canada (Colvine et al., 1984; Groves & Phillips, 1987; Pearton, 1982; Skwarnecki, 1987; 1988; Viljoen, 1984).

In addition to their interest from exploration point of view, komatiites have been subjected to intensive study and documentation since their discovery and definition by Viljoen and Viljoen (1969). This is partly due to a more general interest in these rocks, as they may provide significant information about mantle processes (Keays, 1984). Their high heat content and consequent

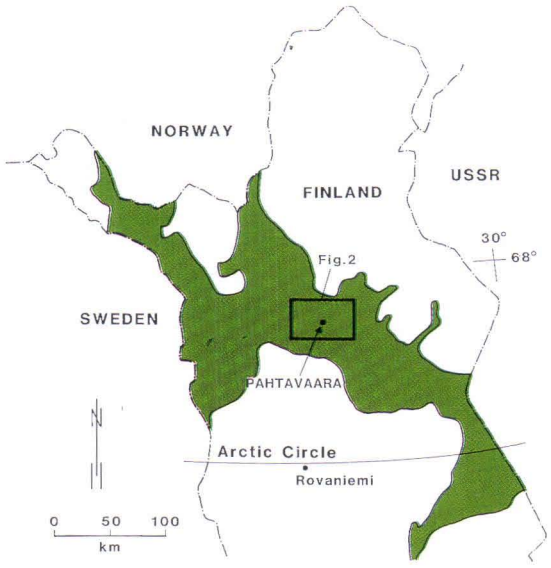

Fig. 1. Location of the Pahtavaara gold deposit within the Lapland Greenstone Belt (green), northern Finland. The outlined area is shown in Figure 2.

thermal effects may also have implications for the genesis of nickel ores (e.g. Groves et al., 1986; Korkiakoski, 1985). It has also been suggested by Brugmann et al. (1987) and Keays (1984) that komatiites may represent primarily gold-enriched rocks, although this is still disputed (cf. Kerrich & Fryer, 1979).

Thus, komatiites are an interesting class of rocks which, besides their economic significance, also offer important insights into petrogenetic problems such as fractional crystallization, partial melting and mantle processes in general. Due to their susceptibility to alteration, they are also sensitive indicators of the nature of hydrothermal processes in gold-enriched environments, which is of great significance and relevance to the present study.

Research aims

The purpose of this study is (1) to give a detailed mineralogical and geochemical description and assessment of the metakomatiite-hosted Pahtavaara gold deposit and (2) to present a model for its origin. Geologically Pahtavaara offers an excellent environment for studying hydrothermal alteration processes. This is partly due to the inferred homogeneous primary composition of the komatiitic host rocks and protoliths, and partly a result of their general chemical reactivity and susceptibility to alteration, as well as variability in the extent and type of alteration.

Recognition of alteration zones in gold prospecting is important because they offer a much larger exploration target than the mineralized rocks themselves and are analytically easier to distinguish. They also provide substantially more information on the gold-mineralizing event than studies restricted to ore samples and veins.

To determine the geochemical and volume changes during the alteration processes relating to the precipitation of gold, the least altered varieties of komatiites were used as reference material in mass balance calculations, using the procedure of Gresens (1967) and its later modification by Grant (1986).

The ultimate purpose of this study, therefore, is to define the geochemical factors associated with the hydrothermal alteration of komatiites, and the factors controlling the precipitation and occurrence of gold at Pahtavaara. This information can be directly applied during subsequent exploration programmes and also in correlation studies between the bedrock and the overlying till.

Terminology

All rocks discussed in this paper have been metamorphosed to greenschist facies grade during regional metamorphism and have undergone hydrothermal alteration to varying degrees. However, the prefix 'meta' has been, for convenience, deliberately omitted from rock names throughout the text.

The rocks in this study and comparable areas in the northern Finland have formerly been referred to as amphibole-chlorite rocks of picritic composition (Mikkola, 1941), ultrabasic extrusives (Paakkola, 1971) and ultramafic volcanic rocks (Tyrväinen, 1983). More recently they have been described as komatiites (Mutanen, 1976; Räsänen, 1983; Saverikko, 1983; 1985), a term first introduced in South Africa by Viljoen and Viljoen (1969) and which is currently defined as an ultramafic volcanic rock containing greater than 18 percent MgO (Arndt & Nisbet, 1982).

Rocks in the study area have been classified on the basis of their present mineralogical composition into three major groups. These consist of (1) amphibole-chlorite schists considered to present the least altered type, (2) biotite schists, and (3) coarse-grained amphibole rocks. All of these rocks show varying amounts of talc-carbonate alteration and, as detailed discussion based on geochemical and textural evidence will later show, are interpreted as having originally been komatiites. Amphibole-chlorite schists are the dominant rock type throughout the whole Sattasvaara Komatiite Complex, but are only sporadically present amongst the biotite schists and amphibole rocks at Pahtavaara. In order to keep terminology consistent, the amphibole-chlorite schists containing variable amounts of talc and carbonate are referred to throughout the text as 'weakly altered' and the others as 'altered types'. Furthermore, the term 'least altered rocks' refers to the four amphibole-chlorite schist samples selected as representing the least altered compositions (Table 1; anal. 1).

Previous and preliminary work

The present lithogeochemical study was preceded by an extensive geochemical mapping of till and drainage commenced by the Geological Survey in 1971 (Pulkkinen, 1983). The eastern, komatiitic part of the CLGB is ca. 300 km^2 in area and is reflected by high contents of Mg, Ca, Cr, Ni and Co in till. Furthermore, geochemical mapping revealed some specific Ni-Cu-Co-Pb anomalies within the komatiitic area. A preliminary project was established in 1984 to investigate these anomalies because it was thought that Cu enrichment in till corresponded to sulphide-bearing zones in the bedrock (Pulkkinen et al., 1986). During the follow-up work anomalous areas were studied in more detail by sampling the till with a grid spacing 100 m × 50 m, in conjunction with lithological mapping of bedrock. This work showed that one of the areas, namely Pahtavaara, also contained increased values of gold (up to ppm level).

During the subsequent stage of research, through 1985/1986, 621 samples of weathered bedrock were taken by percussion drill at 5 m intervals along traverses with 50 m spacing. This was combined with detailed lithogeochemical mapping of exposures and exploration trenches totalling 600 m in length. As a result, a hydrothermally altered zone -hereafter called »the (Pahtavaara) alteration zone» showing increased gold contents was outlined, over an area approximately 100 m × 600 m in extent (Fig. 3).

During the summer of 1986, a preliminary shallow drilling program was commenced, which continued through winter 1986/1987, along with drilling of a profile across the whole alteration zone. In the summer of 1987 the Pahtavaara al-

teration zone was drilled in collaboration with the Exploration division of the GSF on a 50 m × 50 m grid. Gold was analyzed systematically from the drill cores and samples for detailed geochemical and mineralogical study were chosen. The alteration zone has also been used in applying and developing geobotanical and biogeochemical exploration methods (Pulkkinen, 1987; Pulkkinen et al., 1989). Alteration features of the Sattasvaara komatiites have also been recently described (Hulkki, 1990).

In addition, a geogas test was carried out in July to August 1988, using the method described in detail by Kristiansson and Malmqvist (1987) in order to evaluate the information available from geogas in the Pahtavaara gold deposit. This new prospecting technique is based on the presence of a very weak stream of gas bubbles which emanates from bedrock through waterfilled, very deep fractures and fissures (see Malmqvist & Kristiansson, 1984).

The geogas survey at Pahtavaara was supervised by Dr. L. Malmqvist of the Scandinavian Emission Technology AB (SEMTEC) in Lund, Sweden, and entailed collecting 107 samples from four profiles across the alteration zone. Collecting funnels with membranes were exposed for eight weeks before treatment and analysis at the SEMTEC. The collection time was unusually long because the contents of several elements known to be sensitive for the geogas method were very low in account of the komatiitic host rock.

The ascending microflow of gas was guided with an inverted funnel into a collecting membrane made of polystyrene. During collection funnels were placed in holes about 50 cm deep. The matter collected on the membranes was analyzed with the PIXE method (an X-ray analysis technique which uses protons from a small accelerator for the excitation of the inner shells of the atoms).

The preliminary results of the geogas measurements were reported and interpreted by Malmqvist (1988). For the metals Cu, Zn and Pb, comparatively low values were obtained, whereas values for Cr and Ni were higher. This partly reflects the ultramafic nature of the bedrock but, markedly, unusually high emission of these metals occurs close to the alteration zone. High abundances of the volatile elements Cl, S and Br seem to clearly delineate the alteration zone. This is particularly the case with Cl and Br, with the latter having been found in association with several gold mineralizations. Measurements also show some high values of S. In summary, the geogas prospecting technique appears to be a good indicator of mineralization even in a relatively sulphide-poor area such as Pahtavaara.

Present study

The author joined the exploration team led by E. Pulkkinen in spring 1986 and has been involved in the research carried out from then up until June 1989. In 1987 more detailed research into the lithogeochemical characteristics of the Pahtavaara gold deposit was commenced, distinct from the more regional exploration project. The results of these lithogeochemical investigations form the subject of this paper, although some preliminary reports have previously been published (Korkiakoski, 1987; Korkiakoski et al., 1987; 1988; 1989).

MATERIALS AND METHODS

Samples and sample handling

During the work 134 representative bedrock samples of geologically well-defined varieties of weakly altered and altered types were selected for detailed study. Most of them were taken from drill cores but some were collected from outcrops. The latter type of samples generally represent weakly altered background samples and were taken from outside the Pahtavaara alteration zone.

Drill cores were split in half by diamond saw and approximately 1 meter long segments of the core were crushed with a jaw crusher preparatory to analysis. For detailed petrological study, polished thin sections were prepared for every sample.

Analytical methods

Half of the samples (n = 67) were analyzed by X-ray Assay Laboratories Ltd. (XRAL) in Canada using their so-called research package (multi-method multi-element quantitative analysis) for 52 elements including rare earth elements. Major elements were determined by X-ray fluorescence (XRF) spectrometry with a routine precision of better than 1 % for most major components and better than 5 % for Na and minor components (cf. Campbell et al., 1984). All analyses were normalized to 100 % volatile free. Selected rare earth elements (La, Ce, Nd, Sm, Eu, Tb, Yb and Lu) and additional trace elements Au, Sc, and Cr were determined by instrumental neutron activation analysis (INAA). Detection limits are in the order of 2 ppb for Au, 0.01 ppm for Sm and Lu, 0.05 — 0.1 ppm for Eu, Yb, La, Tb, and Co, 0.5 ppm for Cr, 1 ppm for Ce and 3 ppm for Nd. Vanadium, Cu and Zn were determined by direct current plasma (DCP). Detection limits were 2 ppm for V, and 0.5 ppm for the others. Unfortunately, several trace elements, some of which are typically associated with gold deposits, had values below their respective detection limits (shown in parentheses) and it therefore proved impossible to assess their significance in this study. This was the case for As (< 1 ppm), Br (< 0.5 ppm), Mo (< 2 ppm), Ag (< 0.5 ppm), Ir (< 0.5 ppm), Pb (< 2 ppm), Th (< 0.2 ppm), Y (< 10 ppm) and Zr (< 10 ppm).

The remaining half of the samples were analyzed for major elements and for Ba, S, Cr, and CO_2 plus H_2O by V. Hoffren at the GSF. Major components were determined after lithium metaborate fusion and trace elements measured by inductively coupled plasma-atomic emission spectrometry (ICP-AES) after total dissolution with HF/boric acid, with the exception of Cr, Ba and Sr, which were analyzed by XRF. On the basis of duplicate analyses whole rock data is comparable to that carried out by the XRAL. However, the detection limit for K_2O is higher for samples analyzed at the GSF than those determined by the XRAL, being 0.1 and 0.01 wt. %, respectively.

Vanadium, Sc, Co and Zn were analyzed for 5 samples (Drill core 509 / 88.80 — 116.40 m) by ICAP (method 710P) at the GSF by E. Kallio. Sulphur and CO_2 contents were determined by the LECO glow discharge system. Sulphur contents represent sulphur associated with sulphides rather than the total amount present since the method used was not capable of dissolving all sulphur from barite. In addition, 621 samples of weathered bedrock were analyzed semi-quantitatively by optical emission quantometer (OES). In spite of the limitations in its accuracy, this

method was found very suitable for distinguishing the hydrothermally altered zone (cf. Fig. 3).

Gold was analyzed systematically from all drill core samples by E. Kontas and his staff at the GSF laboratory in Rovaniemi using a graphite furnace atomic absorption spectrometer (GFAAS), with gold separation by reductive precipitation using Hg as collector (Kontas, 1981; Kontas et al., 1986). These results were then compared to the results obtained by the XRAL. In spite of the different sample weights used in the analyses (3 g at the GSF and 20 g at the XRAL), results were highly comparable. In addition, the samples with the highest gold content were reanalysed at the GSF by the lead fire assay method using a 50 g weighting. Again, the results were found to be comparable with those previously obtained.

Tellurium was analyzed by E. Kontas at the GSF laboratory in Rovaniemi by GFAAS using the same separation method as for gold, with a detection limit of 3 ppb (cf. Kontas et al., 1986).

Silicate mineral analyses were carried out by P. Kylmäluoma at the Institute of Electron Optics, University of Oulu, using a computer-controlled JEOL JCXA-733 electron probe X-ray microanalyser. All analyses were performed using a silicate-programme at 15 keV with a probe current of 3.3 nA and a beam diameter of 10 µm. Results were corrected using the ZAF correction programme. In order to obtain a clearer understanding of general carbonate compositions, systematic X-ray diffractometer measurements were made by P. Kouri at the GSF in Rovaniemi on 65 samples from drill cores 506 — 509 and 512. The composition of gold was analyzed by Bo Johanson at the GSF with a JEOL JXA-733 Super Probe. Grains were analyzed three times for a fixed interval of 10 seconds and corrected using the ZAF correction program. The accelerating voltage was set at 15 keV and the probe current at 400 nA.

Stable isotope analyses of carbon and oxygen from carbonates were carried out by J. Karhu at the GSF Isotope Laboratory at Espoo. Results for carbon isotope composition are reported as a $\delta^{13}C$ values relative to the $^{13}C/^{12}C$ ratio of the Chigaco PDB standard ($^{13}C/^{12}C$ = 0.0112372; Craig, 1957), and for oxygen as $\delta^{18}O$ values relative to Standard Mean Ocean Water (SMOW) determined by Craig (1961). Values represent isotopic ratios between samples and a standard and are expressed in ‰.

For analysis, CO_2 was liberated from carbonates by reaction with about 100 % phosphoric acid at 100 °C using the procedure of Rosenbaum and Sheppard (1986). Since all carbon is oxidized to CO_2 during this reaction, the value determined is the same as that of the carbonate. For oxygen the situation is more complex as only 2/3 of the oxygen in carbonate is liberated, resulting in fractionation of isotope compositions. Because the degree of fractionation is related to the temperature during the reaction, the composition of carbonate is not known exactly. The results for oxygen isotope compositions were calculated according to the procedure of Rosenbaum and Sheppard (1986) using fractionation factor of 1.00913.

Data handling

The geochemical data were processed at the GSF on a MICROVAX 2 computer using HST-software (Kaivosoja & Koivumaa, 1984). Factor analysis was carried out by CORRFAC-programme at the Geochemistry Department of the GSF using factor loadings in a 5-factor model after rectangular varimax rotation.

PROPERTIES OF GOLD AND CHARACTERISTICS OF GOLD DEPOSITS

Geochemistry of gold

Gold belongs to Group IB of the periodic table, along with copper and silver and follows these elements during processes such as magmatic differentiation. It has a distinct siderophile tendency with a secondary chalcophile tendency. Besides native gold, two ionic forms, Au^{1+} (aurous) and Au^{3+} (auric), occur in nature but at typical geological temperatures and oxygen fugacities only the 1 + oxidation state is common. Gold can be mobilized and precipitated in a wide variety of environments, ranging from those affected by weathering and biogeochemical processes to deep crustal levels associated with pluton emplacement and high-grade metamorphism (Boyle, 1979; Fyfe, 1986; Seward, 1979).

Significant variations in gold content occur between and within rock types. On the basis of data presented in the Geochemical Atlas of Finland, the average gold concentration in Finnish bedrock is 0.2 — 1.5 ppb. (Koljonen, in prep). The mean value is generally somewhat higher for ultramafic rocks, around 6 ppb (Romberger, 1986).

The solution chemistry of gold is reasonably well understood in spite of its low solubility in most solutions of geologic interest. The geochemical properties of gold in hydrothermal systems have been reviewed by a number of authors (Boyle, 1979; Fyfe, 1986; Phillips & Groves, 1983; Romberger, 1986; 1988; Seward, 1984). According to these studies gold is transported in aqueous solutions as a variety of complexes, of which aurous chloride or bisulphide complexes, depending on temperature and solution composition, are those most likely to be found in natural hydrothermal fluids. Thioarsenide and telluride complexes have also been postulated because of the common occurrence of arsenic and tellurium with gold (Seward, 1979). However, in most deposits formed between 200 and 350 °C, gold is best transported under reducing conditions as a bisulphide complex in which sulphur is present as either H_2S or HS^-. Auriferous chloride complexes will predominate only at higher temperatures, under acidic, oxidized conditions where haematite or other oxides are stable.

By considering solubility relationships at elevated temperatures comparable to those in nature as a function of pH, oxygen and sulphur activities together with the observations concerning stable mineral parageneses in gold deposits, it is possible to approximate ambient chemical conditions, as well as changes that may have occurred during deposition. However, the contrast between the geochemical environments of the source and host rock and the composition of derived fluids are probably most significant factors controlling chemical changes and, consequently, ore deposition. The stability fields of sericite and pyrite, both of which characteristic minerals in a number of gold deposits overlap the area of optimum gold solubility as bisulphide, suggesting a genetic relationship during gold deposition. Accordingly, if gold is transported as bisulphide complexes, oxidation and, to a lesser extent, increase or decrease in pH, and/or decrease in sulphur activity will cause deposition. In contrast, gold transported as chloride complexes will be deposited upon encountering reducing conditions, or by an increase in pH and/or decrease in temperature. Oxidation, which is probably the dominant cause for the deposition of gold from bisulphide complexes may be result of mixing of rising hydrothermal solutions with cooler oxygenated ground water, boiling (cf. Drummond & Ohmoto, 1985) or contact with more oxygenated, e.g. carbonated host rock (Henley, 1973; Romberger, 1986; 1988; Seward, 1984). Furthermore, the influence of salinity on the solubility of gold as bisulphide complexes is emphasized by Cathles (1986) since it explains the observed bimodal populations of base metal-rich, gold-poor,

and base metal-poor, gold-rich deposits. The solutions responsible for the deposition of the former are Cl-rich, whereas the latter typically have low salinity, being Cl-poor and HS^--rich (Kerrich & Hodder, 1982).

Classification and genetic models of gold deposits

Precambrian gold deposits can be classified into three major groups: (1) greenstone-hosted lodes, including deposits associated with syn- and post-orogenic felsic intrusive rocks, (2) paleoplacers, and (3) greywacke- or turbidite-hosted ores (Colvine et al., 1984; Hutchinson, 1987). Younger, post-Precambrian gold deposits are reviewed only briefly here. These include (4) Carlin-type deposits, which form a major source of gold in the western U.S.A., and (5) epithermal deposits, which are generated at upper crustal levels during groundwater convection. This last type also includes deposits formed in present-day epithermal systems (Foster, 1990).

The **Carlin-type deposits** are hosted by fine clastic and carbonaceous sediments which have been variously subjected to silicification, decarbonation and argillization (Berger & Bagby, 1991). **Epithermal deposits** occur in volcanic environments and are typically related to active plate margin and attendant subductive processes, such as in island archs of the Pacific rim. They appear to be transitional into deeper-seated porphyry Cu-Mo deposits (Foster, 1990; Sillitoe, 1991), the main alteration types being characterized by K-silicates. Such deposits appear to be lacking from Precambrian terrains, a feature attributed by Hutchinson (1987) to the removal of these near-surface deposits by erosion.

Amongst Precambrian deposits, the **turbidite-hosted** deposits are the least important type. They are otherwise widely distributed globally, and while found in rocks ranging in age from Archaean to Tertiary, they are most characteristic of the middle Palaeozoic, represented by the deposits of the Meguma Terrane in Nova Scotia, Canada (Graves & Zentilli, 1982; Keppie, 1976), and the Ballarat — Bendigo district in Victoria, Australia (Bowen & Whiting, 1975). Tectonically these deposits may be related to post-accretional stages in continental plate margin settings. Gold occurs in native form in these deposits, within structurally controlled quartz veins (saddle reefs). Wall rock alteration effects are commonly minimal but may include silicification, arsenopyritization and chloritization. As turbidite-hosted deposits are enriched in all of the elements associated with their host rocks (Au, Cu, Ag, Mg, Ca, Zn, B, Si, S etc.) metamorphic segregation of gold into quartz veins is considered the most likely explanation for their origin (Boyle, 1986).

Paleoplacer deposits have also been found in most Precambrian shields, generally being restricted to the base of the Proterozoic succession resting unconformably on an eroded Archaean basement. Of these, only the giant Witwatersrand deposits are of major economic importance, with a net production about 10 times greater than the entire Abitibi belt in Canada — the world's largest gold-producing greenstone belt. The Witwatersrand deposits are hosted by quartz-pebble conglomerates having a pyritic matrix (up to 20 %). Besides gold, paleoplacer deposits have also been an economic source of uranium. A number of hypotheses have been proposed for their origin. The most favoured paleoplacer model advocates the primary deposition of gold as detrital placer grains derived from the erosion of greenstone terrains, followed by subsequent mobilization and recrystallization during metamorphism. However, several notable features are also consistent with a hydrothermal origin for these deposits. These include (i) the fine grain-size of gold, (ii) the presence of gold throughout the sedimentary sequence, instead of

being restricted to basal lag deposits in conglomeratic units, (iii) the probability of the bulk of the pyrite being post-depositional rather than detrital in origin, and (iv) the presence of sericite, chlorite, carbonate, tourmaline and other hydrothermal minerals (Boyle, 1979; 1984). Hutchinson (1987) has also argued that only a minor proportion of gold is of detrital origin the bulk being hydrothermal.

In Finland, paleoplacer gold deposits are represented by the subeconomic Kaarestunturi occurrence (Härkönen, 1984), which is hosted by quartzite-conglomerates deposited in a delta or fluvial fan and resting unconformably on the CLGB. Clasts within conglomerates include vein quartz, jasper and jaspilite while the matrix consists of quartz, sericite and chlorite with abundant magnetite and haematite. Gold occurs at the base of conglomerate lenses, and derives from the weathering of gold-bearing quartz-sulphide-carbonate veins of the CLGB.

Greenstone-hosted lodes occur in compositionally diverse Archaean volcano-sedimentary successions. Gold provinces are typically associated with mafic rocks, often including an ultramafic (komatiitic) component. However, at the scale of individual mines, small felsic intrusives are relatively abundant (Hodgson et al., 1982). Other important host rocks are pyritic tuffs and pyritic and graphitic interflow sediments, sulphide facies iron-formations, and pyritic quartz-feldspar porphyries (Boyle, 1984; Hutchinson, 1987).

On the basis of the recently proposed and prevalent models, Archaean greenstone-hosted gold deposits have been classified as (1) structurally controlled epigenetic and (2) stratigraphically controlled syngenetic mineralizations (Kerrich, 1983; Pearton, 1984). Consequently, this has led to an on-going debate and controversy between the synvolcanic and epigenetic models, which in turn influences exploration strategies, depending on the extent to which they emphasize the importance of either favourable stratigraphical sequences and horizons or alternatively structural features. These differ from earlier magmatic-hydrothermal models, according to which hydrothermal fluids were derived from granitoids, moved along major structures and deposited gold and associated minerals within structurally generated dilatation zones (Hodgson, 1989).

Syngenetic gold mineralizations are generally associated with iron-formations and carbonaceous sediments. They are interpreted as sea-floor exhalites, which have subsequently undergone complex metamorphism and remobilization, resulting in the multistage enrichment and separation of gold into veins from strata that were initially enriched in Au as result of sea-floor and subsea-floor hot spring activity (Fryer & Hutchinson, 1976; Fyon & Crocket, 1982; Hutchinson & Burlington, 1984; Karvinen, 1982; Steefel, 1987).

However, the majority of recent models emphasize an epigenetic origin and intimate association with metamorphic fluids (the so-called metamorphic hydrothermal model; Boyle, 1984; Colvine et al., 1984; 1988; Groves et al., 1985). These structurally controlled epigenetic gold deposits are typified by extensive hydrothermal alteration zones which are easiest to distinguish in mafic and ultramafic rocks because of their general susceptibility to alteration. The most marked types of alteration are carbonation, K-metasomatism (sericitization), silicification, albitization, chloritization, sulphidization (particularly pyritization) and tourmalinization. Gold generally occurs in sulphidic quartz veins. Of these alteration types, carbonation is generally the most extensive; in proximity to ore deposits carbonate is typically Mg- and Fe-bearing (magnesite — siderite — ankerite) but further away it tends to be calcite and dolomite (Colvine et al., 1984).

Geochemical alteration is typically associated with the addition of the following elements: CO_2, K, Si, S, Na and to a lesser extent As, W, Mo, Sb, Cr, B and Ba (Boyle, 1979; 1984; Colvine et al., 1984; Pearton, 1984). Although the origin of greenstone-hosted lodes is still controversial, most investigators seem to invoke

auriferous CO_2-H_2O-rich metamorphic fluids, which were focused along crustal-scale fault and shear zone systems and then deposited in favourable structural sites in suitable host rocks. According to the metamorphic hydrothermal model, deposition of gold took place at temperatures below the amphibolite-greenschist facies transition and was related to sulphidation of Fe-rich host rock (Colvine et al., 1984; Groves et al., 1985; 1987; Phillips & Groves, 1984).

Recent studies in active hydrothermal areas have provided additional information about conditions during the transportation and deposition of gold (Drummond & Ohmoto, 1985; Romberger, 1986). These data, in combination with detailed fluid inclusion (e.g. Ho et al., 1985; Roedder, 1984), isotope and experimental (Seward, 1984) studies of ancient gold deposits have given further support for the metamorphic hydrothermal model (Colvine et al., 1984; Fyfe & Kerrich, 1984; Groves & Phillips, 1987; Groves et al., 1985). However, some geologic, geochemical and isotopic data are more consistent with derivation of ore fluids from oxidized CO_2-rich felsic magmas, suggesting a magmatic origin for some gold deposits (e.g. Cameron & Hattori, 1987).

In addition, the importance of porphyry intrusions and associated albitite dikes in the genesis of gold deposits in Timmins, Canada, has been stressed by Mason and Melnik (1986). They have argued that hydrothermal alteration and associated mineralization occurred after emplacement of albitite dikes but before regional metamorphism. Associated regional deformation modified all pre-existing shapes, including those of mineralized structures and formed the distinctive high strain zones. Thus, mineralization is, according to this model, younger than its host rocks, and is related to the intrusion of porphyry-type magmas and circulation of magmatic fluids. Moreover, the Hollinger-McIntyre deposit, which is the largest known Au-quartz vein/shear zone system in the Superior province in Canada (total reserves about 1000 tonnes of Au with the grade of 10 g/t) is also considered to be a magmatically derived deposit, on the basis of stable isotope data (Wood et al., 1986).

In spite of the marked increase in understanding the genesis of the gold deposits, many problems, including for example the source of gold, and the nature of the fluid from which gold is deposited, are still unresolved. The origin of some deposits, such as Hemlo in Ontario, Canada, is still vigorously debated and a number of different models have been proposed; Hemlo has, for example, variously been considered as a syngenetic (Cameron & Hattori, 1985), structurally controlled (Burk et al., 1986), and porphyry-type of deposit (Kuhns, 1986). However, none of these models alone appear adequate to explain the features of the deposit as a whole.

Most greenstone-hosted gold deposits are late Archaean in age whereas gold deposits in otherwise similar early Proterozoic greenstone belts such as CLGB are generally less significant. This contrast may be connected with the oxygenation of the atmosphere and hydrosphere during early Proterozoic time. Examples of such younger gold deposits include those in the Birimian greenstones of West Africa (Black, 1980), the Guiana shield of South America (Gibbs & Barron, 1983), Nor Acme in Manitoba and deposits of the Gunnison gold belt in Colorado (Hutchinson, 1987), Bidjovagge in northern Norway (Björlykke et al., 1987) and numerous small domestic occurrences throughout Finland.

REGIONAL GEOLOGY

General overview

The bedrock in Finnish Lapland consists of two major units: (1) the Archaean Basement Complex (3.1 — 2.5 Ga) and (2) the overlying early Proterozoic cover. The former group consists of Archaean migmatite gneisses which, together with some subordinate greenstones and locally occurring komatiites (i.e. Tuntsa supergroup; Juopperi & Räsänen, 1989), formed the so-called Saamian Craton (Silvennoinen, 1985; Simonen, 1980). The early Proterozoic cover comprises mainly of Lapponian rocks which can be divided into upper, middle and lower Lapponian (Manninen, 1991). The lower and upper Lapponian rocks consist dominantly of volcanites, whereas the middle Lapponian is composed mainly of metasediments. These sediments were deposited in a shallow marine environment in an intracratonic setting after stabilization of the Saamian craton. Sedimentation was followed by rifting and eruption of the voluminous upper Lapponian volcanites resulting in the formation of the CLGB, which now extends in a NW-SE direction across the northern Fennoscandian Shield from Finnish Lapland into northern Norway. These volcanites are mainly tholeiitic although komatiites are also locally abundant.

The age of the Lapponian rocks has been a subject of controversy. Silvennoinen et al. (1980) and Saverikko (1990) regarded the Lapponian Kuusamo and Salla greenstones, and the Jauratsi and Kittilä greenstones as Archaean. In contrast, Gaál et al. (1978) and Gaál (1986) claimed that the western part of the CLGB (i.e. Kittilä greenstone belt) is Proterozoic and only the eastern part, including the present study area, is Archaean and therefore correlative with the Kuhmo greenstone belt, which is unanimously accepted as Archaean (e.g. Piirainen, 1988). Some further contradiction has also been caused by age determinations from the Karasjok greenstone belt in northern Norway (Often, 1985), where the komatiitic continuation of the CLGB yielded a surprisingly young Sm-Nd whole-rock age of 2085 ± 85 Ma (Krill et al., 1985). Most of recent studies, however, consider the volcanites of the CLGB as early Proterozoic (Lehtonen & Rastas, 1988; Lehtonen et al., 1989; Silvennoinen, 1985). The minimum U-Pb age for the middle Lapponian sediments, given by zircons from cross-cutting gabbros and albite diabases, is ca. 2200 Ma (Lehtonen et al., 1985; Rastas, 1980; Silvennoinen, 1985). Furthermore, the middle Lapponian metasediments and associated volcanic formations have recently been correlated with Jatulian rocks (Manninen, 1991).

The youngest supracrustal rocks in central Lapland consist of conglomerates and quartzites of the Kumpu formation, unconformably overlying the CLGB (Silvennoinen, 1985). In contrast to the middle Lapponian metasediments (mainly quartzites) these rocks are continental sediments representing fluvial and alluvial fan deposits (e.g. Nikula, 1988).

The extensive early Proterozoic Granulite Complex in the northeastern side of the CLGB consists of high-grade metapelites and metapsammites with some igneous intercalations (Gaál et al., 1989). It has been thrusted towards the south and interpreted as a collisional orogenic belt (Barbey et al., 1984), with regional granulite facies metamorphism culminating about 1920 Ma ago, possibly as a result of continent to continent collision.

An important stage in the development of the Proterozoic crust was the emplacement of large layered mafic intrusions 2440 Ma ago (Alapieti, 1982; Mutanen, 1989). This was followed by the intrusion of cross-cutting diabase dykes dated back to 2.2 — 2.0 Ga. A major heterogeneous igneous unit in Finnish Lapland is the Central Lapland Granitoid Complex which probably represents to a large extent remobilized Archaean

basement gneiss (Huhma, 1986; Lauerma, 1982; Silvennoinen, 1985). However, the age determinations for these rocks yield the ages corresponding to the Svecokarelian orogeny, between 1.9 and 1.8 Ga. Granitoids formed during the Svecokarelian orogeny were followed by the emplacement of the Nattanen-type post-orogenic granitoids about 1.8 Ga ago (Front et al., 1989).

Central Lapland Greenstone Belt

The Central Lapland Greenstone Belt (CLGB) forms an extensive area of supracrustal rocks which is bordered in the south by the Central Lapland Granitoid Complex and in the north and east by the Granulite Complex and Archaean basement gneisses, respectively. It consists predominantly of rocks belonging to the Lapponian supergroup which have been subdivided into the upper, middle and lower Lapponian (Manninen, 1991). The lower Lapponian volcanites have a relatively restricted distribution in Lapland and are only exposed at Möykkelmä (Räsänen et al., 1989), Rajalompolo, Tojottamaselkä, Peurasuvanto (Lehtonen et al., 1989), Kaukonen (Lehtonen & Rastas, 1988), Teuravuoma (Väänänen, 1989) and Salla (Manninen, 1991).

The lower Lapponian rocks at Möykkelmä, exposed about 4 km north of the Pahtavaara gold deposit (Fig. 2) have been studied in detail recently by Räsänen et al. (1989). These rocks were erupted directly onto Archaean gneisses and now form a distinctive domal structure. Compositionally they are basaltic komatiites and low-Ti tholeiites, the former differing from the dominantly ultramafic komatiites of Pahtavaara. Räsänen et al. (1989) considered the Möykkelmä komatiites as hydrothermally altered. This is indicated by a wide variation in SiO_2 content and their low CaO content, as well as their enrichment in K, Rb and Cs. In addition, anomalous immobile element characteristics (low Ti/Zr and high Al/Ti) suggest a considerable amount of contamination by sialic Archaean crust.

The middle Lapponian metasediments comprise quartzites and mica schists/gneisses bordering the basin into which the upper Lapponian volcanites were erupted (Silvennoinen, 1985). The mutual stratigraphic relation of these units is shown by the sporadic occurrence of komatiitic interbeds in the upper parts of the quartzitic metasediments (Lehtonen et al., 1989).

The detailed stratigraphy and geology of the eastern part of the CLGB have recently been reviewed by Lehtonen and Rastas (1988) and Lehtonen et al. (1989). They divided the upper Lapponian volcanites into three different units V1, V2, and V3 (Fig. 2). The lowermost unit V1, including the present study area, occupies the eastern part of the CLGB and is collectively termed here the Sattasvaara komatiites. It consists mainly of pyroclastic ultramafic and mafic komatiites. Units V2 and V3 appear to form separate volcanic series both beginning with mafic and/or ultramafic komatiites and culminating with tholeiites. The tholeiites of the unit V2 are Fe- and Ti-rich, whereas the unit V3 consist dominantly of Mg-tholeiites. The two units are separated from each other in the Porkonen — Pahtavaara region by sulphide and oxide facies iron-formations.

By comparing the geochemistry of these rocks to recent volcanites from different geotectonic environments, Lehtonen and Rastas (1988) have concluded that they were erupted during different stages of rifting of an ancient continent. Accordingly, they have interpreted unit V2 Fe-tholeiites, which compositionally resemble continental volcanites, to have formed during an early stage of rifting. In contrast, the V3 volcanites were formed during more advanced stage of rifting as indicated by their compositional resemblance to present-day the mid-ocean ridge basalt (MORB). The above authors did not interpret the geotectonic importance of the lowermost V1 unit.

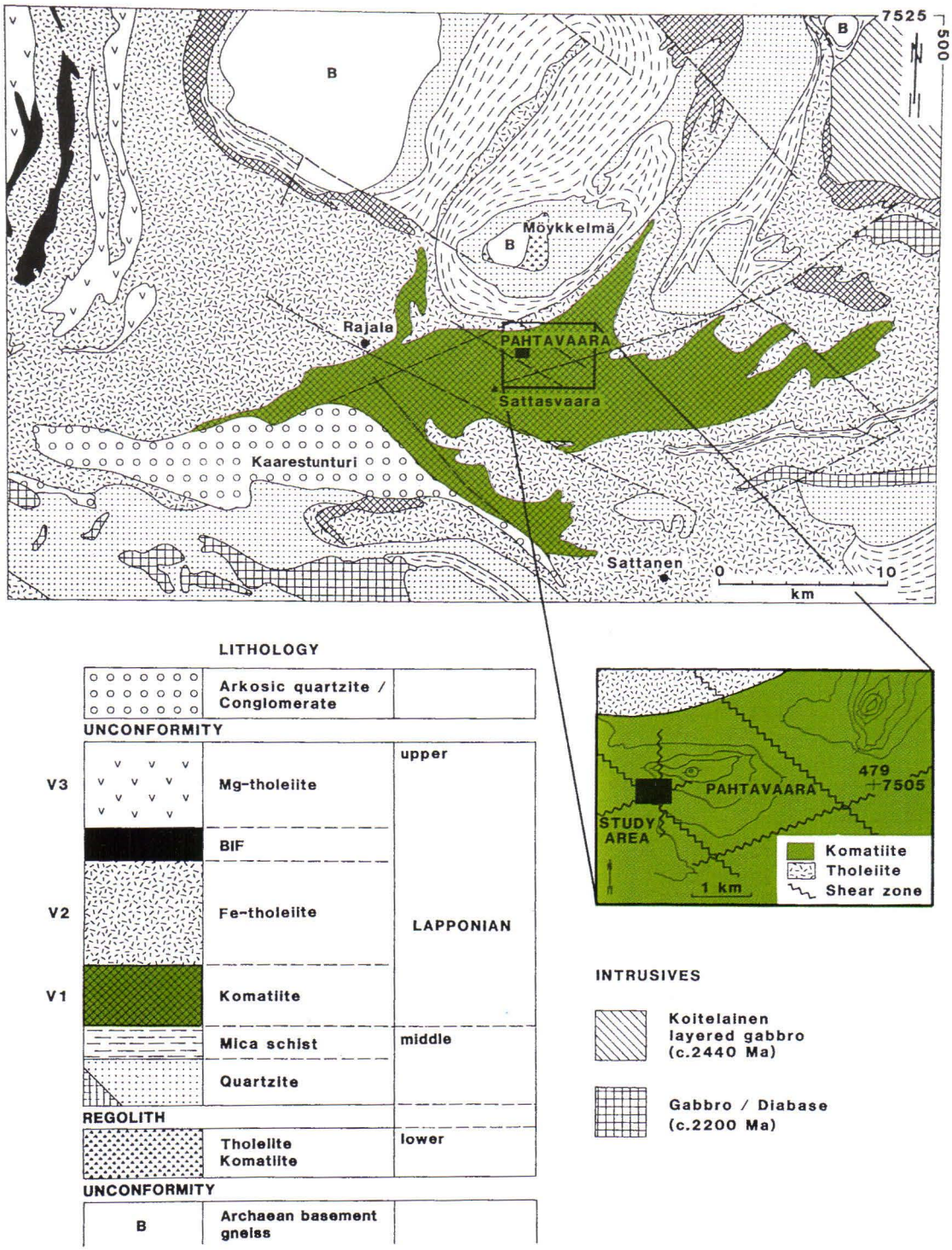

Fig. 2. Generalized geology, stratigraphy and structural features of the eastern part of the early Proterozoic Central Lapland Greenstone Belt (modified after Lehtonen & Rastas, 1986; Lehtonen et al., 1984; Manninen, 1991; Tyrväinen, 1979). The location of the detailed study area on the southwestern flank of hill Pahtavaara is shown on the inset map.

However, its komatiitic nature suggests the existence of deep-seated faults and obvious mantle connection (cf. Groves et al., 1985).

The central part of the CLGB is characterized by low-grade greenschist facies metamorphism which increases to medium-grade towards the granitoid domains in the south (Gaál et al., 1989). Metamorphic grade also becomes higher on the northern side of the Sattasvaara komatiites (Tyrväinen, 1983). In addition to that, wide areas of the CLGB were subjected to extensive synvolcanic albitization (Lehtonen et al., 1989; Ward et al., 1989).

Deformation of the CLGB resembles that in thin skinned fore-land thrust belts and commenced during overthrusting of the Lapland Granulite Complex from the NE. Progressive deformation resulted in further shortening and accommodation to granitoid intrusion around 1.9 — 1.8 Ga with the formation of major NW — SE trending dextral shear systems. Persistent ductile and brittle reactivation of these structures subsequently influenced late orogenic terrestrial sedimentation and granitoid emplacement. Further distinctive structural feature throughout Finnish Lapland, which is probably of more direct significance to the genesis of the Pahtavaara gold deposit, are NE-trending ductile shear zones (Korkiakoski et al., 1988; Ward et al., 1989).

The early Proterozoic CLGB seems to have many features in common with older, Archaean greenstone belts, which have been classified by Groves and Batt (1984) and Groves et al. (1987) into (1) rift-phase greenstones and (2) platform-phase greenstones. The former include several major gold provinces and are characterized by (i) bimodal volcanism, (ii) abundant komatiites, (iii) limited synvolcanic alteration, (iv) major synvolcanic basinal faults and (v) a wide variety of sedimentary facies, including sulphidic deposits. In all, they appear to represent continental rift systems defined by fault-controlled basins and high geothermal gradients. However, the CLGB appears to have more in common with the platform-phase greenstones, which are typified by (i) tholeiitic (and calc-alkaline) volcanites, (ii) lesser komatiites, (iii) intense synvolcanic alteration, (iv) shallow water sedimentary environment and (v) sparsity of sulphidic sediments. As a whole, platform-phase greenstones represent platform sequences developed in shallow, slowly sinking intracontinental basins. Evidence of this in Finnish Lapland is provided by extensive quartzitic sediments which represent shallow marine deposits (Nikula, 1988). Gravimetric anomalies suggest that the thickness of the CLGB in Kittilä area is about 6 km, forming an E — W trending, nearly linear trough (Elo et al., 1989; Lanne, 1979), again consistent with an intracratonic setting.

PAHTAVAARA GOLD DEPOSIT

General features

The Pahtavaara gold deposit is situated in the eastern part of the CLGB (Fig. 2) and is hosted by the Sattasvaara komatiites; formerly termed the Sattasvaara Komatiite Complex by Saverikko (1985) and the V1 Volcanic Unit by Lehtonen and Rastas (1988).

On the 1 : 100 000 scale aeromagnetic graytone pixel map the Sattasvaara komatiites are clearly evident from their distinct positive anomaly. Mikkola (1941) considered them as amphibole-chlorite rocks of picritic composition, and also noted their ferromagnesian nature, ultramafic

composition and extrusive origin. Tyrväinen (1983) classified these rocks into ultramafic and mafic volcanites. The komatiitic composition and pyroclastic nature of these rocks have been discussed by Räsänen (1983) and Saverikko (1983). Saverikko (1985) has further classified these rocks geochemically into komatiitic basalts (MgO 9 — 18 wt. %), (basaltic) komatiites (MgO 18 — 29 wt. %), and komatiites (MgO >29 wt. %; all on an anhydrous basis).

As stated above, the stratigraphical and lithological aspects of the eastern part of the CLGB have been recently described by Lehtonen and Rastas (1988), and Räsänen et al. (1989). According to these authors, ultramafic komatiites of Volcanic Unit V1 are depleted in Al as well as in both light (LREE) and heavy (HREE) rare earth elements. Comparable komatiites from the Karasjok greenstone belt in adjacent northern Norway, which have been dated back to about 2100 Ma, also appear to have been derived from a source region depleted in LREE (Krill et al., 1985).

The Pahtavaara alteration zone covers an area of approximately 100 m × 600 m and is geochemically distinguished from the surrounding komatiitic terrain in that weathered bedrock typically has higher abundances of Ba, K, Sr and Mg and lower Mg, Co, and Zn contents (Fig. 3; Korkiakoski, 1987; Korkiakoski et al., 1988; 1989). The currently estimated gold reserves are about 350,000 t of ore grading 6 g/t (A. Karvinen, pers. comm.). The ENE-trending alteration zone dips subvertically towards the NNW, at an angle of ca. 80 — 85 degrees (Fig. 19). Lithologically, the alteration zone is typified by the abundance of biotite schists and amphibole rocks. Some blocks of weakly altered amphibole-chlorite schists are also preserved within the alteration zone. As a whole, the zone is compositionally heterogenous with all the different rock types alternating irregularly with one other. The alteration zone is enveloped by talc and carbonate-rich amphibole-chlorite schist, and the abundance of talc-carbonate veins diminishes away from the alteration zone. Comparable features have also been described from other komatiite-hosted gold deposits (e.g. Kerr-Addison mine in Ontario; Kishida & Kerrich, 1987). On the northern side of the alteration zone, where some primary features are still preserved, komatiitic pillow lavas have been recognized.

Three major rock types, variously intercalated with one other have been recognized in the study area. These are: (1) amphibole-chlorite schists, (2) biotite schists and (3) coarse-grained amphibole rocks and associated quartz ± barite lenses, veins and irregular pods (Figs. 4 — 6), which may locally contain visible free gold. Talc-carbonate ± pyrite veins are common in all lithologies, but are particularly abundant in the biotite schists (Korkiakoski, 1987; Korkiakoski et al., 1987; 1988; 1989). Amphibole-chlorite schists are the dominant rock type outside the Pahtavaara alteration zone. They represent the regional greenschist facies metamorphic mineral assemblage and are therefore considered to correspond to the most typical and least altered rock type of the Sattasvaara komatiites. This rock type occurs only rarely within the Pahtavaara alteration zone.

Structurally Pahtavaara area is typified by NE — SW, NW — SE, and NNW — SSE trending shear zones (Figs. 2 and 4). According to the interpretation of gravity data, a generally E-W trending vertical fault several km in extent occurs along the southern flank of Pahtavaara hill (E. Lanne, pers. comm.).

Lithology and petrography of the rock types

Unaltered komatiites typically consist of an olivine — pyroxene assemblage with minor plagioclase, chromite and glass (Arndt et al., 1977; Lesher, 1983; Nisbet et al., 1987). However, this

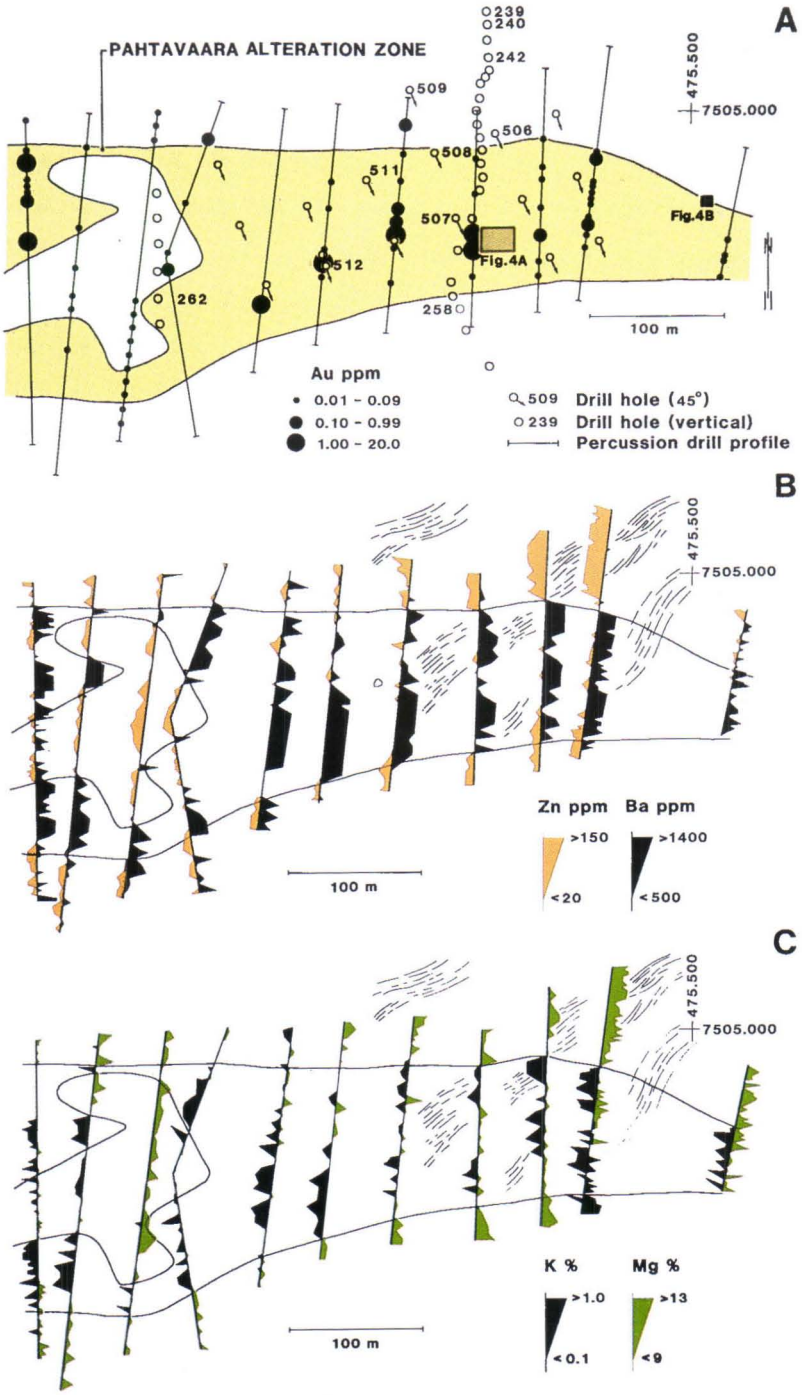

Fig. 3. Pahtavaara alteration zone within the detailed study area.

A; Location diagram showing drill holes, percussion drill profiles and bedrock gold contents.

B; Alteration zone is clearly delineated by low Zn and high Ba contents in weathered bedrock compared to those in the surrounding areas. Note the difference of about 20 degrees in direction between the ENE-WSW trending alteration zone and the major NE-SW schistosity, shown by discontinuous lines. Data based on 621 samples, analyzed OES.

C; Alteration zone indicated by low Mg and high K contents of weathered bedrock with respect to those of surrounding area. Data based on 621 samples, analyzed OES.

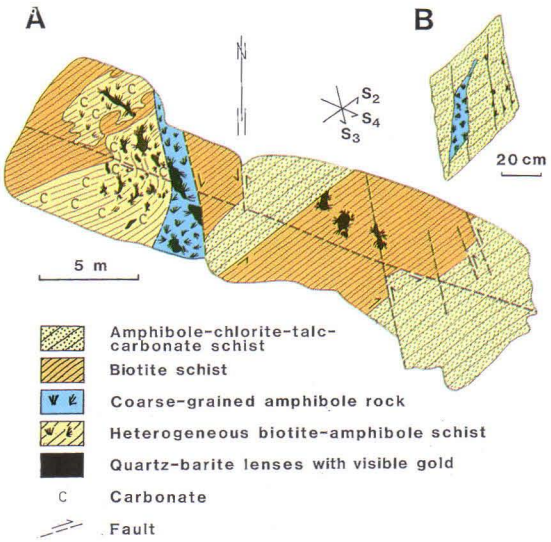

Fig. 4A. Geology and structural features of the Exploration Trench 5, showing the major hydrothermally altered rock units. Amphibole—chlorite—talc—carbonate schist represents weakly altered tuffitic komatiite. Note also the regional NE-SW schistosity (S_2), and NNW-shearing (S_3) associated with the coarse-grained non-schistose amphibole rock and quartz-$\pm$barite lenses containing visible gold. S_4 represents later crenulation and kinks, with no influence upon mineralization. For location, see Figure 3A.

Fig. 4B. Detailed sketch of relation between the weakly altered amphibole-chlorite schist and coarse-grained amphibole rock. Note the association of the latter with S_2 and S_3 structures. For location, see Figure 3A.

Fig. 5. Drill core samples of variably altered rock types from Pahtavaara. Drill cores are 4 cm in diameter.

A; Biotite-chlorite-magnetite schist (biotite and magnetite = black; chlorite = green) with pyrite-bearing (yellow) talc-carbonate vein (white to light grey). Drill core 508/95.70 m.

B; Parallel zones of biotite-chlorite-magnetite assemblage (patchy grey) and talc-carbonate vein (white to light grey). Both are cross cut by coarse-grained and radiating amphibole crystals (light green). Abundant pyrite (yellow) is associated with areas where the amphibole rock overlaps with formerly magnetite-rich parts of the rock. Drill core 508/117.30 m.

C; Biotite-chlorite-magnetite schist (black to dark grey) and dolomitic carbonate (light grey). Note the overgrowth of coarse-grained amphibole (green) along the carbonate vein at the right end of the core. Drill core 511/84.20 m.

Fig. 6. Drill core samples of variably altered rock types from Pahtavaara. Drill cores are 4 cm across.

A; Fine-grained amphibole-chlorite-carbonate schist representing weakly altered komatiite. Drill core 509/36.40 m.

B; Detailed section of the drill core 508/117.30 m shown in Figure 5B (opposite side). Biotite-chlorite-magnetite assemblage is shown in black and dark grey, concordant talc-carbonate-minor magnetite vein in white to grey, and radiating amphibole overgrowth in green. Note also the presence of pyrite (yellow) at the upper centre.

assemblage is only rarely preserved due to subsequent metamorphism and various kinds of hydrothermal alteration, including early serpentinization and carbonation (cf. Eckstrand, 1975). Hence, apart from sporadic chromite, no primary minerals or even serpentine have been found at Pahtavaara. In the following section, the lithological and petrographical features of the three major mineralogical types are described.

Amphibole-chlorite schist

Amphibole-chlorite schists are the most characteristic lithology within the Sattasvaara komatiites. They occur only rarely within the Pahtavaara alteration zone but some talc and carbonate-rich varieties have been observed. As a whole, the amphibole-chlorite schists are relatively homogeneous and fine-grained, the present mineral composition being formed as a result of greenschist facies regional metamorphism.

The komatiitic nature of these weakly altered rocks was recognized by Räsänen (1983), Saverikko (1983; 1985) and Lehtonen et al., (1989). Although they are generally schistose, their pyroclastic nature is shown by the local preservation of lapilli tuffs and agglomerates. Primary

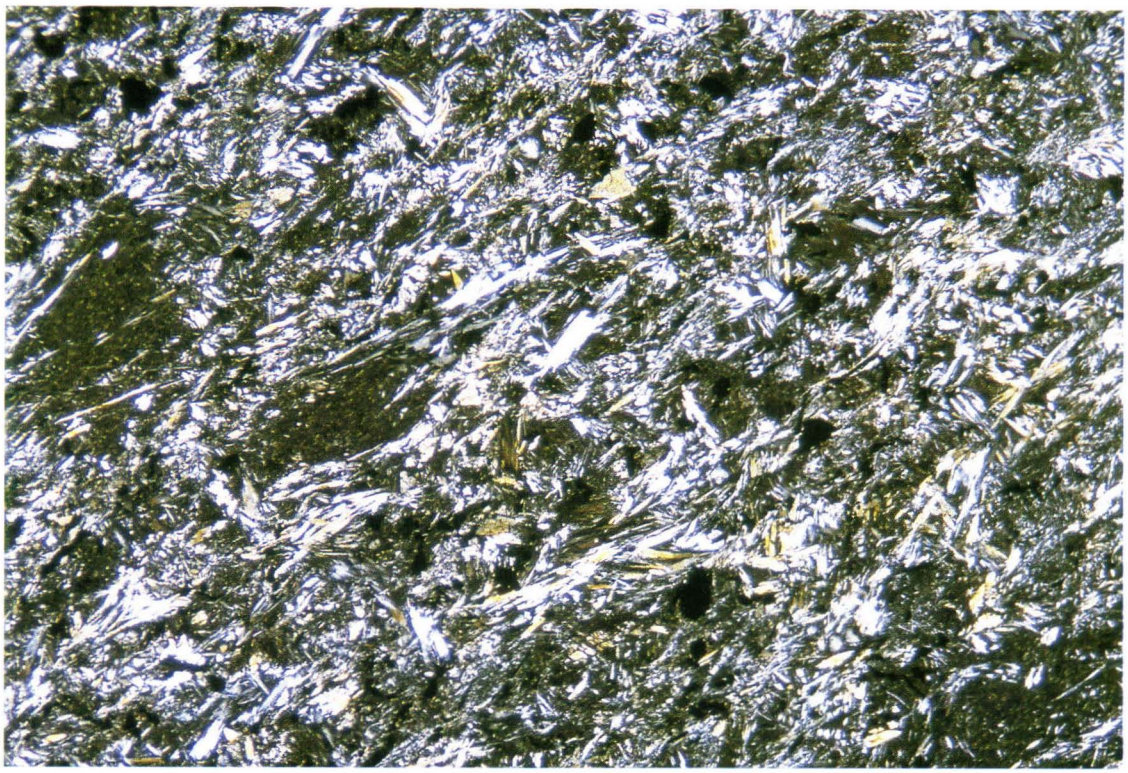

Fig. 7. Amphibole-chlorite schist representing weakly altered komatiite. Elongate amphibole crystals (tremolite-actinolite) are shown in bright colours, chlorite in dark green and magnetite in black. Note the dark chlorite patches probably representing relict primary lapilli structures. Drill core 230/33.40 m. Field of view is 5 mm in width.

textural features are particularly well-preserved at the hill Sattasvaara where both pyroclastic and pillowed structures are common (Saverikko, 1985). In addition, komatiitic and tholeiitic dykes have been reported (Lehtonen et al., 1989). Some pillowed, amygdaloidal and massive varieties have also been observed, for example at the top of the hill Pahtavaara. However, no spinifex textures typical for many komatiites have been found or reported from the Sattasvaara komatiites.

Mineralogically, rocks at Pahtavaara consist predominantly of amphibole and chlorite with variable carbonate and talc contents (Figs. 6A and 7). Talc and carbonate occur both as porphyroblasts and veinlets. They increase in abundance as the Pahtavaara alteration zone is approached, and the overall proportion of veins also increases. A small amount of pyrite also occurs in association with talc-carbonate veins but apart from some rare chromite rimmed by magnetite, no primary minerals have been preserved. Typical accessory minerals are magnetite, formed at least partly as a result of serpentinization (cf. Eckstrand, 1975), and ilmenite.

Texturally these komatiitic rocks are fine-grained and relatively homogeneous. Due to the homogeneity of the material, the intensity of foliation development and the lack of any marker horizons, determination of primary bedding is generally difficult or impossible. However, outside the Pahtavaara alteration zone, ultramafic komatiites can in places be distinguished in outcrop from mafic varieties by their browner

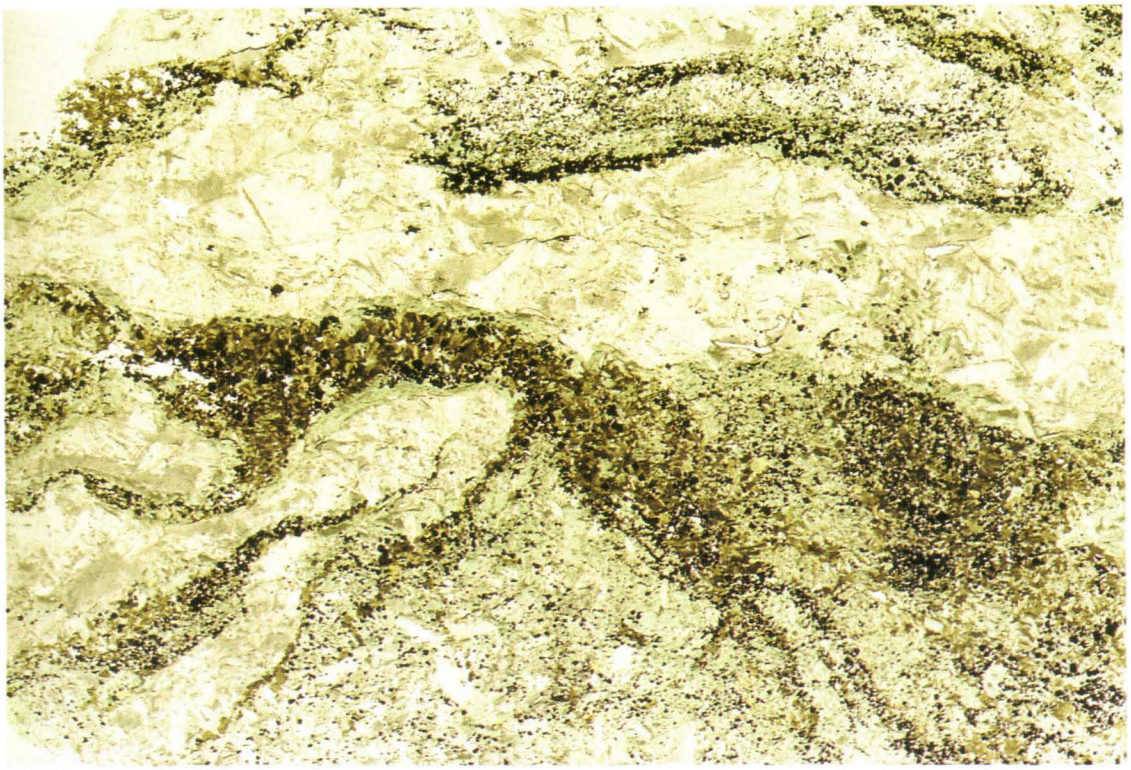

Fig. 8. Heterogeneous biotite-chlorite-magnetite schist with talc-carbonate vein. Biotite is shown in brown, chlorite in green, magnetite in black, and talc-carbonate vein in light grey. Some albite is also present. Drill core 256/26.45 m. Field of view is 2.6 cm in width.

weathering surface in the least altered and well-exposed areas. Mineralogically the mafic varieties differ from the more Mg-rich types by the presence of albite (cf. Saverikko, 1985).

Biotite schist

Due to their dark colour, biotite schists are the easiest distinguishable rock type in the Pahtavaara alteration zone. Because they are soft and prone to weathering, they have only been encountered in exploration trenches. Furthermore, because of a well-developed foliation parallel the regional NE — SW schistosity, unweathered samples for detailed study are available only from drill core material.

As a whole, the biotite schists are heterogeneous, fine-grained rocks which consist of variable proportions of dark mica (biotite-phlogopite, termed hereafter biotite) and chlorite with variable proportions of talc-carbonate ± pyrite veins (Figs. 8 — 10). Under the microscope, biotite is generally brown but locally green varieties can also be observed. Magnetite and, to a lesser extent, albite are the most typical accessory minerals. Chromite crystals surrounded by magnetite rims occur in places. Some tourmaline has also been detected.

The abundance of magnetite is related to that of biotite and may locally attain 10 %. The amount of magnetite is much higher in the biotite schist than in the amphibole-chlorite schists, suggesting that in biotite schist it is at least in part a product of the hydrothermal alteration processes.

Comparable examples of ultramafic and maf-

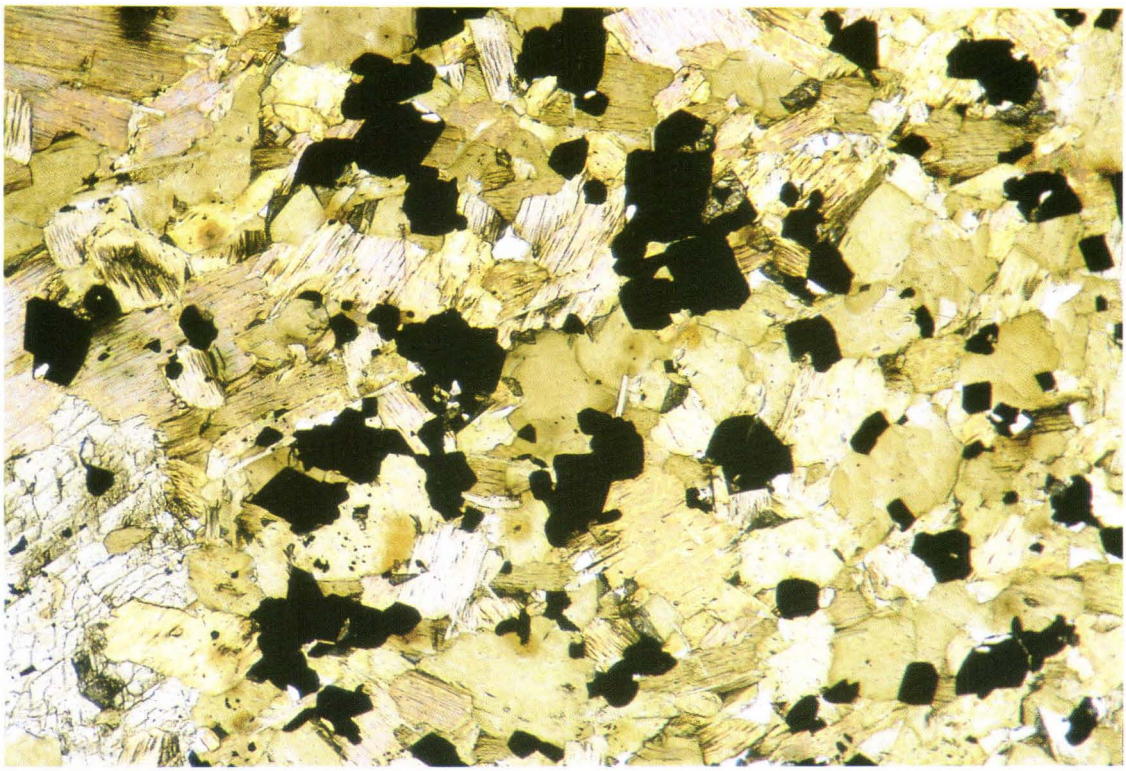

Fig. 9. Biotite-magnetite schist with some amphibole (light green; lower left corner). Biotite is in brown and magnetite in black. Drill core 506/28.40 m. Field of view is 2 mm in width.

ic volcanites containing magnetite have been described from the Hunt Mine, at Kambalda, Western Australia, where a marked increase in the abundance of magnetite is associated with the concomitant disappearance of amphibole and appearance of chlorite. These features suggest that magnetite and chlorite have been produced by carbonation/hydration reactions consuming amphibole (Neall & Phillips, 1987). Another, and more probable alternative is that at least some of the magnetite at Pahtavaara formed as a result of serpentinization of olivine and/or glass, the serpentine having later altered to chlorite (cf. Korkiakoski, 1985).

The distribution of biotite is closely related to that of chlorite, which has evidently been replaced by the former. Often these two minerals are crystallographically contiguous and display parallel extinction. In some alteration types biotite as well as chlorite may occur nearly monomineralally. This is particularly the case where talc-carbonate ± pyrite veins are common. In general, the amount of biotite is at its highest adjacent to the these veins and diminishes further away from them (Fig. 10). This suggests that alteration of chlorite to biotite is broadly synchronous and closely related to the formation of these veins. In places, magnetite is observed at the contact zone between such veins and the biotite-rich host rocks.

The occurrence of talc and carbonate, which together with serpentine are the most typical alteration product of ultramafic rocks (see Eckstrand, 1975), is not however, entirely restricted

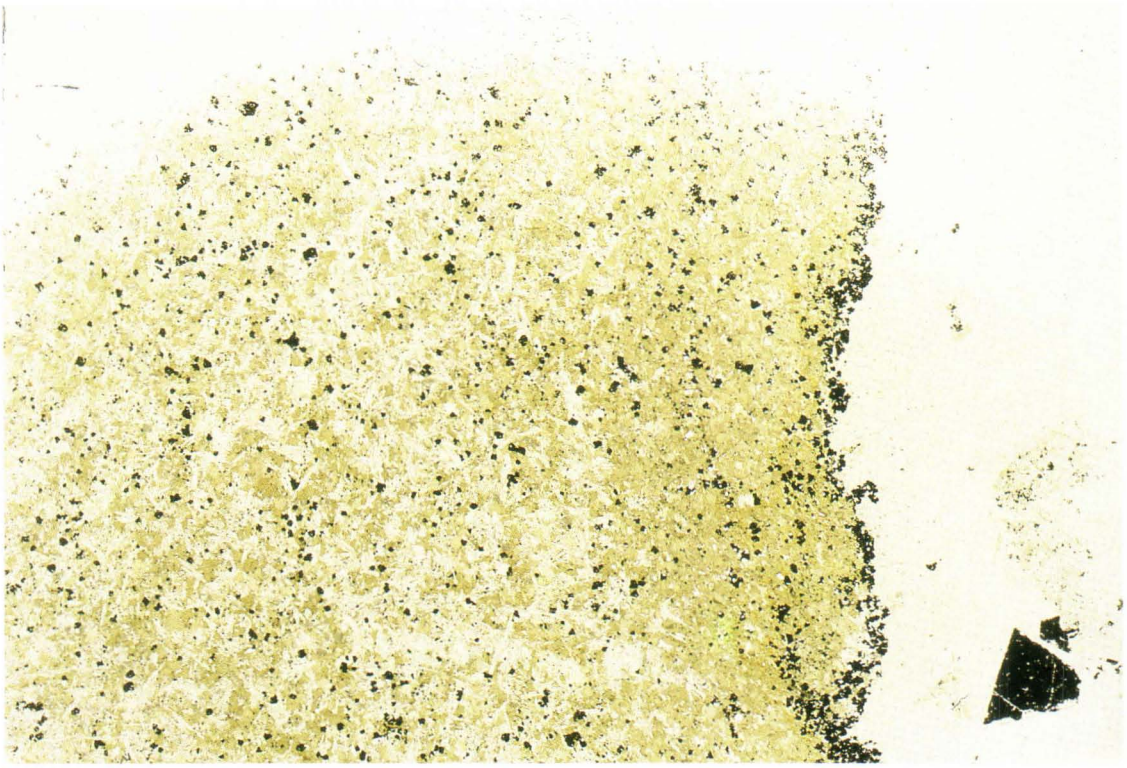

Fig. 10. Biotite schist with associated talc-carbonate vein (light). Note abundant magnetite (black) at the contact, and transition from biotite-rich rock (brown) at right to the amphibole-chlorite-rich assemblage at left. Large euhedral pyrite crystals also occur in the vein (lower right corner). Drill core 255/12.00 m. Field of view is 2.6 cm in width.

to the talc-carbonate veins. These minerals are also present in the biotite- and chlorite-dominated units where they occur as evenly distributed disseminations.

Biotite schists seem to grade transitionally into both amphibole-chlorite schists and also the coarse-grained amphibole rocks. This is indicated by the local occurrence of biotite in the other rock types.

Amphibole rock

In contrast to all the other rock types in the study area, amphibole rock is typically coarse-grained and non-schistose and is locally associated with heterogeneous patches and veins of quartz and barite (Fig. 4A). Being relative hard, it is better exposed than biotite schist and can form outcrops several meters in diameter. It is mineralogically more homogeneous than the other rock types in the area, consisting dominantly of amphibole which may form up to several cm long radiating sheafs or rosettes (Figs. 11 and 35). Accessory minerals include carbonate, talc, albite and locally abundant quartz and barite (Fig. 12). Magnetite, which is in many places completely absent, may elsewhere form discontinuous veinlets along the schistosity and across some large amphibole crystals. Sulphides are represented by pyrite and minor chalcopyrite which are often associated with the quartz ± barite veins and pods. Some albite-rich veins also occur locally.

A type transitional between the fine-grained amphibole-chlorite schist and coarse-grained amphibole rock consists of large crystals of colour-

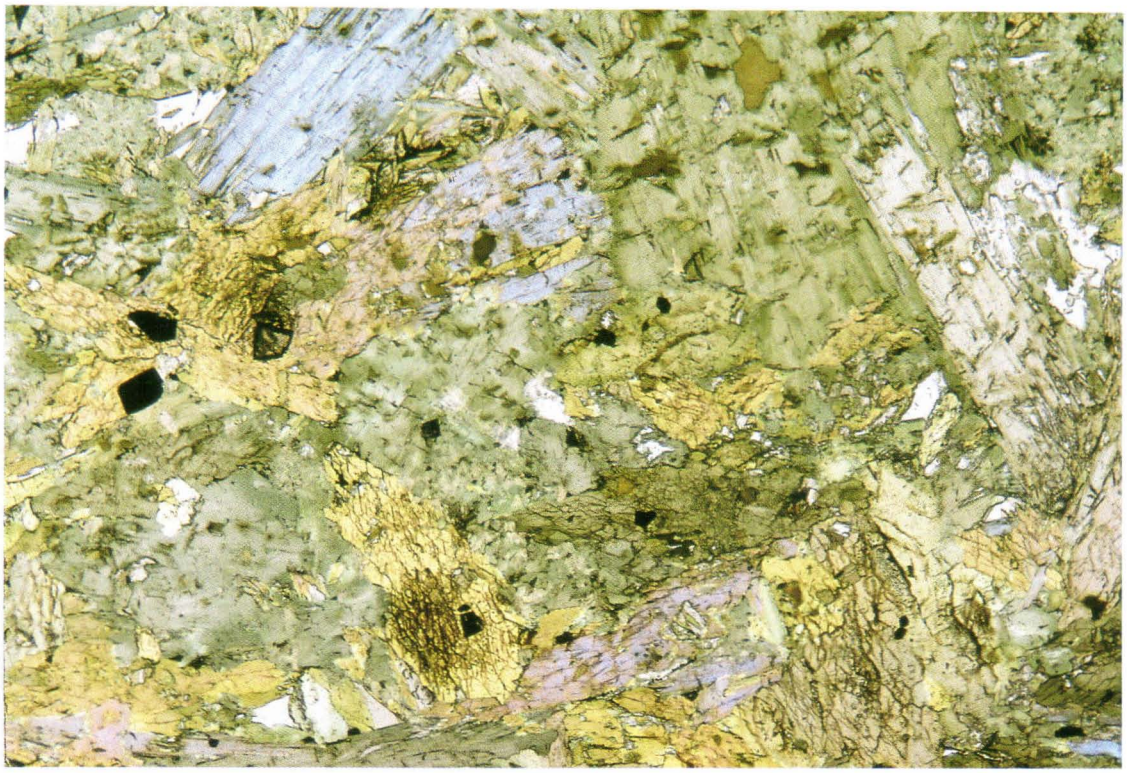

Fig. 11. Coarse-grained amphibole rock with radiating amphibole (mainly green). Some biotite (upper centre, brown) occurs as inclusions in amphibole. Minor albite, carbonate and magnetite are also present. Drill core 512/13.70 m. Field of view is 5 mm in width.

less or light green amphibole porphyroblasts occurring in a fine-grained talc-carbonate ± chlorite matrix (Figs. 13 and 14). Hereafter this type is termed **'amphibole porphyroblastic talc-carbonate schist'.**

Two different types of coarse-grained amphibole rocks, which are however compositionally gradational into one another, can be distinguished: (1) dark amphibole rock and (2) light amphibole rock representing high-alumina and low-alumina types, respectively (see discussion below). The latter type is generally sulphide-bearing and typically associated with the talc — carbonate — amphibole veins as well as being gradational into them.

In spite of local folding of the amphibole rock there are several pieces of textural evidence indicating that amphibole growth resulting in the formation of the amphibole rock took place late in the metamorphic and hydrothermal history and therefore postdates the generation of biotite schist and talc-carbonate veining. These include the clearly cross-cutting nature of the amphibole rock relative to the other rock types, and the lack of regional NE — trending schistosity (Figs. 2, 3 and 4). At a smaller scale this is shown by the obvious textural overgrowth of coarse-grained amphibole crystals into the surrounding biotite schist (Figs. 5B and 6B).

Additional evidence for the relatively young age of the amphibole rock is given by the local occurrence of biotite as remnant-like inclusions

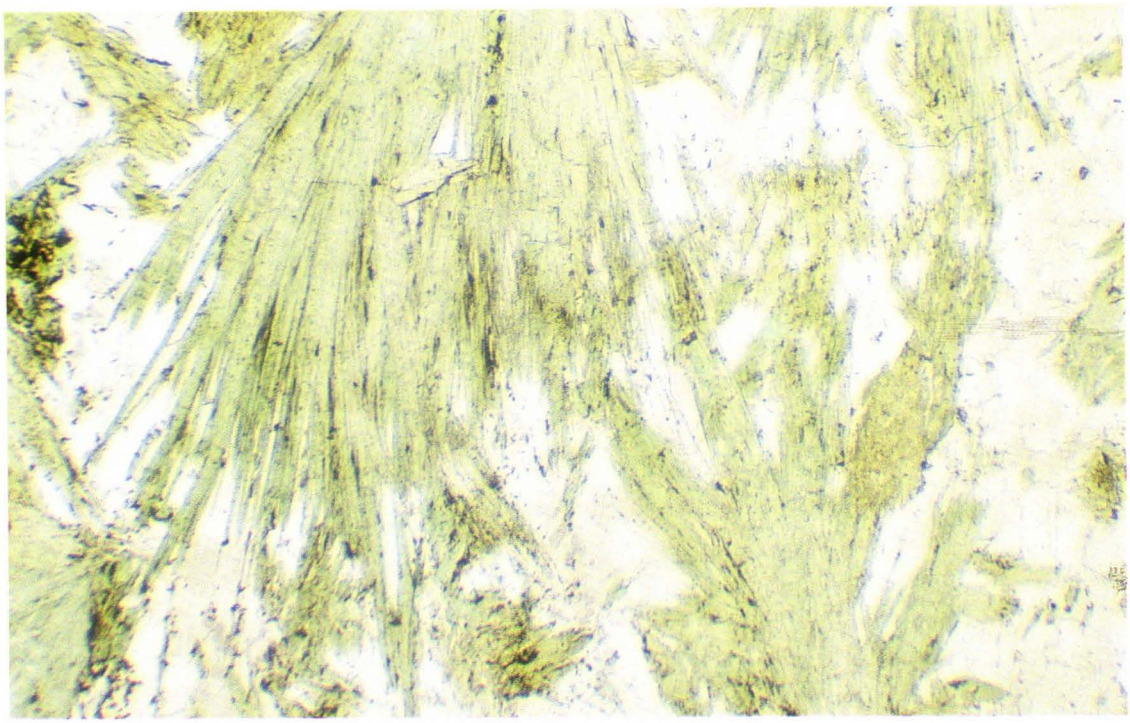

Fig. 12. Coarse-grained radiating amphibole rock (amphibole in green) with abundant carbonate and quartz with minor albite (light grey). Drill core 239/8.10 m. Field of view is 2.0 cm in width. Photographed by S. Gehör.

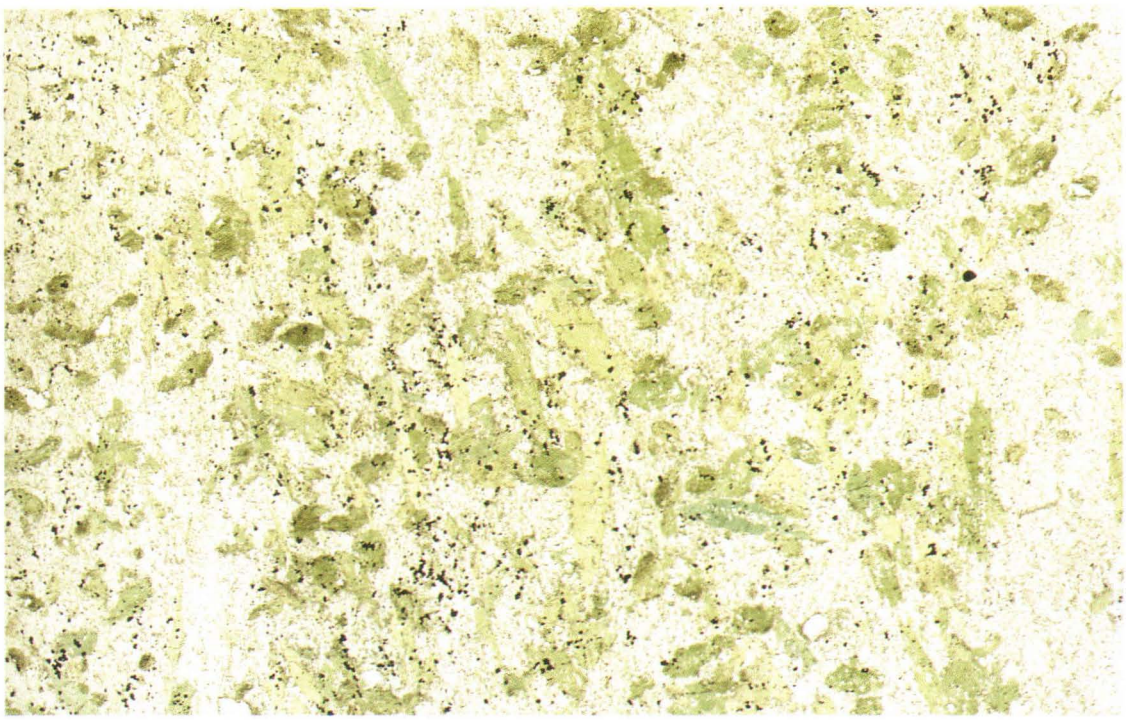

Fig. 13. Amphibole porphyroblastic (green) talc-carbonate schist representing a transitional type between coarse-grained amphibole rock and fine-grained amphibole-chlorite schist. Some magnetite (black) is also present. Drill core 256/33.55 m. Field of view is 2.5 cm in width.

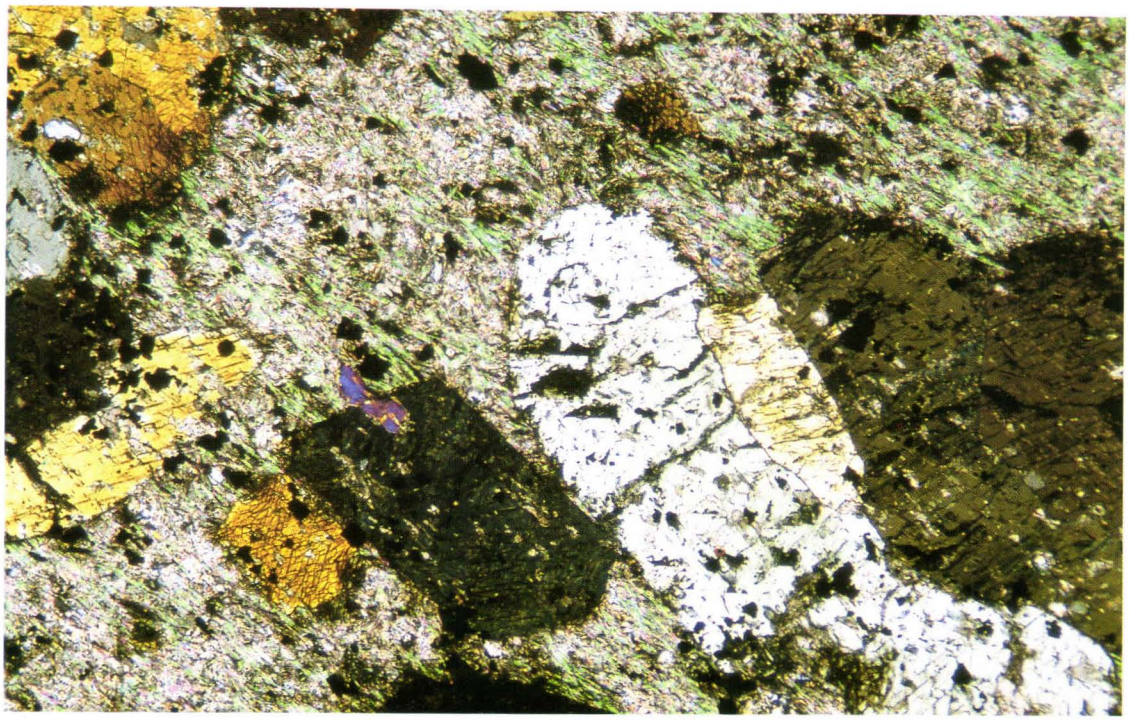

Fig. 14. Amphibole porphyroblastic talc-carbonate-chlorite schist. Large amphibole crystals shown in variable colours, fine-grained talc in green and carbonate-chlorite in grey. Some magnetite (black) also occurs. Drill core 508/128.90 m. Field of view is 5 mm in width.

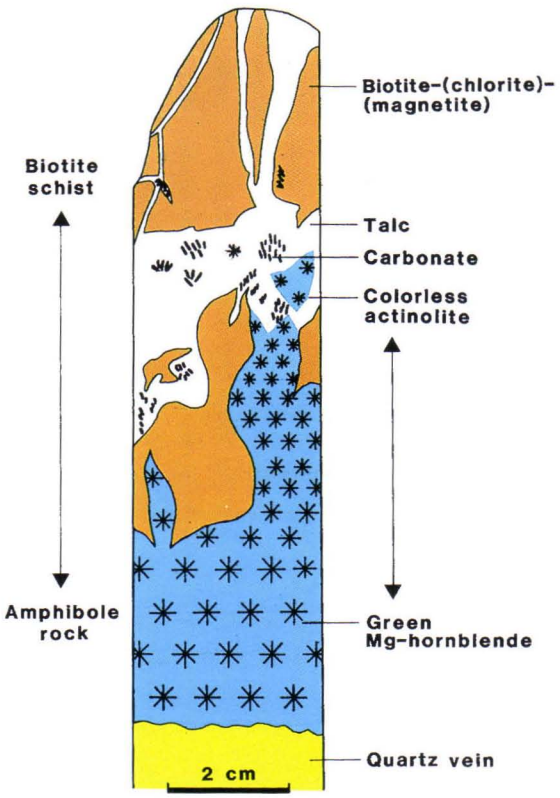

Fig. 15. Schematic description of gradational change between schistose biotite — chlorite — magnetite schist containing talc-carbonate veins, and non-schistose coarse-grained amphibole rock related to quartz vein. Amphiboles associated closely with talc-carbonate vein are colourless and actinolitic, whereas amphiboles associated with quartz are green and Mg-hornblende in composition. Note that amphiboles follow the talc-carbonate vein. Drill core 253/6.70 m. For more details, see Figure 27.

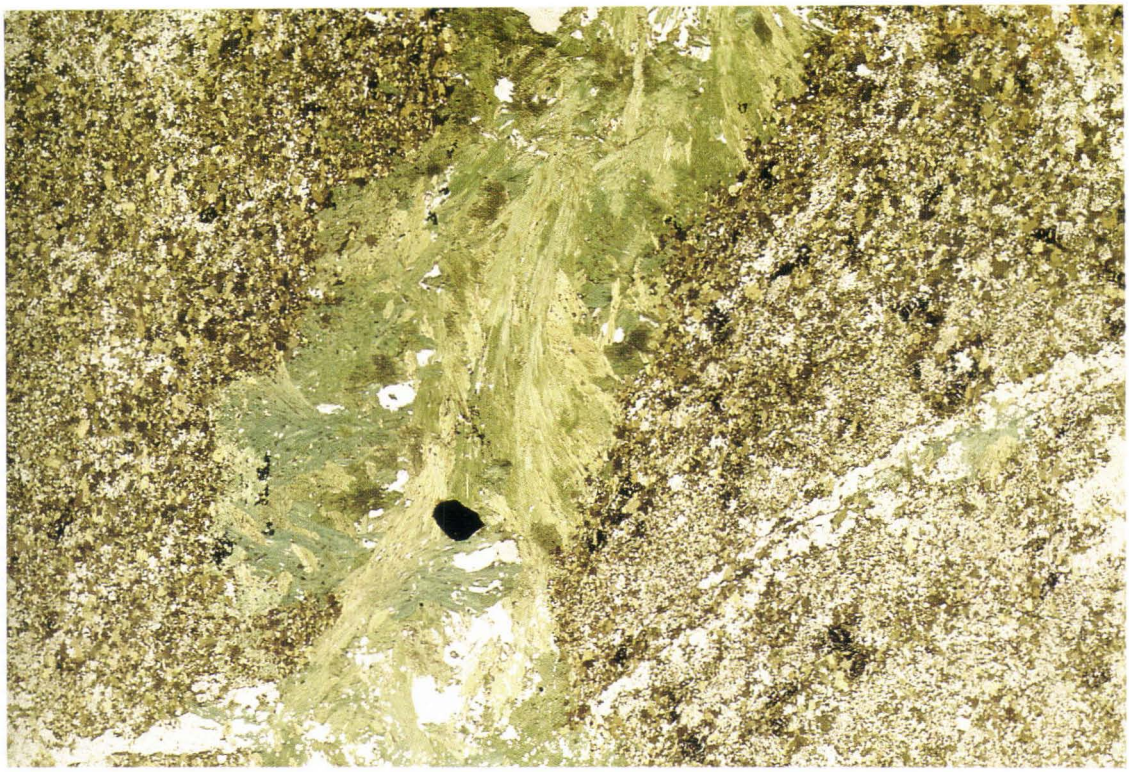

Fig. 16. Biotite-quartz-talc schist (brown) with coarse-grained amphibole-quartz vein (green/white). Amphibole has replaced the former talc-carbonate vein. Drill core 506/98.20 m. Field of view is 2.5 cm in width.

in amphibole rock (Fig. 11). Furthermore, there are also examples where a clear textural and mineralogical gradation occurs between non-schistose coarse-grained amphibole rock and foliated biotite schist, as schematically presented in Figure 15. Close to the quartz vein the rock consists totally of amphibole which appears to preferentially follow the talc-carbonate veins towards the biotite schist. This is associated with the change in the composition of amphibole discussed in more detail below and illustrated in Figure 27. Furthermore, amphibole may also occur as vein-like features in biotite schist (Fig. 16), probably indicating the total replacement of talc-carbonate veins by amphibole.

Veins

The veins in the study area can be divided into two main groups representing end members of more heterogeneous groups. These are (1) talc-carbonate ± pyrite veins and (2) quartz ± barite veins and irregular pods. Visible gold occurs locally in the latter type. A continuum exists between these end members, and in addition, amphiboles occur in variable amounts in all veins. In places, amphibole may be the dominant vein mineral, almost totally replacing its talc-carbonate precursor (Figs. 5C, 15 and 16). A similar occurrence of vein amphibole (actinolite) has also been reported from the Macassa gold mine in Ontario (Kerrich & Watson, 1984).

The veins of the first group characterize the whole study area. They occur most abundantly in biotite schist but are also typical as minor constituents in the amphibole-chlorite schist and amphibole rock.

The second group, namely quartz ± barite veins, is dominantly associated with the light-coloured coarse-grained amphibole rock and is in fact gradational into it. Although quartz veins are very common in a number of gold mines they are relatively rare at Pahtavaara and generally occur, along with minor barite, as small patches and lenses. Nevertheless, in places such veins attain 0.5 m in width (Fig. 4A). Barite, which is the most common of the alkaline earth sulphates in hydrothermal systems (Barnes, 1979), has been documented from many other gold deposits as well, including gold-bearing quartz-carbonate veins in the Lake Shore and Macassa Mines at Kirkland Lake, Ontario (Cameron & Hattori, 1987).

On the whole, talc-carbonate-amphibole ratios in the veins vary considerably. There also appears to be a gradational mineralogical change from amphibole-bearing veins to light-coloured coarse-grained amphibole rock, as described in the previous chapter.

Ore mineralogy

Ore minerals of the Pahtavaara gold deposit consist of various oxides and sulphides, the most common of these being magnetite and pyrite.

Magnetite is distributed heterogeneously throughout the different rock types. It is most abundant in the biotite schists and may locally comprise more than 10 % of the rock. Magnetite occurs as euhedral to subhedral grains up to 2 mm in diameter and tends to concentrate towards contact zones with talc-carbonate veins. Inclusions in magnetite consist of droplet-like pyrrhotite, chalcopyrite and pentlandite. On the other hand, magnetite can occur as inclusions in pyrite. Some gold is also associated with magnetite.

The amount of magnetite in amphibole-chlorite schists is relative small (<2 %) but on the basis of its even distribution, it is very probable that magnetite formed from Fe released during the serpentinization of olivine/glass (olivine → serpentine + magnetite; cf. Eckstrand, 1975). As alteration progressed further, serpentine was evidently replaced by chlorite; no serpentine has been observed within the Pahtavaara alteration zone but it occurs frequently in other parts of the Sattasvaara komatiites (Saverikko, 1985). The above reaction is typical in many comparable komatiites such as at Kambalda, Western Australia, where the regular distribution of magnetite around primary olivine crystals (now totally altered to chlorite) still reveals the original spinifex textures (Korkiakoski, 1985). Therefore, the abundance of magnetite in the biotite schist and the presence of sulphide inclusions indicate that some Fe was mobile during hydrothermal alteration. Furthermore, the virtual absence of magnetite from some amphibole rocks indicates the complexity of the deposition of magnetite and Fe-mobility.

Other oxide minerals are present only in small amounts in the mineralized area, and include chromite, ilmenite, haematite and rutile. Chromite is typically zonal, with the cores being more Cr-rich than the margins and is rimmed by magnetite. Ilmenite has been partly or in some instances entirely altered to rutile. Haematite occurs as inclusions in ilmenite or, alternatively, as a secondary alteration product of magnetite (martite).

Pyrite is heterogeneously distributed and is everywhere the dominant sulphide. The overall proportion is variable but relatively low, typically comprising less than 1 % of the rock in both amphibole rocks and in biotite schists. In the latter rock type it is typically associated with talc-carbonate veins, whereas in amphibole rock it occurs as disseminations or patches up to 1—2 cm in diameter. However, it is most characteristic of contact zones with other rock types where it may be accompanied by visible gold. In places, excep-

tionally large amounts of pyrite (up to several percent) seem to be related to some magnetite-rich parts in biotite schist. This is shown for example in Figure 5B, where pyrite is mainly restricted to areas where coarse amphibole crystals cut across the pre-existing magnetite-rich biotite schist and talc-carbonate veins. Pyrite also forms irregular aggregates in amphibole rock (Fig. 6B), although it usually occurs as randomly distributed disseminations.

Other sulphides at Pahtavaara include pyrrhotite, chalcopyrite, pentlandite and violarite, all of which typically occur as inclusions in pyrite. In addition, millerite occurs intergrown with pentlandite which is locally altered to violarite. Pentlandite may form flame-like exolution lamellae in pyrrhotite. Chalcopyrite also occurs as free crystals, sometimes having cubanite lamellae. Rarer ore minerals that have been detected include clausthalite (PbSe), merenskyite (PdBiTe) and some other Bi-Se-Te minerals (Kojonen & Johanson, 1989).

The distribution and nature of gold is discussed in more detail in a separate section, but in general seems to differ between each of the different rock types. In biotite schists it is fine-grained and associated with magnetite and the pyrite-rich parts of talc-carbonate veins. Microscopically gold in these veins has been observed on only one occasion, where it may in fact represent an inclusion in a vein-related pyrite grain (Fig. 34). Gold in amphibole rock is coarse and typically found at contact zones against quartz ± barite veins, where it occurs in the native state, occasionally forming aggregates up to nearly 1 cm in length (Fig. 35). In places gold occupies the interstices between several cm long amphibole laths or rosettes. Gold can also be associated with magnetite, which may represent remnants of former biotite schist.

WHOLE-ROCK GEOCHEMISTRY

Introduction

In the following, the geochemical characteristics of the three dominant rock types supplemented by the compositional data from different veins are presented with respect to major and selected trace elements plus CO_2. Ba is also included in the major elements due to its integral part in the alteration process and locally high abundances (up to 2.6 wt. %; Tables 1 and 2; Figs. 17 — 24; App. 1). To exclude the effects of carbonation and hydration, and to facilitate comparison between variably altered samples, the major element data for all analyses were recalculated to 100 % on a volatile-free basis. Gold content and its relationship to other element abundances together with chondrite-normalized rare earth element contents are also described in separate sections.

Geochemical distinction between different alteration types is sometimes difficult since more than one type may be present in a single sample and, consequently, the chemical analysis of the bulk rock often reflects the mixing of several alteration types. In order to solve this problem, and to obtain good mineralogical and compositional control for different samples, special attention was given to sample selection and detailed microscopical examination.

The use of element ratios in characterizing elemental mobility or immobility in alteration studies has been successfully applied in a number of investigations (e.g. Beswick, 1982; Campbell et al., 1984; Finlow-Bates & Stumpfl, 1981; Floyd & Winchester, 1978). Of significance to this study is the fact that element ratios can be

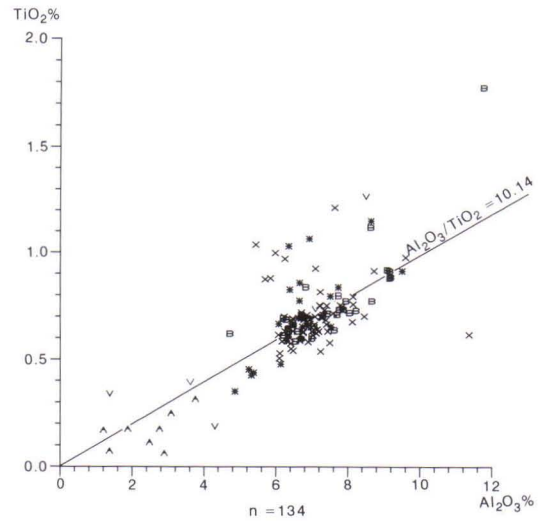

Fig. 17. Al_2O_3 vs.TiO2 diagram of variably hydrothermally altered rocks from Pahtavaara. Ratio 10.14 represents the average value for the four least altered samples (Table 1; anal 1). Rock symbols (cf. Appendix 1): ● = amphibole-chlorite schist (4 least altered samples), X = weakly altered rock types including some amphibole growth and/or talc-carbonate alteration, B = biotite schist, * = high-alumina amphibole rock (>4 wt. %), A = low-alumina amphibole rock (<4 wt. %), V = vein (carbonate or quartz-rich).

used to determine the protolith compositions in hydrothermally altered zones (Vance and Condie, 1987). Relatively constant ratios between the immobile elements Al and Ti plus, to a lesser extent, Cr suggest a common, komatiitic origin for all samples in the present study area irrespective of their degree of alteration (Fig. 17). Additional evidence for this is given by the evident geochemical and mineralogical gradation between the pervasively altered and the least altered samples, which show the characteristic geochemical features of komatiites (Figs. 20 — 23). This is also supported by the local occurrence of less altered blocks within the Pahtavaara alteration zone and the occurrence of differently altered rock types as an irregular and heterogeneous mixture.

In estimating the degree of alteration, the four least altered samples collected outside the intensively altered area were used as reference material against which the composition of altered samples were compared. They were selected on the basis of their low CO_2, high MgO and, in particular, low Ba and K_2O contents (Table 1; anal. 1). The last two elements were found to be the most useful and sensitive indicators of hydrothermal alteration at Pahtavaara since the abundances of these elements are negligible in unaltered komatiites but increase markedly at even low degrees of alteration.

Certain trace elements have also played an important part in hydrothermal alteration and mineralization processes, such as Co, Cu, Sr, Te, V, Zn, and W. Of these, increased Cu contents were some of the first indicators of mineralization, with Cu contents up to 3.2 % having been detected during the early stages of research (Pulkkinen et al., 1986).

In contrast to a number of gold deposits, Pahtavaara is characterized by relatively low overall S contents (generally <0.2 %). Comparably low values have also been reported from the Macassa gold mine in Kirkland Lake, Ontario (Kerrich & Watson, 1984), and the Kolar gold deposits in India (Hamilton & Hodgson, 1986). Although values up to 1.6 % were determined from Pahtavaara, the total S content may locally be somewhat higher, since not all of the sulphur associated with barite was dissolved during analysis.

Major elements

General

Compositional variations of selected major and trace elements plus gold for variously altered rock types from drill core intersections through the hydrothermally altered zone at Pahtavaara are given in Figures 18 and 19, and Appendix 1. Spatial variations correspond to mineralogical

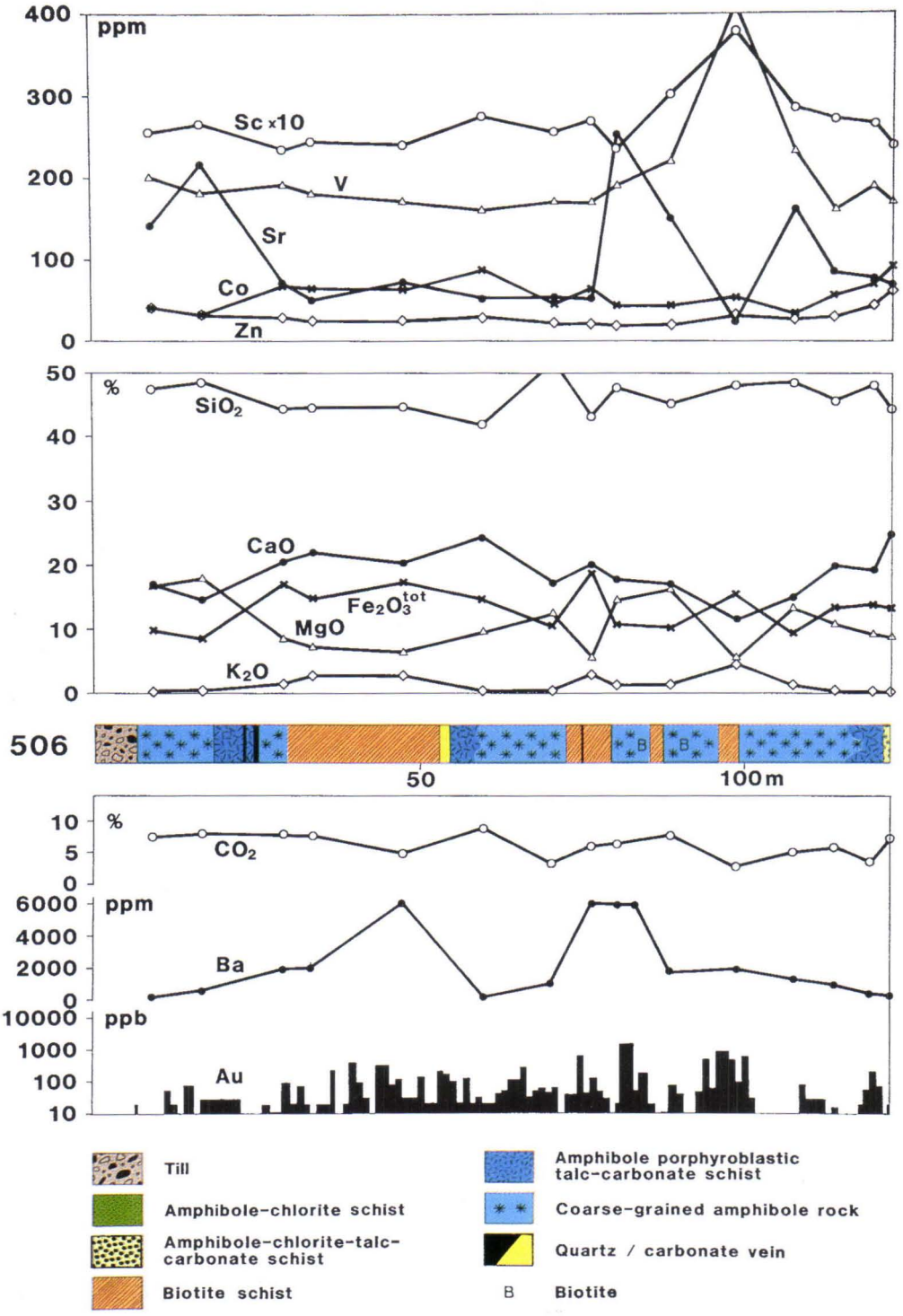

Fig. 18. Geochemistry and lithology of drill core 506 at Pahtavaara with respect to major and selected trace elements. Major element compositions recalculated to 100 %, on a volatile-free basis. For location of drill core, see Figure 3A.

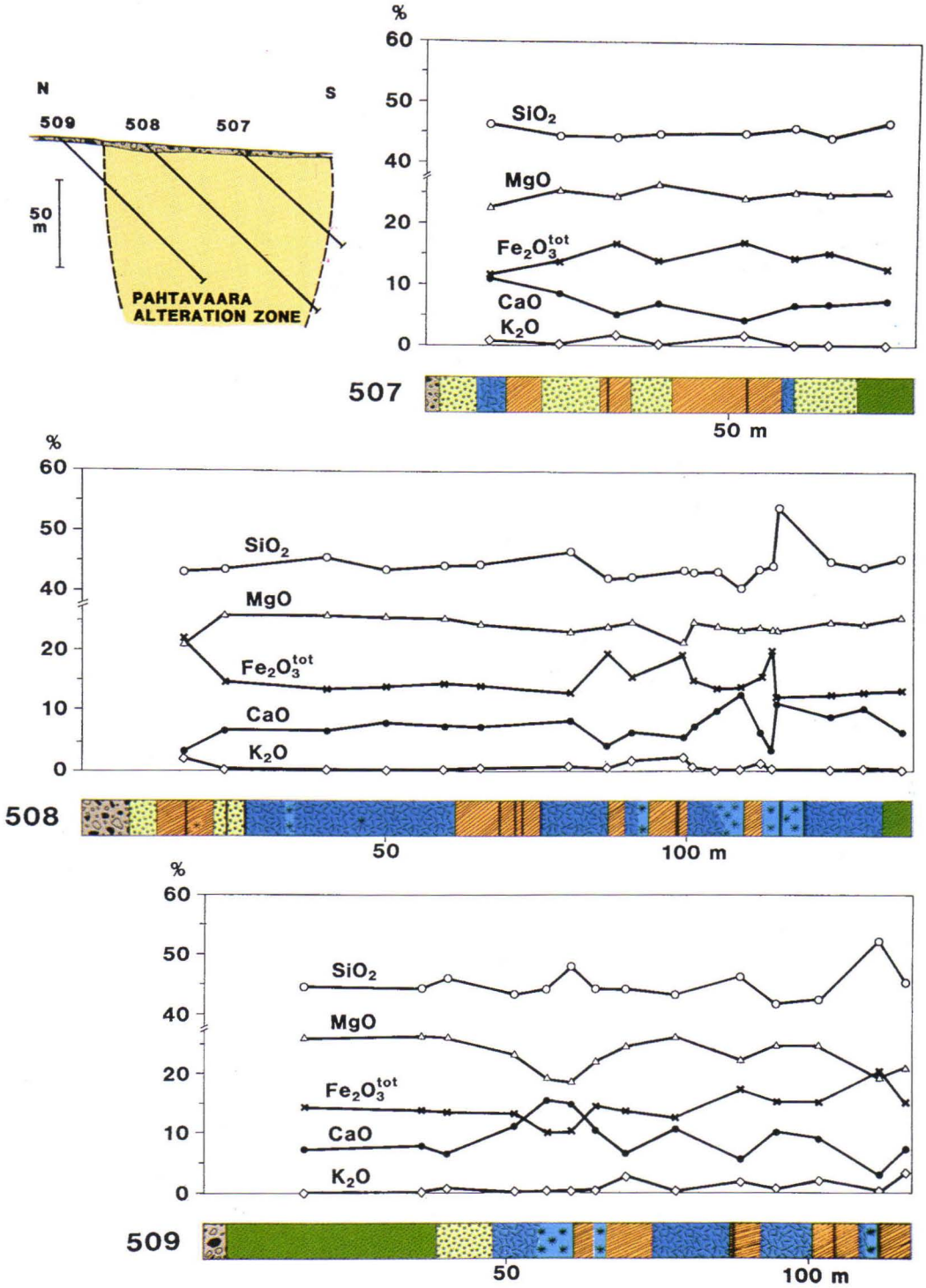

Fig. 19. Major and selected trace element geochemistry across the Pahtavaara alteration zone along drill cores 507-508-509. Vein thicknesses have been exaggerated. For locations, see Figure 3. Lithological symbols as in Figure 18.
Fig. 19 A; Major elements.

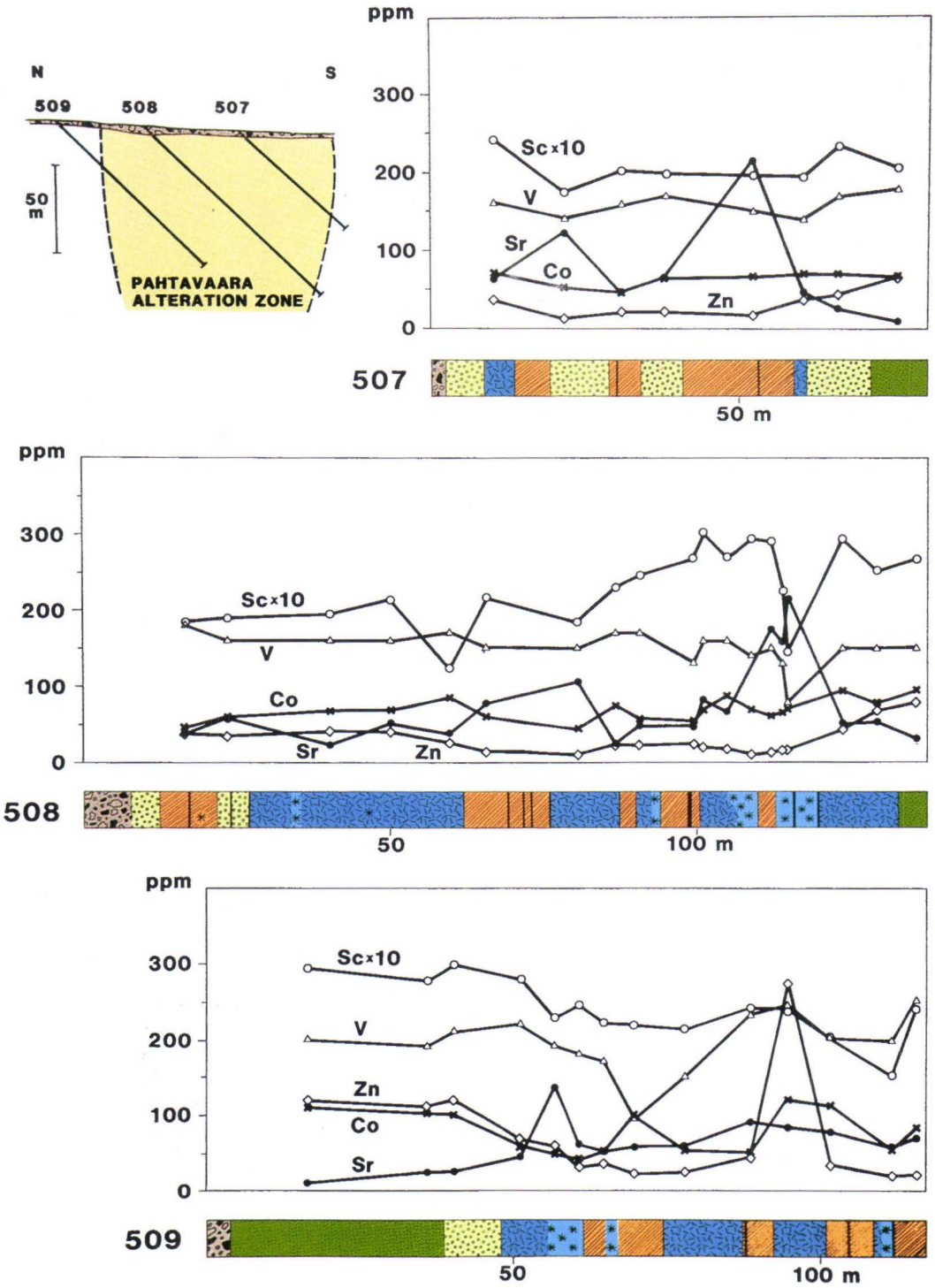

Fig. 19 B; Selected trace elements.

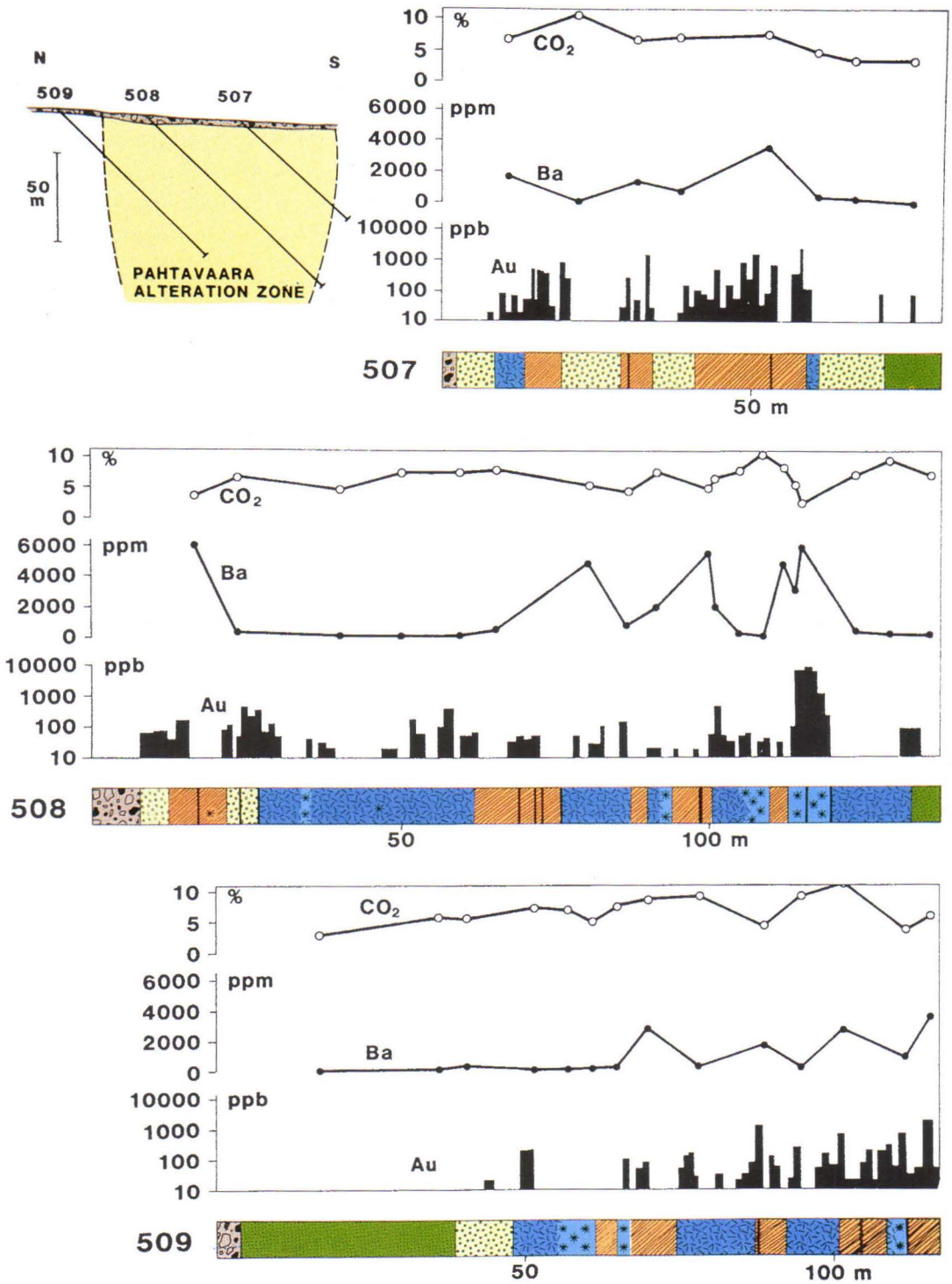

Fig. 19 C; Au, Ba and CO_2.

Table 1. Composition of weakly altered komatiites from Pahtavaara and selected comparable regions.

	1	2	3	4	5	6
(n)	(4)	(4)	(12)	(18)		(4)
SiO_2 (%)	45.87	46.28	45.2	47.28	46.05	50.30
TiO_2	0.65	0.62	0.6	0.34	0.32	0.49
Al_2O_3	6.59	5.77	7.2	7.80	7.41	7.21
$Fe_2O_3^{tot}$	13.31	11.11	12.5	12.68	11.51	10.79
MnO	0.20	0.24	0.2	0.20	0.22	0.20
MgO	25.44	27.98	26.3	23.69	26.53	21.65
CaO	7.67	7.88	7.5	7.72	7.41	8.82
Na_2O	0.18	0.06	0.0	0.15	0.45	0.41
K_2O	0.04	0.05	0.0	0.06	0.10	0.06
P_2O_5	0.05	0.00	0.0	0.08	0.00	0.05
Total	100.00	100.00	100.00	100.00	100.00	100.00
Au (ppb)	2	n.d.	n.d.	n.d.	n.d.	n.d.
S (%)	0.01	n.d.	n.d.	0.39	n.d.	n.d.
CO_2	1.34	n.d.	n.d.	0.65	n.d.	n.d.
LOI	6.79	n.d.	n.d.	6.56	n.d.	5.5
Ba (ppm)	63	n.d.	37.5	n.d.	n.d.	n.d.
Cr	2353	n.d.	2664	n.d.	n.d.	n.d.
Al/Ti	10.14	9.03	12.0	22.94	23.16	18.03

1= Average of the least altered amphibole-chlorite schist samples, Pahtavaara gold deposit (reference composition).
2= Average of the pyroclastic amphibole-chlorite schists, Sattasvaara area (Mikkola, 1941; Papunen et al., 1977).
3= Average of the pillowed and pyroclastic komatiites from Sattasvaara (Lehtonen et al., 1989).
4= Average of the samples from the flow top of the Lunnon metapicrite, Kambalda, Western Australia (Gresham & Loftus-Hills, 1981).
5= Average of peridotitic komatiites with MgO <30%, Munro Township, Canada (Arndt et al., 1977).
6= Average of Geluk-type basaltic komatiites, Komati Formation, South Africa (Viljoen & Viljoen, 1969).

All results recalculated to 100 wt. %, volatile-free. Al/Ti ratio in oxide.

changes in the rocks but, as stated above, compositions are transitional into one another and may in some cases represent a mixture of different alteration types.

The major elements Ca, Fe, Mg and Si show the greatest proportional variation in abundances since they have behaved in a mobile manner during hydrothermal alteration. They illustrate the dominant trends in whole rock composition and also best describe the compositional fields of different rock types and gradation between them, as portrayed in Figures 20—23.

Amphibole-chlorite schist

The recalculated volatile-free compositions of amphibole-chlorite schists are relatively homogeneous in spite of variations in degree of hydration and talc-carbonate alteration. The least altered types are characterized by high MgO (ca. 24 — 26 wt. %), low CO_2, alkalis (K_2O, Na_2O) and Ba (Table 1; anal. 1; App. 1). Besides these, amphibole-chlorite schists have other features typical of komatiites according to the definition of Arndt and Nisbet (1982). These include high Cr (>2000 ppm) and Ni (>1000 ppm) contents and low TiO_2 and alkali contents (<1 wt. %). Accordingly, the least altered amphibole-chlorite schists clearly correspond compositionally to komatiitic rocks and, as shown by the most commonly used discrimination diagrams (Fig. 20), are comparable to komatiites from other regions.

According to the Jensen cation plot, amphibole-chlorite schists are compositionally equivalent to ultramafic komatiites, or Geluk-type (basaltic) komatiites as defined by Viljoen and Viljoen (1969) and Viljoen et al. (1982). The komatiitic nature of these rocks was recognized earlier by Räsänen (1983) and Saverikko (1983; 1985).

In the original definition of komatiites Viljoen and Viljoen (1969) strongly emphasized the high CaO/Al_2O_3 ratio of about 1.5 although it has

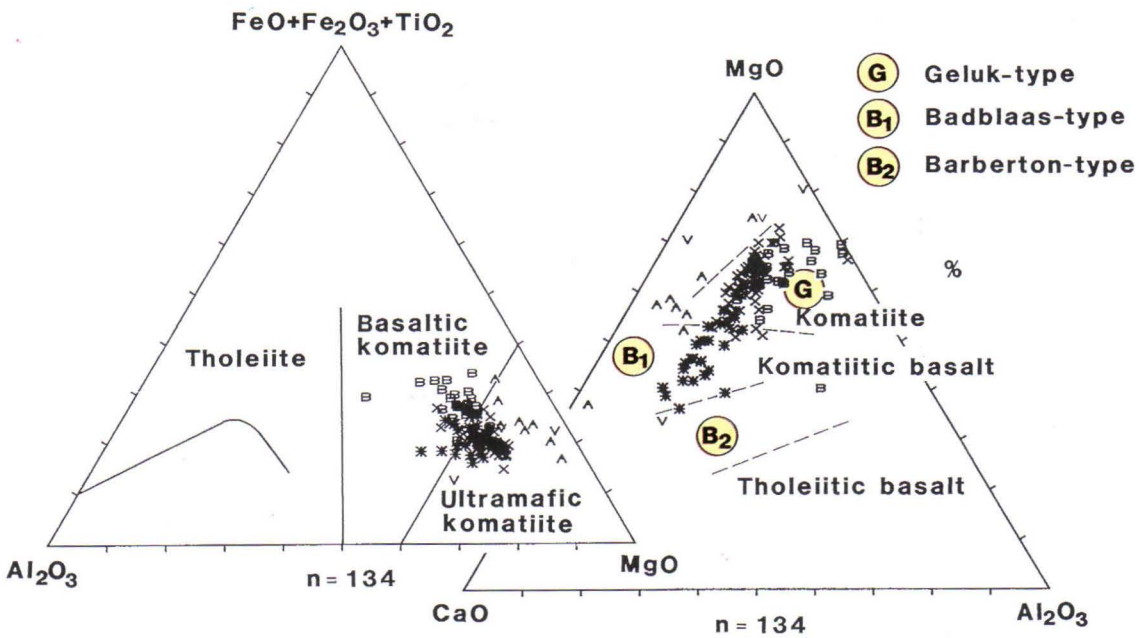

Fig. 20. Chemical compositions of variably altered komatiitic rocks from Pahtavaara gold deposit presented on Jensen cation plot and CaO-MgO-Al_2O_3 diagram. Compositional fields as defined by Jensen (1976), Viljoen and Viljoen (1969), and Viljoen et al. (1982). For rock symbols, see Figure 17.

subsequently been pointed out by several authors that for most komatiites this value is lower (e.g. Arndt et al., 1977; Gresham & Loftus-Hills, 1981). The high ratio can be explained by the mobile nature of Ca in hydrothermal systems, as shown by Lesher (1983), further suggesting that these komatiites were hydrothermally altered at an early stage, at least with respect to Ca contents.

Nesbitt et al. (1979) classified komatiites into Al-depleted and Al-undepleted types. The former have high CaO/Al_2O_3 (about 1.5) and low Al_2O_3/TiO_2 ratios (about 11), whereas the latter are typified by ratios close to unity and ca. 20 (chondritic), respectively. On the basis of the Al_2O_3/TiO_2 ratio, the amphibole-chlorite rocks at Pahtavaara are similar to the other Sattasvaara komatiites, which are considered to be Al-depleted komatiites by Räsänen et al. (1989) and Lehtonen and Rastas (1988). This conclusion is also supported by rare earth element (REE) data showing depletion relative to both light and heavy REE. However, the CaO/Al_2O_3 ratio is close to unity for the weakly altered Pahtavaara komatiites, and thus more consistent with the Al-undepleted type. Furthermore, it appears that the Pahtavaara komatiites are more TiO_2-rich than other Al-depleted komatiites, the Al_2O_3 content being comparable to that for Al-undepleted komatiites. Hence, the low Al_2O_3/TiO_2 ratio at Pahtavaara may rather be related to enrichment of Ti, and not to the depletion of Al.

Biotite schist

Biotite schists as represented in Figures 18 — 23 and Table 2 are typified by higher Fe, K and Ba contents and lower Si, Mg and Ca contents compared to the amphibole-chlorite schist. $Fe_2O_3^{tot}$ is generally between 18 — 22 wt. % but values up to about 25 wt. % have been recorded. Mineralogically the maximum iron values are associated with increased amounts of magnetite plus pyrite. K_2O and, to a lesser extent, Ba are related to biotite. However, as barite is also present, Ba values are highly variable, ranging between 0.14 and 1.2 wt. % (average 0.42 %). K_2O contents vary between ca. 1 and 4.7 wt. % (average 2.6 %) being therefore markedly higher than in unaltered komatiites (i.e. <0.1 %). Al_2O_3 and TiO_2 contents are a little higher than in amphibole-chlorite schists but the elemental ratio is the same (Fig. 17). Chromium contents are also high (typically >2000 ppm of Cr) reflecting the ultramafic parentage of the biotite schist.

SiO_2 content vary between 39 and 48 wt. % clustering typically between 42 — 45 wt. % and are inversely proportional to the CO_2 abundance; accordingly, the lowest SiO_2 contents are related to the most carbonated samples. Typical MgO contents are between 20 and 22 wt. % which is ca. 4 to 5 % lower than in the least altered type. Samples with MgO <20 wt. % are either exceptionally Fe-rich (e.g. anal. 46; App. 1) or Si-rich due to the presence of quartz (anal. 65; App. 1). CaO contents are highly variable, being between about nil and 9 wt. %, which is clearly a function of the degree of carbonation, samples having the lowest CO_2 contents being almost devoid of CaO. Na_2O values are typically very low (<0.1 wt. %) but as some of biotite schists are albite-bearing contents may attain 0.8 wt. %. MnO contents are between 0.24 and 0.6 wt. %, being slightly higher than in both the weakly altered amphibole-chlorite schists (0.16 — 0.21 wt. %) and amphibole rocks (0.23 — 0.4 wt. %).

The biotite schists represent a compositionally variable but distinctive rock type in the study area. In terms of dominant major elements it differs form other lithologies at Pahtavaara in its high $Fe_2O_3^{tot}$ and low CaO contents, and high abundances of immobile Al and Ti. On the Jensen cation plot, biotite schists occur in the basaltic komatiite field and on the $MgO\text{-}CaO\text{-}Al_2O_3$ diagram, in the field of Geluk-type komatiites (Fig. 20). However, as a CaO-poor rock it differs from the weakly altered type by being closer to the $MgO\text{-}Al_2O_3$ line. Compositional gradations into other rock types is also evident as displayed in Figures 21 — 23.

Table 2. Composition of hydrothermally altered rocks from Pahtavaara and selected comparable regions.

	1	2	3	4	5	6	7	8
(n)	(31)	(13)	(21)	(15)	(7)	(6)	(1)	(1)
SiO_2 (%)	44.45	42.49	45.22	50.03	55.02	52.91	49.40	48.47
TiO_2	0.71	0.75	0.67	0.66	0.17	0.57	0.25	0.25
Al_2O_3	7.12	7.55	6.94	6.51	2.61	5.49	6.19	7.04
$Fe_2O_3^{tot}$	14.82	18.29	13.82	11.53	13.38	10.99	11.72	11.53
MnO	0.30	0.45	0.27	0.32	0.49	0.22	0.23	0.58
MgO	24.23	21.79	23.75	17.63	17.99	15.45	21.43	11.43
CaO	7.68	5.74	8.48	12.06	9.79	13.00	10.69	18.58
Na_2O	0.40	0.09	0.47	0.82	0.37	1.23	0.00	0.00
K_2O	0.25	2.81	0.34	0.38	0.02	0.09	0.04	2.09
P_2O_5	0.03	0.03	0.05	0.04	0.16	0.05	0.05	0.03
Total	100.00	100.00	100.00	100.00	100.00	100.00	100.00	100.00
Au (ppb)	20	2465	27.3	3132	5736	n.d.	n.d.	n.d.
S (%)	0.03	0.09	0.04	0.09	0.21	n.d.	n.d.	n.d.
CO_2	7.14	7.01	5.96	2.66	0.99	0.17	n.d.	n.d.
LOI	11.37	10.37	10.01	4.86	2.73	2.31	21.98	22.07
Ba (ppm)	795	4310	868	4310	4741	n.d.	n.d.	n.d.
Cr	2278	2080	2387	1910	556	n.d.	1169	1877
Al/Ti	10.03	10.07	10.36	9.86	15.35	9.63	24.76	28.16

1 = Amphibole-chlorite schist with talc-carbonate alteration, Pahtavaara.
2 = Biotite schist, Pahtavaara.
3 = Amphibole porphyroblastic talc-carbonate schist, Pahtavaara.
4 = High-alumina amphibole rock, Pahtavaara.
5 = Low-alumina amphibole rock, Pahtavaara.
6 = Badblaas-type basaltic komatiite, Komati formation, South Africa (Viljoen & Viljoen, 1969).
7 = Altered komatiite; a grey schist (carbonate-chlorite schist) adjacent to mineralization, Sugar Loaf, Barbrook prospect, South Africa (Houston, 1987).
8 = Altered and gold-mineralized komatiite; a green schist (carbonate-fuchsite-quartz-white mica schist), Crown mine, Barbrook prospect, South Africa (Houston, 1987).

All results recalculated to 100 wt. %, volatile-free. Al/Ti ratio in oxide.

In all, biotite schists are easily distinguishable geochemically from the surrounding amphibole-chlorite schists by their salient concentrations of K and Ba. In addition, immobile element contents of are higher than in other rock types. Mineralogically the formation of biotite schist corresponds to the alteration of chlorite to biotite by adding K and removing MgO.

Amphibole rock

In spite of its mineralogical homogeneity the coarse-grained amphibole rock is nevertheless compositionally heterogeneous and can be divided on the basis of Al contents into two types: (1) high-alumina ($Al_2O_3 > 4$ wt. %) and (2) low-alumina ($Al_2O_3 < 4$ wt. %) types. The former type is compositionally closely related to amphibole-chlorite schist, whereas the latter appears to be compositionally gradational into amphibole-rich talc-carbonate veins. As a whole, the amphibole rocks differ from the amphibole-chlorite schist in their higher CaO and SiO_2 and lower MgO contents (Figs. 21 — 23). In addition, Al contents vary sympathetically with Ti and Cr contents. In the following, the geochemical features of the high-alumina and low-alumina types are described separately (Table 2).

The **high-alumina amphibole rock** has a variable but characteristically high SiO_2 content (47 — 52 wt. %). This corresponds in part to the appearance of minor quartz. Aluminum and Ti contents are comparable to those in the amphibole-chlorite schists, ranging between 5 and 9 wt. %, and between 0.35 and 1.1 wt. %, respectively. The Al_2O_3/TiO_2 ratios are approximately the same as in typical Sattasvaara komatiites. However, some samples are relatively Ti-rich (Fig. 17). The presence of albite appears to correlate with the highest values of Al and Na, probably reflecting the availability of these elements during hydrothermal alteration.

As stated above, the CaO content of the amphibole rock is remarkably high, averaging about 12 wt. %, although values up to 16 % are relatively common. This high CaO content can only be partly attributed to the abundance of amphibole as the most typical amphibole mineral present contains 11 — 12 % CaO. Since samples practically devoid of CO_2 contain only about 9 wt. % of CaO, at least part of the CaO is associated with carbonates. Furthermore, the samples with the highest CO_2 content have also the highest CaO. These features, as well as the increased CaO/Al_2O_3 ratio, indicate an absolute addition of Ca during alteration processes (cf. Kerr-Addison mine, Kirkland Lake, Ontario; Kishida & Kerrich, 1987).

MgO and $Fe_2O_3^{tot}$ contents in high-alumina amphibole rock are lower than in weakly altered lithologies at Pahtavaara, ranging typically between 16 — 20 wt. % and 9 — 13 %, respectively. In contrast, K_2O contents vary from ca. 0.1 wt. % up to 1.6 % (average 0.3 — 0.4 %). Mineralogically this corresponds to the sporadic presence of biotite in amphibole rock. Variations in Na_2O reflect the heterogeneous distribution of albite, and local presence of Na-amphibole, with values displaying comparably variation from ca. zero up to 1.8 % (average 0.8 %). This is clearly higher than contents in both biotite schists (0.2 — 0.7 wt. %) and in weakly altered amphibole-chlorite schists (typically 0.1 — 0.2 wt. %).

Mineralogically and compositionally, the high-alumina amphibole rocks resemble the Badblaas-type basaltic komatiites defined in an early paper by Viljoen and Viljoen (1969) (or Badblaas-type komatiitic basalt of Viljoen et al., 1982). On the Jensen cation plot they plot within the field of ultramafic and basaltic komatiites (Fig. 20). Originally, the above authors considered that this type of komatiite represented a primary magma type and concluded that high Si, Mg and Ca, and low Al (hence high Ca/Al) and alkalis were related to the primary abundance of diopsidic pyroxene and absence of olivine. However, in a more recent paper Viljoen et al. (1983) have interpreted comparable rocks in South Africa as representing zones through which significant amounts of fluid have passed. This resulted in the addition of Si, Ca, Na, Sr, and Cu, while im-

mobile element ratios (e.g. Al/Ti), although remaining constant, have nevertheless had their relative proportions diluted. Therefore it appears that the Badblaas-type komatiites, as defined by Viljoen and Viljoen (1969), do not represent a primary compositional type of basaltic komatiite but rather a hydrothermally altered variety. Similarly, high-alumina amphibole rocks at Pahtavaara are considered as hydrothermally modified komatiites in which some primary geochemical features are nevertheless still recognizable. Furthermore, it is important to bear in mind that increased K_2O contents and local presence of biotite in some amphibole rocks may indicate that at least some of them have also undergone potassic alteration similar to that which resulted in the formation of biotite schist. Therefore these rock types probably had at least in part a common alteration history.

The **low-alumina amphibole rock** is more silica-rich than the other rock types at Pahtavaara and closely associated with quartz veins, SiO_2 contents varying between 54 and 58 wt. %. Al_2O_3/TiO_2 ratios are broadly similar to those for other rock types, although absolute contents are appreciably lower (Fig. 17). A good example of this is the analysis of sample 051/0.0 taken from exploration trench 5, and containing visible gold (Fig. 4A; App. 1; anal 2). This shows that values for all the above elements and Cr are about a half of respective abundances in the weakly altered amphibole-chlorite schist. The MgO content of the low-alumina amphibole rock is similar to that of high-alumina amphibole rock, being 18 wt. % in average. Iron contents are higher and Ca contents lower than in the latter. Na_2O is lower than in the high-alumina type but still markedly higher than in the amphibole-chlorite schists. Importantly, the low-alumina amphibole rock is characterized by low CO_2 and extremely low K contents. The latter feature, together with the low immobile element contents, is similar to the amphibole-rich talc-carbonate and quartz ± barite veins. This, supported by mineralogical gradations suggests a close relationship between these types and a vein-type nature of the low-alumina amphibole rock. Furthermore, these features also indicate that K was not mobile during the formation of veins and low-alumina amphibole rocks as no biotite has been observed within them. If this deduction is accepted it seems likely that the high K_2O of some high-alumina amphibole rocks is related to their association with biotite schist and a common alteration history referred above.

To summarize, amphibole rocks are divided compositionally into high-alumina and low-alumina types. They are all CaO, SiO_2 and Na_2O-rich and have low $Fe_2O_3^{tot}$ and MgO contents compared to the least altered amphibole-chlorite schists. Geochemically the high-alumina amphibole rock resembles the Badblaas-type basaltic komatiite described by Viljoen and Viljoen (1969). However, it is not considered here as a primary magma type but regarded as representing hydrothermally altered komatiites. High-alumina and low-alumina amphibole rocks are compositionally and texturally gradational into amphibole-chlorite schist, and talc-carbonate-amphibole and quartz ± barite veins, respectively.

Veins

Compositions of veins vary depending largely on mineralogical assemblage. As discussed earlier they can be broadly subdivided into (1) talc-carbonate ± pyrite veins and (2) quartz ± barite veins, with both types containing variable proportions of amphibole. The former type is typically associated with biotite schists and the latter with amphibole rocks but as these rock types are intimately intercalated no detailed conclusion concerning their mutual relationships can be drawn. In practice the above classification is only descriptive as mineralogical relations and hence also chemical compositions are extremely variable and transitional into each other. Accordingly, by selective sampling it is possible to obtain any kind of mineralogical combination. The appearance of free quartz is clearly reflected in the composition of veins, evidently indicating satu-

ration of hydrothermal fluid with respect to silica. A similar situation exists where high Ba contents correspond to the appearance of barite, although Ba content can also increase due to the presence of biotite.

In all, due to the complexity of vein mineralogy and composition, and the limited number of samples, it has only been possible to demonstrate the chemical composition of veins on a tentative basis. All veins are, however, Al-poor and therefore comparable with, and probably gradational into low-alumina amphibole rocks/veins.

Compositional gradation

As noted above, altered lithologies at Pahtavaara display mineralogical and compositional gradations (Figs. 15 and 20 — 23). This is best shown geochemically by those major elements which were also integrally involved in alteration processes, namely CaO, $Fe_2O_3^{tot}$, MgO and SiO_2. In spite of the compositional gradation, distinct fields for different rock types can nevertheless be distinguished. It is important to note that, even though the whole rock data were recalculated according to volatile-free composition, the variable carbonate content still has some effect on the results. This can be seen particularly in the general increase in CaO and MgO content together with the carbonate contents (typically ferroan dolomite), coinciding with a concomitant reduction in the relative proportions of elements not present in carbonates, namely Si, K and, to a lesser extent, Fe. Furthermore, it is also difficult to distinguish carbonation geochemically from other Ca-related mineralogical changes such as amphibole growth when interpreting the relationships between mineralogical and geochemical features.

In the MgO vs. $Fe_2O_3^{tot}$ diagram (Fig. 21) the weakly altered rocks can be distinguished by their high MgO (ca. 24 — 26.5 wt. %) and intermediate $Fe_2O_3^{tot}$ contents (ca. 12 — 15 wt. %) from biotite schists, which have $Fe_2O_3^{tot}$ up to 25 wt. %, and also from coarse-grained amphibole

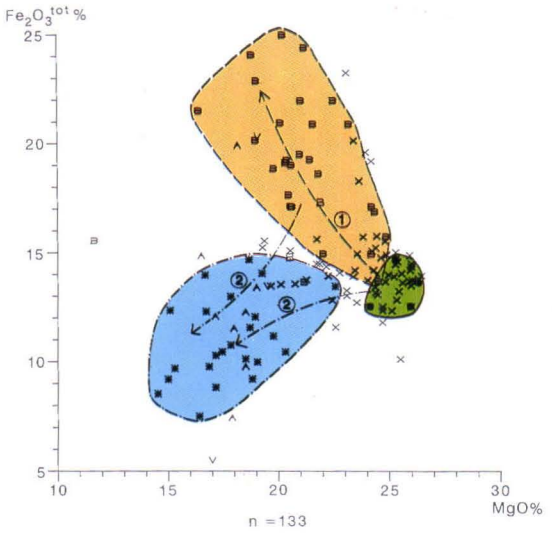

Fig. 21. MgO vs. $Fe_2O_3^{tot}$ diagram for variably hydrothermally altered rocks from Pahtavaara gold deposit. For rock symbols, see Figure 17 (colours as in Fig. 18). Note the clear separation of different rock types as well as gradation between them. The arrows indicate trend from the least altered composition towards higher degrees of alteration. On the basis of structural evidence, biotite alteration (1) preceded the development of amphibole rock (2).

rocks, which have lower $Fe_2O_3^{tot}$ contents (down to 7 wt. %). This is accordingly reflected in Fe/Mg oxide ratios which are 0.6 — 1.4 for biotite schist, 0.4 — 0.8 for amphibole rock, and ca. 0.5 for the least altered amphibole-chlorite schists (Fig. 22). When these data are combined with variations in CaO content, the dominant rock types will clearly plot in different fields on the $Fe_2O_3^{tot}$/MgO vs. CaO diagram, in spite of the effects of gradation. An apparent gradation also exists with respect to CaO and SiO_2 contents, as portrayed in Figure 23.

Furthermore, when observing elemental transitions in terms of different rock types, it is easy to notice that the trends are bidirectional. For example, biotite schists have a trend towards more Fe-rich compositions and amphibole rock towards Fe-poor compositions compared to least altered amphibole-chlorite schists (Fig. 21). A similar pattern exists in regard to CaO and SiO_2 (Figs. 22 and 23).

Altogether these features, along with addition-

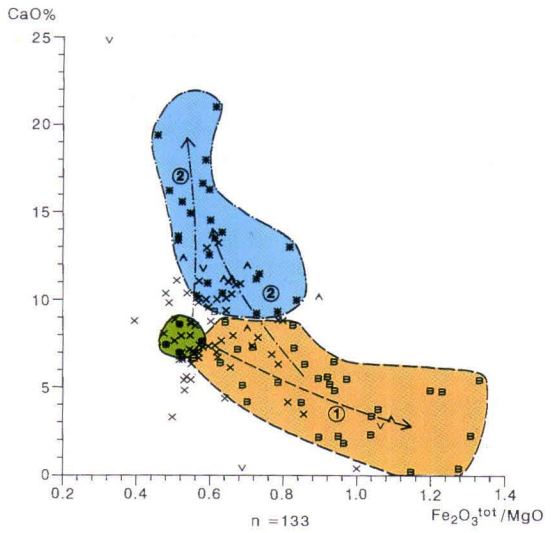

Fig. 22. $Fe_2O_3^{tot}/MgO$ vs. CaO diagram for variably hydrothermally altered rocks from Pahtavaara gold deposit. For rock symbols, see Figure 17 (colours as in Fig. 18). Note the clear separation of different rock types as well as gradation between them. Arrows as in Figure 21.

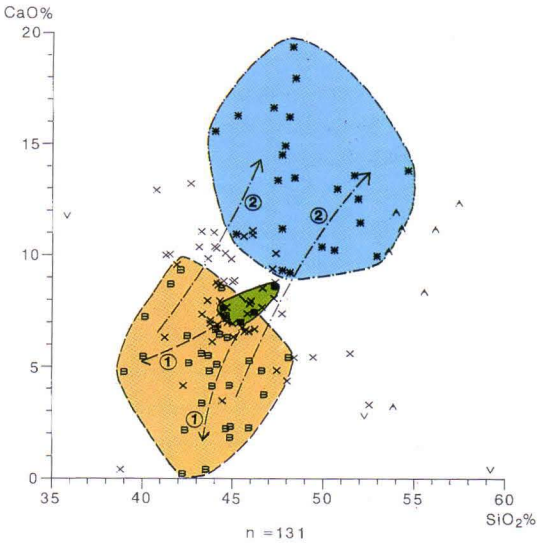

Fig. 23. SiO_2 vs. CaO diagram for variably hydrothermally altered rocks from Pahtavaara gold deposit. For rock symbols, see Figure 17 (colours as in Fig. 18). Note the clear separation of different rock types. Arrows as in Figure 21.

al textural evidence, suggest that the hydrothermal alteration that resulted in the formation of the variable rock types included at least two geochemically different stages. During the first stage of alteration, which resulted in the formation of the biotite schists, the original komatiitic rock become enriched in elements such as Fe plus K and Ba and depleted in Mg (Fig. 21) and Ca (Fig. 22). In the second stage the previously heterogeneously altered, as well as unaltered rocks became enriched in Ca and Si (Figs. 21 and 22). These additions, along with other changes discussed more detail below resulted in the generation of amphibole rock. It is important to note that the later stage of alteration was superimposed either directly upon the least altered komatiitic compositions or, alternatively, previously altered biotite schists. Evidence for the latter is shown by the local occurrence of biotite remnants in amphibole rock.

Trace elements

The contents of several trace elements typically associated with gold mineralization were mostly below the detection limit for the method used at Pahtavaara. These elements include As, Ag, Be, B, Br, Pb, Mo and U, which is compatible with their negligible abundances in both the komatiitic host rocks and also in the mineralizing fluid.

However, the concentrations of some trace elements, namely Co, Sc, Sr, Te, V, W and Zn were sufficiently variable and high to enable detailed studies relative to the different rock types (Figs. 18, 19B and 24; App. 1). The results show that Te, W and Sr contents are higher in altered rocks, whereas Co and Zn contents are lower. These features suggest that the above elements have been respectively added or depleted during hydrother-

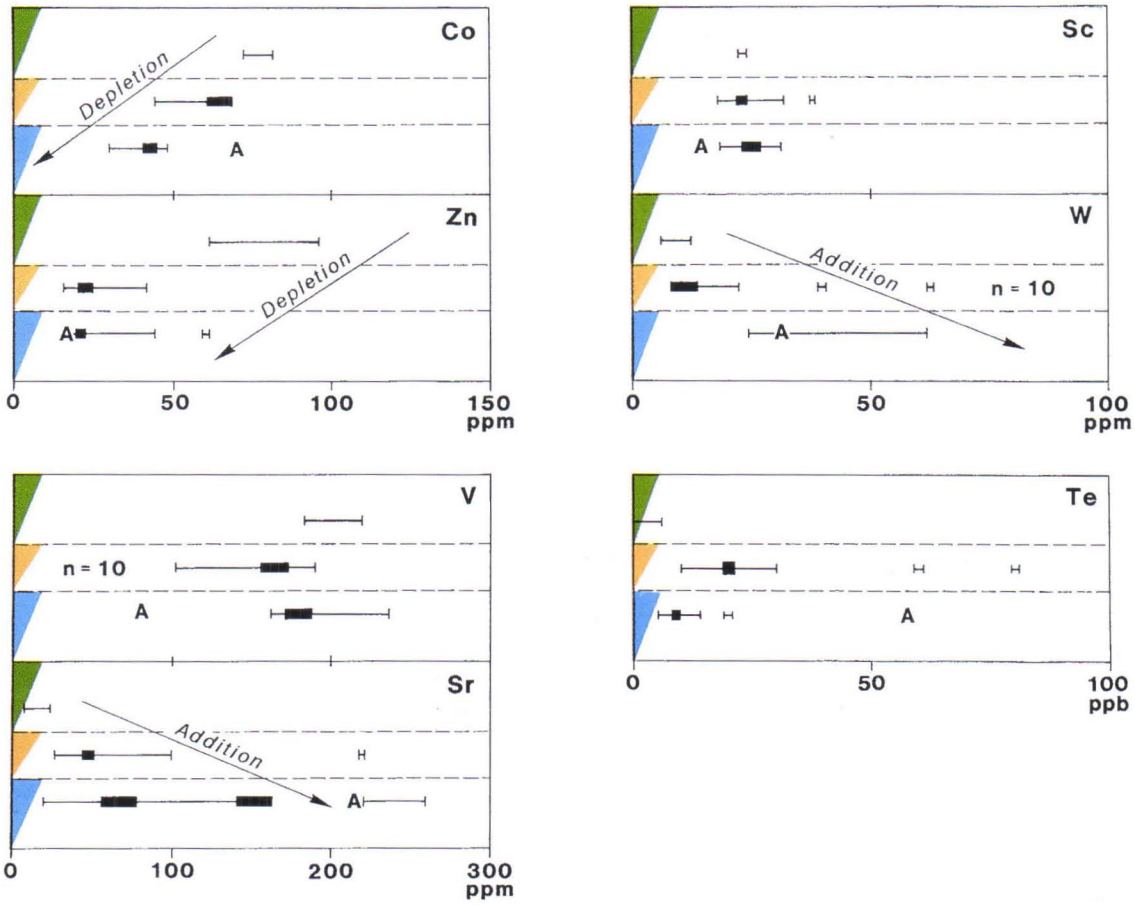

Fig. 24. Ranges of selected trace elements for major rock types from Pahtavaara gold deposit. The uppermost line (green) for each element represents the weakly altered amphibole-chlorite schist (n = 4), the middle one (orange) biotite schist (n = 11, where not otherwise indicated), and the lowermost (blue), high-alumina amphibole rock (n = 11). A single analysis of the low-alumina amphibole rock is shown by A. Thick line shows dominant compositional clusters. For further discussion, see text.

mal alteration. Scandium and V contents are approximately the same in both altered and weakly altered types (= amphibole-chlorite schists). However, there is probably a minor decrease in V content in the altered rocks and the major cluster of Sc values in the biotite schists appears to be slightly lower than in the least altered samples and amphibole rocks.

Ranges for the above trace elements relative to different rock types are displayed in detail in Figure 24. Strontium in the amphibole rock is highly variable, ranging between 20 to 260 ppm, with the most common values falling between ca. 55 — 80 and 140 — 160 ppm. These concentrations are markedly higher than in biotite schist (typically 40 — 50 ppm) and in least altered amphibole-chlorite schist with values between 5 and 25 ppm. Strontium content is closely related to CO_2 content, indicating mobility of Sr during carbonation. Vanadium contents for the least altered rock types vary between 180 — 215 ppm which is only slightly higher than the most typical values for amphibole rocks. Furthermore, V contents in biotite schists are lower, ranging be-

tween 100 and 190 ppm with modal concentrations around 155 — 175 ppm.

It is impossible to make any distinction between the biotite schist and amphibole rock in terms of Zn content; contents are, however, markedly lower in altered rocks (15 — 40 ppm) than in the weakly altered amphibole-chlorite schists (60 — 100 ppm). Cobalt contents are highest (ca. 70 — 80 ppm) in the least altered samples but only slightly lower in biotite schist (45 — 70 ppm; modal content of 65 ppm). The lowest values are found in amphibole rocks, ranging between 30 and 50 ppm with major clustering at ca. 40 ppm. Accordingly, Co content is a good indicator of the degree of alteration at Pahtavaara. In contrast, W content displays an opposite if less well-developed trend relative to alteration, being lowest in the least altered type (6 — 12 ppm), with values in biotite schists being slightly higher, typically between 8 — 22 ppm, with major cluster at 8 — 13 ppm; isolated values of ca. 60 and 150 ppm have however been detected. On the whole, amphibole rocks have the highest W contents, varying between 24 and 62 ppm.

The Sc contents of both biotite schists and amphibole rocks range between 18 and 31 ppm, the modal values for the former being 21 — 23 ppm, which is the same as for typical amphibole-chlorite schist compositions. For amphibole rock Sc contents in general overlap with the other types but is, however, to a small extend higher. Proportion of Te, which is among the one of the rarest elements in the crust, seems to be a good indicator of alteration. It is very low in least altered samples being generally below the detection limit (3 ppb) for the method used, whereas values up to 80 ppb have been measured for biotite schist, the major concentration being between 10 — 30 ppb. The contents for high-alumina amphibole rock are generally slightly lower being typically between 5 and 15 ppb (maximum 20 ppb). Furthermore, single analysis of low-alumina amphibole rock displays higher Te content of about 60 ppb. Nurmi et al. (1991) have also reported high Se (11.8 ppm) and U (3.6 ppm) contents of the ore sample from Pahtavaara. The former feature is supported by the occurrence of Se minerals as documented by Kojonen and Johanson (1989).

In summary, trace element contents are very variable in the present study area and some of them, namely Sr, Co, Zn and W appear to display gradational trends between least altered and more altered types. Tellurium also appears to be a good indicator of hydrothermal processes. These data suggest that abundances of these elements can be used in general to estimate the degree of alteration at Pahtavaara.

MINERAL COMPOSITIONS

Amphiboles

Amphiboles are an essential component of the Pahtavaara deposit and have therefore been studied in detail. On the whole their composition varies depending on their geological environment. When interpreting the mineralogical data, it is important to distinguish hydrothermal amphiboles from those recrystallized isochemically during regional metamorphism. The former tend to be mono- or bimineralic and are highly variable, so that amphibole compositions reflect the influence of the chemical potentials of species in the hydrothermal fluid phase rather than simply pressure and temperature. Accordingly, only the latter kind of amphiboles can be used when determining regional metamorphic grade (Evans, 1982).

Nomenclature of amphiboles follows Leake (1978) and Hawthorne (1981), who classified am-

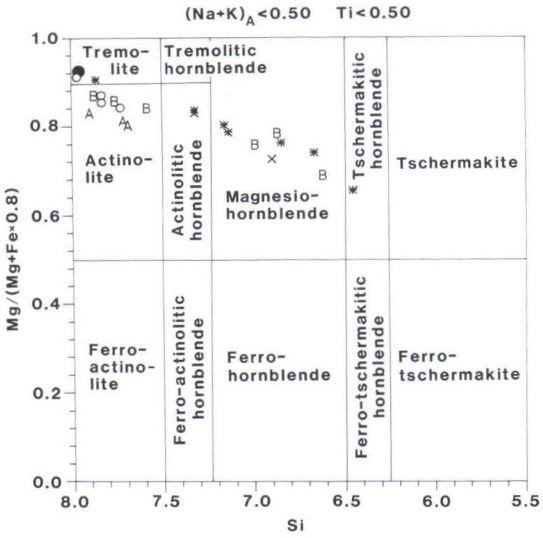

Fig. 25. Chemical compositions of dominant calcic amphiboles from Pahtavaara gold deposit. Nomenclature after Leake (1978) and Hawthorne (1981). Rock types are also indicated; symbols as in Figure 17, excluding ○ (= amphibole-chlorite schist with weak talc-carbonate alteration) and × (= amphibole porphyroblastic schist).

phiboles into four principal groups on the basis of the number of atoms of (Ca + Na) and Na. Within these groups amphiboles are classified using the number of Si atoms and Mg/(Mg + Fe^{2+}). Some inaccuracy is inevitable however, because the Fe^{2+}/Fe ratio cannot be determined by electron microprobe. A ratio of 0.8 is nevertheless considered as a reasonable estimation; in the vein-type Con and Giant Mines in the Yellowknife district, Canada, the whole-rock ratio

Fig. 26. Compositionally heterogeneous amphibole crystal in amphibole rock with some carbonate, chlorite and talc. The inner part consists of green Mg-hornblende (dark grey) and rim of colourless actinolite (light grey). Numbers refer to microprobe analyses in Table 3. Drill core 232/6.80 m. Field of view is 1.2 mm in width.

for unmineralized metabasaltic background samples is 0.7, compared with 0.9 for reduced carbonate-muscovite schists enveloping Au-bearing quartz veins (Kerrich & Fyfe, 1981). Furthermore, as the amphiboles at Pahtavaara are all Mg-rich, the effect of uncertainty concerning Fe atomic proportions on the nomenclature is only of minor importance.

Compositionally, the majority of amphiboles from Pahtavaara belong to the monoclinic calcic amphibole group as presented in Figure 25 and Table 3 although orthorhombic anthophyllites belonging to the Fe-Mg-Mn amphibole group have also been recorded (Table 3; anal. 23 — 25). In addition, a blue alkali amphibole (Table 3; anal. 26) occurring together with anthophyllite has been found in one vein.

Calcic amphiboles display a clear compositional gradation from colourless tremolite-actinolite to green magnesium hornblende and tschermakitic hornblende, with the colour apparently related to Cr content. In general, the amphiboles in weakly altered samples are tremolite-actinolite, whereas amphiboles in altered rocks and in veins are, due to their hydrothermal nature, compositionally more variable.

Tremolite-actinolite has MgO contents between 17 and 22 wt. % and SiO_2 contents between 53 and 57 wt. %, whereas the proportion of CaO is relatively constant at around 11 — 12.5 wt. %. Chromium occurs only in small quantities and does not correlate with Al_2O_3 content in spite of constant ratio in the whole-rock analyses. TiO_2 contents are also lower than in hornblendes. On the whole, amphiboles in weakly altered samples have more Mg and Si, and less Fe and Al than amphiboles in altered samples. Because the amphiboles in the latter type are so heterogeneous, it is not possible to further discriminate between hydrothermally altered amphiboles and those formed as a result of regional metamorphism.

Besides tremolite-actinolite, the amphibole rocks contain alkali amphiboles and anthophyllites. Compositionally different amphiboles may occur in the same sample either as separate or composite crystals (Fig. 26; Table 3; anal. 3 and 15). Examples of the latter are given by analyses from drill cores 506/87.9 m (Table 3; anal. 12 and 22) and 508/80.2 m (Table 3; anal. 13 and 17). It is also interesting to note that Al-rich amphibole may occur as either the core to Al-poor crystals or rim crystals having Al-poor cores.

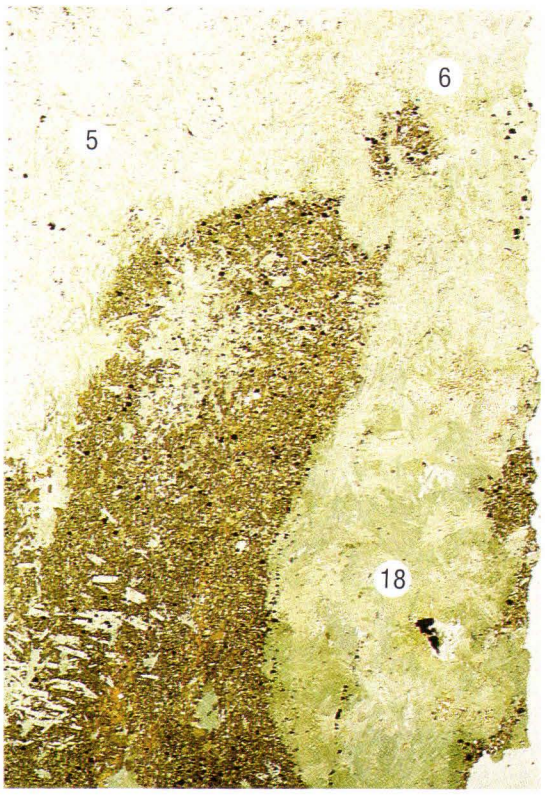

Fig. 27. Transitional zone between biotite schist (brown) with talc-carbonate vein and coarse-grained amphibole rock (detail of Fig. 15). Amphiboles occurring together with talc and carbonate consist of coarse-grained green Mg-hornblende which is gradational upwards into colourless actinolite. Numbers refer to microprobe analyses in Table 3. Drill core 253/6.70 m. Field of view is 1.8 cm in width.

Additionally, amphiboles in amphibole-rich talc-carbonate veins in biotite schist may display gradational changes from green Mg-hornblende (Table 3; anal. 18) to colourless actinolite (Table 3; anal. 5 and 6) over a distance of a few cm (Fig. 27; cf. also Fig. 15). In such cases, amphiboles closer to quartz veins in amphibole rock are

Table 3. Composition of amphiboles from Pahtavaara. Rock symbols as in Appendix 1.

	1	2	3	4	5	6	7	8	9	10	11	12	13
SiO_2 (%)	56.19	57.50	55.43	55.20	56.26	54.37	54.83	54.19	52.89	54.81	52.90	49.12	50.84
TiO_2	0.02	0.03	0.04	0.05	0.04	0.07	0.04	0.05	0.15	0.08	0.18	0.28	0.29
Al_2O_3	0.17	0.37	0.80	1.55	1.59	2.52	1.38	2.13	3.65	0.91	2.49	5.42	5.38
FeO	4.00	4.67	4.94	6.55	6.74	7.08	7.34	7.84	7.91	8.51	9.61	7.36	8.23
MnO	0.14	0.20	0.17	0.15	0.34	0.26	0.14	0.15	0.31	0.36	0.36	0.19	0.27
MgO	21.57	21.50	21.20	19.66	19.96	18.95	19.26	18.89	18.62	18.65	17.45	16.80	17.90
CaO	12.61	12.51	12.17	12.14	11.75	11.60	11.96	11.90	11.44	11.50	11.33	12.01	11.77
Na_2O	0.09	0.17	0.33	0.32	0.26	0.38	0.55	0.70	0.42	0.34	0.65	0.72	1.10
K_2O	0.02	0.08	0.01	0.02	0.01	0.02	0.03	0.02	0.02	0.01	0.01	0.10	0.02
V_2O_3	0.01	0.01	0.02	0.04	0.03	0.05	0.04	0.05	0.04	0.02	0.04	0.05	0.05
Cr_2O_3	0.01	0.01	0.06	0.18	0.00	0.01	0.07	0.19	0.09	0.00	0.17	0.54	0.08
NiO	0.10	0.07	0.13	0.08	0.16	0.08	0.08	0.08	0.06	0.08	0.06	0.09	0.06
Total	94.92	97.11	95.30	95.94	97.14	95.38	95.72	96.20	95.60	95.25	95.25	92.70	96.00
	Atomic proportions			mg = Mg/(Mg + 0.8*Fe)									
Si	7.976	7.990	7.881	7.848	7.886	7.785	7.848	7.748	7.604	7.913	7.705	7.335	7.340
Ti	0.002	0.003	0.004	0.005	0.004	0.008	0.004	0.005	0.017	0.009	0.019	0.032	0.032
Al	0.028	0.061	0.134	0.260	0.263	0.425	0.232	0.359	0.619	0.156	0.427	0.954	0.915
Fe	0.475	0.542	0.587	0.779	0.790	0.848	0.879	0.937	0.952	1.028	1.170	0.920	0.994
Mn	0.017	0.024	0.021	0.018	0.040	0.032	0.017	0.019	0.038	0.044	0.044	0.024	0.033
Mg	4.564	4.453	4.493	4.167	4.171	4.045	4.110	4.026	3.991	4.013	3.788	3.740	3.852
Ca	1.918	1.862	1.853	1.849	1.764	1.779	1.834	1.823	1.762	1.779	1.769	1.921	1.821
Na	0.026	0.044	0.092	0.087	0.072	0.105	0.152	0.196	0.117	0.096	0.183	0.210	0.308
K	0.003	0.014	0.003	0.003	0.001	0.004	0.004	0.004	0.003	0.002	0.002	0.020	0.004
V	0.001	0.001	0.002	0.004	0.004	0.006	0.005	0.006	0.004	0.002	0.005	0.006	0.005
Cr	0.001	0.001	0.006	0.021	0.000	0.002	0.008	0.021	0.010	0.000	0.020	0.063	0.009
Ni	0.012	0.008	0.015	0.009	0.018	0.010	0.009	0.090	0.007	0.009	0.007	0.011	0.007
mg	0.923	0.911	0.905	0.870	0.868	0.856	0.854	0.843	0.840	0.830	0.802	0.836	0.829

SAMPLE	MINERAL	COLOUR	ROCK SYMBOL
1 = 230/33.45	Tremolite-actinolite	Colourless	●
2 = 248/27.0	Tremolite-actinolite	Colourless	O
3 = 232/6.8	Tremolite-actinolite	Colourless	*
4 = 248/27.0	Tremolite-actinolite	Colourless	O
5 = 253/6.7	Tremolite-actinolite	Colourless	B (vein)
6 = 253/6.7	Tremolite-actinolite	Colourless	B (vein)
7 = 232/34.2	Tremolite-actinolite	Colourless	O
8 = 232/34.2	Tremolite-actinolite	Colourless	O
9 = 506/46.6	Tremolite-actinolite	Colourless	B
10 = 051/0.0	Tremolite-actinolite	Colourless	A
11 = 051/0.0	Tremolite-actinolite	Colourless	A
12 = 051/0.0	Tremolite-actinolite	Colourless	A
13 = 506/87.9	Actinol. hornblende	Colourless	*

Table 3. Composition of amphiboles from Pahtavaara (continued).

	14	15	16	17	18	19	20	21	22	23	24	25	26
SiO_2 (%)	49.07	48.42	49.40	46.51	47.95	45.41	46.76	44.58	43.29	56.56	56.22	54.38	55.35
TiO_2	0.34	0.28	0.25	0.40	0.32	0.40	0.31	0.45	0.91	0.01	0.05	0.03	0.05
Al_2O_3	7.43	6.79	6.98	9.96	9.00	11.40	9.61	11.77	12.40	0.78	0.80	2.05	0.69
FeO	8.93	9.69	9.90	10.23	10.60	11.10	11.59	12.90	13.41	13.46	13.74	16.72	23.18
MnO	0.24	0.22	0.25	0.21	0.39	0.29	0.24	0.25	0.31	0.75	1.11	0.87	0.47
MgO	16.31	16.04	16.09	14.74	14.85	14.27	13.76	12.82	11.46	23.83	22.33	21.29	9.53
CaO	11.16	11.33	11.78	11.24	11.18	11.13	11.33	11.12	11.99	0.26	0.26	0.63	0.58
Na_2O	1.08	1.79	1.02	1.86	1.55	1.99	1.47	1.73	1.56	0.10	0.12	0.33	6.68
K_2O	0.06	0.09	0.07	0.07	0.06	0.08	0.07	0.16	0.34	0.00	0.01	0.00	0.01
V_2O_3	0.04	0.07	0.05	0.06	0.06	0.06	0.09	0.10	0.05	0.01	0.00	0.03	0.01
Cr_2O_3	0.36	0.18	0.20	0.05	0.30	0.03	0.45	0.06	0.87	0.03	0.00	0.04	0.02
NiO	0.08	0.08	0.10	0.04	0.06	0.09	0.04	0.09	0.07	0.12	0.11	0.12	0.08
Total	95.11	94.98	96.10	95.37	96.30	96.25	95.72	96.03	96.66	95.92	94.76	96.48	96.66
	Atomic proportions			mg = Mg/(Mg + 0.8*Fe)									
Si	7.172	7.149	6.878	6.858	6.997	6.675	6.909	6.627	6.459	8.008	8.075	7.815	8.310
Ti	0.037	0.031	0.026	0.044	0.035	0.044	0.034	0.051	0.102	0.001	0.005	0.003	0.005
Al	1.280	1.182	1.145	1.731	1.548	1.975	1.674	2.062	2.181	0.131	0.136	0.347	0.122
Fe	1.092	1.197	1.153	1.262	1.293	1.365	1.432	1.604	1.673	1.594	1.651	2.009	2.910
Mn	0.030	0.027	0.030	0.026	0.048	0.036	0.030	0.032	0.039	0.090	0.135	0.106	0.060
Mg	3.553	3.531	3.339	3.240	3.231	3.126	3.030	2.841	2.548	5.028	4.781	4.560	2.133
Ca	1.747	1.793	1.758	1.775	1.749	1.753	1.794	1.771	1.917	0.039	0.040	0.097	0.094
Na	0.307	0.513	0.276	0.532	0.438	0.567	0.422	0.499	0.450	0.028	0.034	0.092	1.943
K	0.011	0.016	0.012	0.014	0.011	0.014	0.013	0.030	0.065	0.000	0.002	0.000	0.002
V	0.005	0.008	0.005	0.007	0.007	0.007	0.010	0.012	0.006	0.001	0.000	0.003	0.001
Cr	0.042	0.021	0.022	0.006	0.035	0.004	0.052	0.007	0.102	0.004	0.000	0.004	0.002
Ni	0.009	0.010	0.012	0.005	0.007	0.011	0.005	0.011	0.008	0.014	0.012	0.013	0.010
mg	0.803	0.787	0.784	0.762	0.758	0.741	0.726	0.690	0.656	0.798	0.784	0.739	0.478

SAMPLE	MINERAL	COLOUR	ROCK SYMBOL
14 = 253/9.6	Mg-Hornblende	Green	*
15 = 232/6.8	Mg-Hornblende	Green	*
16 = 506/28.4	Mg-Hornblende	Green	B (vein)
17 = 508/80.2	Mg-Hornblende	Green	*
18 = 253/6.7	Mg-Hornblende	Green	B (vein)
19 = 508/80.2	Mg-Hornblende	Green	*
20 = 507/59.7	Mg-Hornblende	Green	X
21 = 506/28.4	Mg-hornblende	Green	B (vein)
22 = 506/87.9	Tscherm. hornblende	Green	*
23 = 511/84.7	Anthophyllite	Colourless	B (vein)
24 = 508/71.9	Anthophyllite	Colourless	*
25 = 506/28.4	Anthophyllite	Colourless	B (vein)
26 = 508/71.9	Alkali amphibole	Blue	V

more Al, Fe, Na, and Cr-rich and contain less Mg and Si than those further away. This probably reflects the composition of the original material in which the amphibole growth took place, and its Al-content in particular.

In intensively altered rocks amphibole is typically green Mg-hornblende while veins typically contain colourless tremolite-actinolite. This probably reflects the availability of Al during alteration and the capacity of different minerals for accommodating Al during crystallization. The variable Al-contents of rims and cores of amphibole crystals described above can be explained similarly. In weakly altered amphibole-chlorite schist, amphibole is typically Al-poor tremolite-actinolite since Al appears to be preferentially hosted by chlorite if the latter is present. The presence of an alkaline amphibole in veins is probably related to the paucity of Al and increased Na-activity in the hydrothermal fluid.

To summarize, it appears that amphibole composition is primarily related to the original composition of the rock and hence to the availability of Al during hydrothermal alteration and metamorphism but may also depend upon different tendencies for minerals to host Al. Accordingly, it appears that in the least altered, regionally metamorphosed amphibole-chlorite schists amphibole tends to be Al-poor tremolite-actinolite, the Al present being preferentially partitioned into, or remaining in chlorite. In contrast, hydrothermal amphiboles in altered rocks are compositionally heterogeneous. Amphiboles associated with talc-carbonate veins are Al-poor, as suggested by the low Al-content of the veins, whereas hydrothermal amphiboles forming nearly monomineralic high-alumina amphibole rock are commonly Al-bearing, probably due to the absence of other minerals suitable for taking Al into their lattices. In low-alumina amphibole rocks, amphibole is naturally Al-poor, whereas amphiboles in biotite schist are compositionally heterogeneous and no detailed conclusion concerning their nature can be drawn.

Carbonates

Carbonates are one of the most characteristic mineral groups in a number of greenstone-hosted gold deposits and have also been widely used as a guide in exploration (Davies et al., 1982; Fyon & Crocket, 1982; Fyon et al., 1983; Karvinen, 1982). Carbonation is a particularly important alteration process in ultramafic rocks due to the high abundance of Ca and Mg available for reaction with the CO_2-rich fluids that are typically associated with Au mineralization (Kerrich, 1983). The composition of carbonates often reflects the original composition of the rock as well. Generally the degree of carbonation and the composition of carbonates change from calcite and dolomite to Fe and Mg-carbonates towards the centre of a deposit (Colvine et al., 1984). This is also evident in an increase of the CO_2/CaO ratio; in the highly mineralized Timmins area for example this ratio is 0.67, whereas in adjacent unmineralized areas nearby it is only 0.13 (Davies et al., 1982).

At Pahtavaara, the dominant carbonate is ferroan dolomite (Table 4) and hence compositionally similar to carbonates in major gold deposits, although some more magnesian varieties as well as some relatively pure calcites have also been identified (Table 4; Fig. 28). To complement the microprobe data, and to obtain a more comprehensive view of the carbonate compositions, systematic X-ray diffractometer determinations were made from drill cores 506 — 509 and 512. This revealed that ca. 85 % of the carbonates analyzed from Pahtavaara were ferroan dolomite, the rest being calcite and magnesite.

In short, carbonates in mineralized rocks at Pahtavaara are compositionally relatively homogeneous ferroan dolomites and are therefore comparable with carbonates from many

Table 4. Composition of carbonates from Pahtavaara.

	1	2	3	4	5	6	7	8	9	10	11	12
MgO (%)	18.13	17.87	17.65	17.46	0.54	18.25	18.41	17.90	18.08	21.30	0.49	17.75
CaO	29.98	28.29	27.83	28.36	55.38	29.04	28.94	29.42	29.16	11.84	53.46	30.06
FeO	6.86	4.21	4.75	4.70	0.34	4.01	3.49	4.02	3.55	6.72	0.35	5.40
MnO	0.23	1.40	0.40	0.34	0.40	0.41	0.31	0.44	0.46	0.10	0.68	0.25
CO_2	44.78	48.22	49.37	49.14	43.35	48.29	48.85	48.22	48.74	60.03	45.01	46.54
Total	100.00	100.00	100.00	100.00	100.00	100.00	100.00	100.00	100.00	100.00	100.00	100.00
Atomic proportions												
Mg	0.866	0.826	0.809	0.802	0.027	0.842	0.844	0.827	0.831	0.890	0.024	0.833
Ca	1.029	0.826	0.916	0.936	1.987	0.963	0.954	0.977	0.963	0.356	1.891	1.014
Fe	0.184	0.109	0.122	0.121	0.009	0.104	0.090	0.104	0.091	0.158	0.010	0.142
Mn	0.006	0.037	0.010	0.009	0.011	0.011	0.008	0.012	0.012	0.002	0.019	0.007
C	1.958	2.043	2.071	2.066	1.982	2.040	2.052	2.040	2.051	2.297	2.028	2.002

Drill Core/ Depth (m)	Mineral	Rock symbol						
1 = 252/7.30	Fe-dolomite	B	5 = 232/34.20	Calcite	O	9 = 232/6.80	Fe-dolomite	X
2 = 252/7.30	Fe-dolomite	B	6 = 511/84.70	Fe-dolomite	B	10 = 248/27.00	Fe-dolomite	O
3 = 242/12.10	Fe-dolomite	O	7 = 506/46.60	Fe-dolomite	B	11 = 506/87.90	Calcite	*
4 = 242/12.10	Fe-dolomite	O	8 = 506/46.60	Fe-dolomite	B	12 = 253/6.70	Fe-dolomite	B

Rock symbols as in Appendix 1.

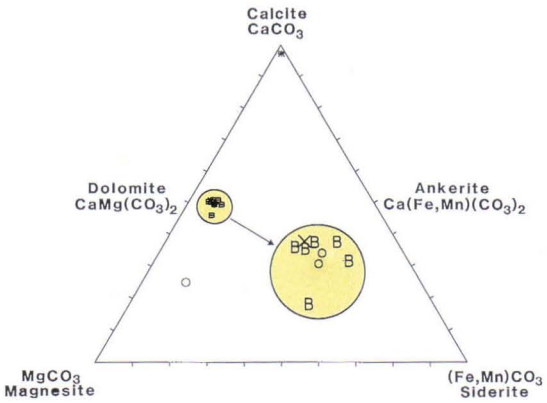

other gold deposits (cf. Fyon & Crocket, 1982; Fyon et al., 1983; Kerrich, 1983). In contrast, carbonates in the weakly altered amphibole-chlorite schist display the greatest variation, being either calcite, Mg-rich dolomite or Fe-dolomite (Fig. 28). Of these, calcite appears to be related to late veins.

Fig. 28. Chemical composition of carbonates from Pahtavaara. Rock symbols as in Figure 17, excluding ○ (= amphibole-chlorite schist with weak talc-carbonate alteration) and × (= amphibole porphyroblastic talc-carbonate schist).

Biotite-phlogopite

Biotites, or more correctly, biotite-phlogopites in the study area form a compositionally relatively heterogeneous group of minerals (Table 5). The term biotite is defined as a Fe-rich mica which is arbitrarily distinguished from phlogopite in having a Mg/Fe ratio, expressed in atomic proportions, of less than two to one (Deer et al., 1967).

Biotite-phlogopites at Pahtavaara are rich in immobile elements and contain up to about 16 wt. % Al_2O_3 and 2 wt. % TiO_2. The high proportions of these elements are also reflected in the whole-rock compositions of the biotite schist. The Fe content of biotite is also high (up to 15 % of FeO^{tot}) although still lower than in the Fe-richest samples of biotite schist, where $Fe_2O_3{}^{tot}$ can be as high as 24 wt. %. This implies that a large proportion of the Fe must also be contained in phases other than biotite, such as magnetite and pyrite.

The most distinctive compositional features of the biotite-phlogopites at Pahtavaara are the high K_2O (typically 8—9 wt. %) and Ba contents (ca. 0.5 %), which are also reflected in the whole-rock chemical data. Accordingly, these elements are reliable and sensitive indicators of the overall biotite-related hydrothermal alteration in the mineralized area. Furthermore, since biotite is practically the only mineral to host K in the study area, the whole-rock K_2O values can be used to estimate the proportion of biotite by volume in the rock. Since biotites at Pahtavaara contain on average 8.5 % K_2O (standard deviation 0.5), 2 wt. % K_2O in whole-rock analyses indicates volume proportion of 2/8.5 or about 24 %. Similarly, Ba concentrations can be used as an indication of the amount of the mineral barite in the rock: when the K_2O/Ba ratio in the biotite schist is less than 17, and the proportions of these elements in biotite (8.5 %/0.5 %, respectively) is allowed for, barite is probably present.

Biotite-phlogopite is Cr and Ni-rich, reflecting the ultramafic parentage of the protolith. Cr_2O_3 contents rise up to 0.8 wt. % resembling in that respect the other Cr-bearing mica, fuchsite (>1 % Cr_2O_3; Deer et al., 1967) which is characteristic of a number of gold deposits hosted by ultramafic rocks (Boyle, 1979; Colvine et al., 1984; Houston, 1987; Pearton, 1979). The 'green carbonate ore' at the Kerr-Addison mine in Ontario is one such example of fuchsite-bearing ore, in which the original komatiitic nature of these highly altered rocks is indicated by local preservation of spinifex textures (Kishida & Kerrich, 1987). The Hollinger mine at Timmins, Ontario, is also typified by Cr-bearing minerals, with vein-related muscovite and chlorite containing about 1 % Cr_2O_3, reflecting the original elevated Cr-

Table 5. Composition of biotite-phlogopites from Pahtavaara.

	1	2	3	4	5	6	7	8	9	10	11
SiO_2 (%)	36.42	35.88	35.63	36.05	36.37	36.00	36.29	37.31	38.85	36.53	(0.99)
TiO_2	1.79	2.02	0.97	2.05	1.66	1.30	1.28	1.08	1.80	1.55	(0.40)
Al_2O_3	12.98	14.84	15.74	14.92	15.04	15.05	14.94	15.20	15.82	14.95	(0.82)
FeO	15.01	14.60	14.81	14.31	14.13	13.09	12.73	12.11	12.66	13.72	(1.07)
MnO	0.14	0.19	0.10	0.11	0.11	0.26	0.12	0.22	0.13	0.15	(0.06)
MgO	12.49	13.82	14.70	14.66	15.40	16.05	16.46	16.47	17.36	15.27	(1.52)
CaO	0.01	0.01	0.02	0.06	0.06	0.05	0.01	0.03	0.01	0.03	(0.02)
Na_2O	0.20	0.28	0.19	0.22	0.32	0.19	0.21	0.28	0.60	0.28	(0.13)
K_2O	9.05	7.45	8.34	8.67	8.68	8.87	8.91	8.72	8.13	8.53	(0.50)
V_2O_3	0.10	0.11	0.11	0.11	0.10	0.09	0.11	0.07	0.08	0.10	(0.01)
Cr_2O_3	0.73	0.19	0.61	0.81	0.51	0.59	0.76	0.57	0.24	0.56	(0.22)
NiO	0.25	0.16	0.28	0.18	0.16	0.16	0.18	0.17	0.30	0.20	(0.06)
BaO	0.24	n.d.	n.d.	n.d.	0.51	0.63	n.d.	0.43	0.80	0.52	(0.21)
Total	89.41	89.54	91.51	92.17	93.06	92.32	91.99	92.66	96.78	92.39	(6.01)
Mg/Fe	1.48	1.69	1.77	1.82	1.94	2.19	2.31	2.43	2.46	2.01	n.d.

Drill core/Depth Mineral

1 = 512/13.7 Biotite
2 = 253/9.6 Biotite
3 = 250/28.0 Biotite
4 = 506/87.9 Biotite

Mg/Fe in atomic proportions.

5 = 506/28.4 Biotite
6 = 506/46.6 Phlogopite
7 = 251/23.7 Phlogopite
8 = 253/6.7 Phlogopite

9 = 508/80.2 Phlogopite
10 = Average (n=9)
11 = Sd. Dev. (n=9)

content of the altered ultramafic host rock (Kerrich, 1983).

In general biotite seems to be more typical of gold deposits in mafic rather than ultramafic lithologies (e.g. Hunt Mine, Kambalda; Neal & Phillips, 1987; Phillips & Groves, 1984). Metamorphic and hydrothermal biotite in mafic and ultramafic rocks appear to be indistinguishable from one another as in highly mineralized Red Lake greenstone belt in Canada. There, biotite in altered deformation zone gives way to sericite as the main expression of potassic alteration where proceeding downgrade from the amphibolite to greenschist facies (Andrews et al., 1986).

Talc

The composition of talc at Pahtavaara is relatively homogeneous, as displayed in Table 6. Only FeO^{tot} and, to a lesser extent, MgO show minor variations and the proportions of immobile elements are low. The MgO content being approximately 26 wt. % is slightly higher but comparable with the overall rock composition. Excluding quartz, talc is the most silica-rich mineral at Pahtavaara, having SiO_2 content of about 59 — 60 wt. %. The low abundances of the immobile elements Al, Ti and Cr suggest that talc at Pahtavaara is of hydrothermal origin (cf. Costa et al., 1980; 1983).

Table 6. Average composition of talc (n=5) from Pahtavaara.

	1	2	3	4
SiO_2 (%)	59.50	(0.52)	60.09	58.74
TiO_2	0.04	(0.04)	0.10	0.00
Al_2O_3	0.83	(0.78)	1.69	0.08
FeO	6.23	(2.08)	8.87	4.47
MnO	0.05	(0.03)	0.10	0.01
MgO	25.83	(1.26)	26.79	24.09
CaO	0.03	(0.02)	0.06	0.00
Na_2O	0.16	(0.17)	0.39	0.00
K_2O	0.01	(0.02)	0.04	0.00
V_2O_3	0.01	(0.01)	0.02	0.00
Cr_2O_3	0.04	(0.03)	0.10	0.02
NiO	0.18	(0.07)	0.30	0.01
Total	92.91	n.d.	93.55	92.36

1 = Average
2 = Sd. Dev.
3 = Maximum
4 = Mimimum

Chlorite and its use as geothermometer

In contrast to talc, chlorite displays marked variations in composition (Table 7). It consists mainly of Mg, Si, Al and Fe but also contains significant amounts of Cr (about 0.5 wt. % Cr_2O_3) reflecting its ultramafic origin. Also the abundance of the other immobile element, namely aluminium, is very high, being up to 20 %. Accordingly, when chlorite is present, as in weakly altered amphibole-chlorite schist, it is the major host of Al. Compared to many other minerals,

Table 7. Average composition of chlorite (n=9) from Pahtavaara.

	1	2	3	4
SiO_2 (%)	28.97	(1.19)	30.70	27.79
TiO_2	0.05	(0.01)	0.07	0.03
Al_2O_3	18.19	(1.59)	20.23	15.46
FeO	11.39	(3.14)	16.00	6.96
MnO	0.13	(0.05)	0.21	0.08
MgO	25.53	(2.39)	29.00	22.43
CaO	0.03	(0.02)	0.08	0.01
Na_2O	0.00	(0.00)	0.00	0.00
K_2O	0.01	(0.01)	0.02	0.00
V_2O_3	0.03	(0.02)	0.06	0.01
Cr_2O_3	0.50	(0.40)	1.45	0.09
NiO	0.20	(0.06)	0.33	0.15
Total	84.99	n.d.	86.77	83.78

1 = Average
2 = Sd. Dev.
3 = Maximum
4 = Minimum

such as biotite, talc and amphibole, the NiO content of chlorite is relative high, at around 0.2 %.

Chlorite compositions have recently been used for geothermometry by Cathelineau and Nieva (1985), who determined temperatures from deep drill holes in the Los Azufres geothermal field in Mexico. The use of chlorite solid solution is based on the correlation between temperature and the tetrahedral AI^{IV} substitution for Si. Kranidiotis and MacLean (1987) studied the compositions of altered, Al-saturated chlorites from Phelps Dodge massive sulphide deposit in Canada and converted the earlier procedure of Cathelineau and Nieva (1985) into the following formula: $T°C = 106Al^{IV} + 18$, where $Al^{IV} = 8\text{-}Si$ formula units (cation formula based on eight $Si + Al^{IV}$ atoms). As Al^{IV} in chlorite also increases with iron enrichment (substitution of Fe for Mg), a correction has to be made; $Al^{IV}_{corrected} = Al^{IV}_{analyzed} + 0.70Fe/(Fe + Mg)$.

This procedure was directly applied to Pahtavaara chlorites, which show replacement of silica by aluminium within the range $Si_{5.65}Al_{2.35}$ to $Si_{6.18}Al_{1.82}$, while $Fe/(Fe + Mg)$ ratios vary from 0.12 for the weakly altered rocks to 0.28 for altered rocks. On the basis of preliminary calculations, formation temperatures for chlorites from weakly altered rocks were 220—240°C, and for altered rocks 260—290°C. Although these values give a reasonable approximation for the temperature during hydrothermal alteration at Pahtavaara in general, it is important to note that the values indicate the formation temperature for chlorite, and not biotite, which is generated at higher temperatures. Besides the limited number of analysis performed, some inaccuracy in calculation may have been caused by the low $Fe/(Fe + Mg)$ ratios of the chlorites from weakly altered rock types. On the whole however, these results are comparable to those obtained by Pankka and Bornhorst (in press) from Kuusamo using the same method. There, calculated temperatures vary from 270°C to 310°C in ore zones and 260—280°C in unmineralized zones and are generally similar to those determined from other gold deposits with various methods.

Plagioclase

Plagioclase is only present in minor amounts but is nevertheless widely encountered. This is reflected chemically by generally low values of Na_2O in the whole-rock analyses. Plagioclase is typically associated with quartz-rich parts of the amphibole rock but may be present in weakly altered types as well. Its presence is also related to the original composition of the rock; in weakly altered types it only occurs in rocks with relative mafic compositions. The common occurrence of

albite in less Mg-rich komatiitic basalts has been documented by Saverikko (1985).

On the basis of the available analyses, plagioclase is compositionally either nearly pure albite or, alternatively, oligoclase with 25 % of anorthite content. Albitic compositions seem to be typical of the metamorphic, greenschist facies assemblage in relatively unaltered komatiites, whereas plagioclase in the altered rock types is either albite or oligoclase.

RARE EARTH ELEMENTS

Geochemical characteristics

The rare earth elements (REE) show distinctive similarities in their chemical behaviour. They are incompatible elements and in igneous processes tend to be enriched in later crystallisation phases. They are generally considered as immobile elements during weathering and alteration processes and are therefore widely used in solving petrogenetic problems such as degree of fractional crystallization and partial melting (e.g. Hanson, 1989; Sun & Nesbitt, 1978). However, there is increasing evidence that, during some alteration processes, the abundances of REE and their distribution patterns may be changed to some degree (e.g. Campbell et al., 1984; Ludden et al., 1984). Accordingly, it is important to evaluate the degree of mobility of these elements during alteration in order to be able to assess the applicability of REE for petrogenetic modelling. The overall gains and losses of REE during hydrothermal alteration depend on the following factors (Humphris, 1984):

(i) The primary REE content in unaltered rock and the distribution of REE in the various mineral phases present, as well as the stability of the mineral phases.

(ii) The concentration of REE in the mineralizing fluid, the partitioning behaviour of REE between the rock and fluid, and the ability of the fluid to transport REE out of the system.

(iii) The ability of secondary minerals formed during the reactions to accommodate the REE released from the original mineral.

The behaviour of REE during hydrothermal alteration associated with gold deposits has been discussed by Kerrich and Fryer (1979) and Kerrich (1983). According to these authors, and also Kerrich and Watson (1984), REE are relative immobile, except under conditions of intense carbonation when the heavy REE are preferentially taken into solution. According to Vance and Condie (1987) heavy REE are relatively stable, whereas the light REE are, in contrast, mobile during hydrothermal alteration processes and may be depleted during alteration as is the case for the Agnico-Eagle gold deposit in Canada (Wyman et al., 1986). Comparable evidence for the mobility of the light REE is also given by Campbell et al. (1984) from hydrothermal alteration pipes below massive sulphide deposits. They have argued that REE mobility increases with the degree of alteration and can therefore be used as a potential exploration method in distinguishing between large and small deposits. Some mobility of these elements has also been observed by Ludden et al. (1984). Therefore, the degree and manner in which REE patterns reflect hydrothermal alteration and mineralization processes is still a matter of debate. In all, it appears that REE behave in an immobile manner during most alteration processes (Nurmi et al., 1991) but some mobility may occur during intensive alteration processes such as carbonation (e.g. Lesher et al., 1985).

REE patterns

Komatiites in general have fairly low REE contents and light REE/heavy REE ratios. Furthermore, they are characterized by a progressive increase in overall REE content and La/Lu ratios from ultramafic through mafic komatiite and tholeiite, indicating that the first type has formed as a result of higher degree of melting (i.e. >50%) of mantle than the later ones (Cullers & Graf, 1984). Similar low REE contents which are close to chondritic values have also been detected for both weakly altered and altered rock types from Pahtavaara, consistent with all of them having a komatiitic origin (Fig. 29).

All rock types at Pahtavaara have gently slop-

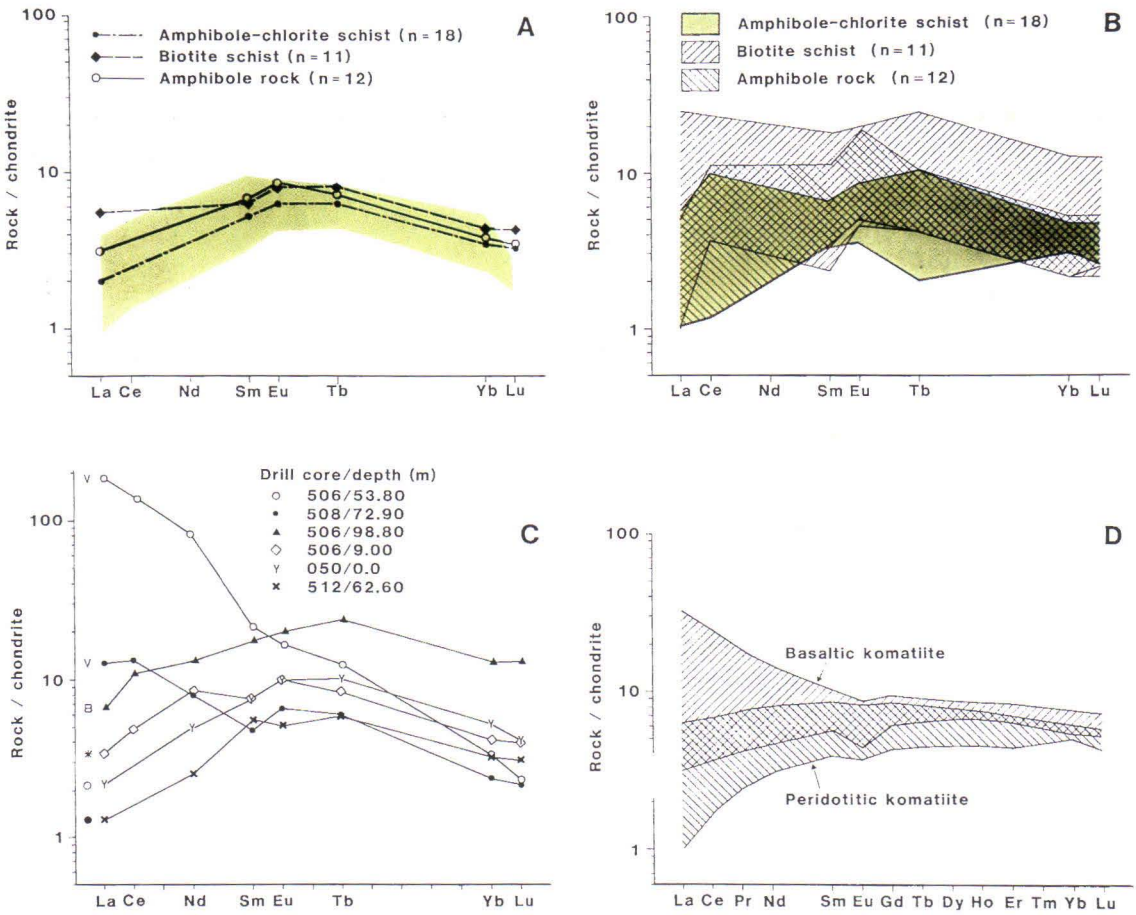

Fig. 29. Chondrite-normalized rare earth element contents of variably altered rocks from Pahtavaara gold deposit and other selected areas.

A; Average compositions of the three major rock types from Pahtavaara. The shaded area represents the field of Sattasvaara komatiites (n = 7) after Lehtonen and Rastas (1988).

B; Field of composition for the three major rock types, Pahtavaara.

C; Selected examples of REE patterns for differently altered rock types, Pahtavaara. Rock symbols shown on the left are as in Figure 17, excluding ○ (= amphibole-chlorite schist with weak talc-carbonate alteration).

D; Compositional field of peridotitic komatiites and basaltic komatiites after Cullers and Graf (1984).

ing heavy REE patterns, and slightly steeper light REE patterns (Fig. 29A). However, the importance of the latter feature is difficult to estimate due to analytical inaccuracies, since the initially low Ce and Nd contents of komatiites are below the detect limit of these elements for the method used. Accordingly, only the higher values were considered to be reliable and practically all the Nd and the lowermost Ce values were omitted in detailed pattern description. However, compositional fields are given for comparison in Fig. 29B, showing that amphibole rocks have a moderately positive Eu anomaly, whereas for other rock types in the study area this might be absent or even negative. Similar variations in komatiitic Eu anomalies of have also been detected by other authors (e.g. Cullers & Graf, 1984). Furthermore, those more mafic samples having the lowest MgO contents appear to have slightly higher REE abundances than similarly altered, more MgO-rich samples, a feature which is inherited from mantle fractionation processes, as described above.

The results obtained in this study are in agreement with those reported by Lehtonen and Rastas (1988) from the western part of the Sattasvaara komatiites (Fig. 29A). The REE pattern shows that these komatiites are depleted in both light and heavy REE. The former feature is interpreted to be an indication of primary magma depletion relative to the light REE. The latter feature may have resulted from the fractionation of garnet during melting of the source (Lehtonen & Rastas, 1988).

In detail, the REE patterns and compositional fields for amphibole-chlorite schists appear to be slightly lower than for more altered amphibole rocks and biotite schists. This feature is in agreement with the enrichment of REE in the biotite schists by leaching other, more mobile elements, resulting in the enrichment of immobile elements through volume decrease. However, if REE were immobile during hydrothermal alteration, respective abundances in amphibole rocks should also be lower due to dilution by other elements (i.e. volume increase). As this is not the case, the formation of amphibole rock requires some REE mobility. However, in spite of this REE patterns and overall low REE abundances in all lithologies still retain features reflecting a common komatiitic origin.

Only two analyses were available from vein material and therefore results are inconclusive. However, it does seem that vein material has been enriched relative to the light REE, whereas the heavy REE have remained relative stable, their slope showing only a minor steepening. The steeper pattern is at least partly related to carbonation, as the sample with the highest CO_2 content (Drill core 506/53.80 m; Fig. 29C) also has the highest light REE content. A similar mobility of light REE compared to heavy REE during carbonation was also demonstrated by Wood et al. (1976) and Campbell et al. (1984). As discussed above, these features are in contradiction with the observation by Kerrich and Watson (1984) according to whom the heavy REE are mobile during carbonation processes. Geochemical data from Pahtavaara suggests that light REE were mobile to some degree during alteration and hence become enriched in the fluid and accommodated into the secondary minerals, especially carbonates.

In summary, the chondrite-normalized REE abundances and patterns are approximately the same for all rock types in the study area, irrespective of variations in degree of alteration. Furthermore, they are also comparable to those reported by Lehtonen and Rastas (1988) from the Sattasvaara komatiites and also similar to the REE pattern of other komatiites (Fig. 29D). The only exception is for Lu, which has somewhat higher contents in this study than the results obtained by the above authors. A possible reason for this is that the REE analyses were performed in different laboratories.

The above features all strongly suggest a common komatiitic origin for all rock types at Pahtavaara, and that hydrothermal alteration has only modified REE patterns to minor extent.

Furthermore, REE appear to have been immobile during the formation of biotite schist, with some evidence for mobilization during the generation of amphibole rock. For intensively carbonated samples and vein material REE mobilization is highly probable. These rocks are relatively enriched in light REE and therefore display steep chondrite-normalized patterns, a feature which may indicate the contamination of the hydrothermal fluid by Archaean basement gneisses. This interpretation may also be related to the high K and Ba contents of altered rocks in the study area, since high values of these elements have been reported also from the Archaean gneiss dome exposed at Möykkelmä, some 4 km north of the study area (Räsänen et al., 1989).

STABLE ISOTOPES

General

Stable isotope analyses of carbonates, which are a major component of a number of gold deposits, can be used to derive information concerning the nature and probable source of fluid involved in the mineralization event. This is based on the assumption that equilibrium isotopic fractionation occurred between the mineralizing CO_2-rich fluid and precipitating carbonates.

Carbon isotopes

The $\delta^{13}C$ (PDB; for definition see p. 10) values for magmatic carbonates generally range between -7 and -3 ‰, whereas seafloor carbonates have values between 0 to +2 ‰, dissolved marine carbonates between -3 and +3 ‰, and organic compounds from -20 to -35 ‰ (Burrows et al., 1986; Colvine et al., 1984; Ohmoto & Rye, 1979).

At Pahtavaara $\delta^{13}C$ values for vein carbonates are between about -2 and -3 ‰ (Fig. 30; Table 8), within the range for magmatic carbonate. Moreover, one analysis of spotted carbonate in weakly altered komatiite (amphibole-chlorite schist) yielded heavier value of -0.40 ‰, which may indicate the existence of some primary sea floor alteration.

The $\delta^{13}C$ values at Pahtavaara are also comparable with the median value of -3.5 ‰ obtained from Australian (Golding & Wilson, 1983) and Canadian gold deposits (Colvine et al., 1988; Wyman et al., 1986). In contrast, carbon isotope determinations from the Saattopora gold deposit near Kittilä typically yield values between -7 and -8 ‰ (Tamminen, in prep.). These are markedly lower than for most gold deposits suggesting a magmatic origin for the Saattopora carbonates. In addition to that, isotope compositions of some carbonates from Saattopora have clearly positive values, up to about +3 ‰, indicating the existence of carbonate sediments in the area. Comparable examples of sedimentary influxes influencing carbon isotope compositions have been described from Timmins, Canada. There vein and replacement carbonates show a general trend towards heavier $\delta^{13}C$ values from -5 ‰ in the outskirts of the district, where carbonaceous sediments are rare, to 0 ‰ in the centre of the Timmins camp, where such sediments are present. These features suggest that the CO_2-bearing fluids reacted with carbonaceous sediments, resulting in the gradual progression towards heavier $\delta^{13}C$ compositions (Colvine et al., 1988).

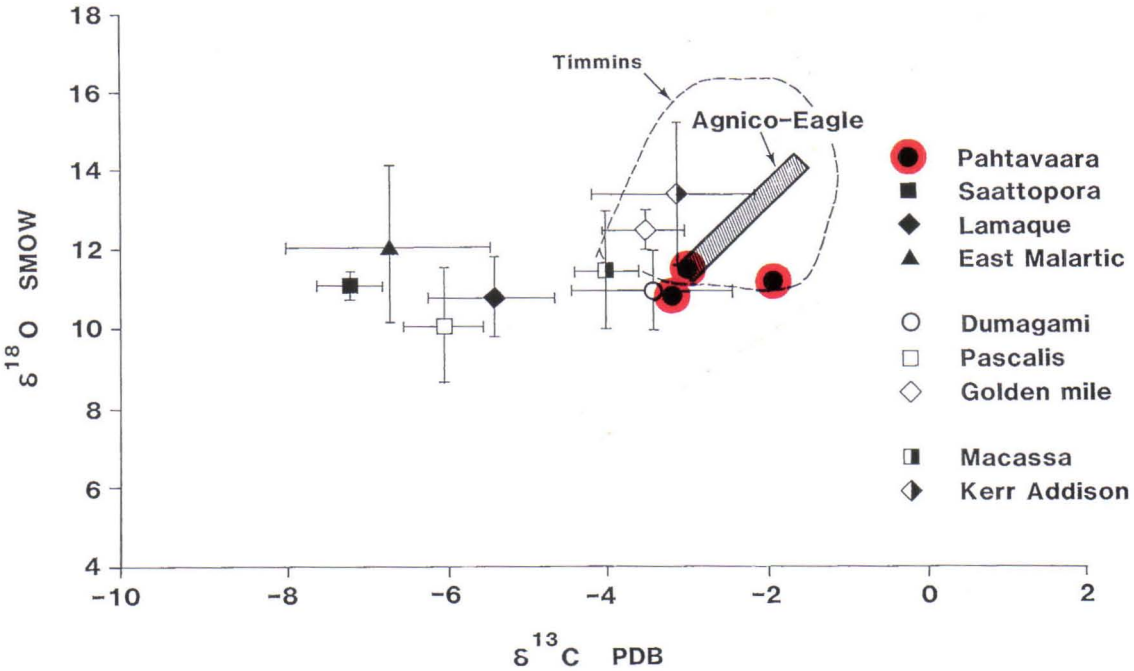

Fig. 30. Carbon and oxygen isotope compositions of carbonates from Pahtavaara and selected gold deposits. Data from Tamminen (in prep.), Golding and Wilson (1983), and Wyman et al. (1986).

Table 8. Stable isotope compositions of carbonates from Pahtavaara. Analysis by J. Karhu.

Drill Core/ Depth (m)	$\delta^{13}C$ (PDB)	$\delta^{18}O$ (SMOW)	Rock type
506/83.00	-1.93	11.22	Carbonate vein in amphibole rock
508/95.70	-2.95	11.47	Talc-carbonate vein in biotite schist
509/16.00	-0.40	---	Carbonate spots in amphibole-chlorite schist (total C)
509/110.9	-3.17	10.82	Talc-carbonate-amphibole vein in biotite schist

In all, the carbon isotope data from Pahtavaara are consistent and comparable with results from major gold deposits, as recently summarized by Colvine et al. (1988). These values are in agreement with both a magmatic (Burrows et al., 1986) or metamorphic origin for the mineralizing fluid (Colvine et al., 1988), but do not unequivocally discriminate between them. However, the existence of carbonaceous sediments at Pahtavaara as argued by Pulkkinen et al. (1986) appears improbable in terms of this data.

Oxygen isotopes

The oxygen isotope compositions of carbonates from Pahtavaara show only minor variation having $\delta^{18}O$ values (SMOW; for definition see p. 10) between +10.8 and +11.5 ‰ (Fig. 30; Table 8). These values are comparable to those from Saattopora (Tamminen, in prep.) and fall well within the range of Archaean gold deposits for which values are typically between +10 to +16 ‰ (Colvine et al., 1984). However, the huge Hollinger-McIntyre deposit at Timmins has values between +3.7 and +5.3 ‰ which, according to Wood et al. (1986), indicates that this deposit was magmatically derived.

In general, oxygen isotope data are difficult to interpret because $\delta^{18}O$ values are subject to modification by water-rock interaction and fractionation of isotopes during analysis. Furthermore, the oxygen isotope values for magmatic and metamorphic fluids are largely overlapping, and the present oxygen results do not discriminate between different genetic models. However, the homogeneous values obtained for many major gold deposits suggest a high fluid to rock ratio and equilibration between the fluid and the wall rock during hydrothermal alteration and deposition of gold (Colvine et al., 1988).

OCCURRENCE OF GOLD AND RELATED ELEMENT ASSOCIATIONS

Mode of occurrence

Gold at Pahtavaara is heterogeneously distributed, tending to be more concentrated towards the southern margin of the alteration zone, where it forms three separate zones. It occurs in both biotite schists and coarse-grained amphibole rock (Figs. 18 and 19C); the latter rock type, together with quartz ± barite veins may form distinct outcrops containing visible free gold, as shown in Figures 4 and 35.

Gold in the poorly-exposed and deeply-weathered biotite schists is related to locally extensive talc-carbonate ± pyrite veins. Consequently, the mode of occurrence of gold can only be studied in detail only from drill core samples. A section containing the highest gold values from drill core 511 is shown in Figure 31. There, the most distinctive geochemical differences between the gold-rich biotite schists and the average composition of the four least altered samples (shown by the horizontal line in Fig. 31; cf. Table 1; anal. 1) are relative enrichments of $Fe_2O_3^{tot}$, K_2O and CO_2, and depletion in MgO, CaO and SiO_2. More specifically, typical $Fe_2O_3^{tot}$ values are about 7 — 8 wt. % higher, and K_2O contents ca. 2 % higher than in the reference samples. CO_2 content is variable but lower in the biotite schists than in other, less altered varieties. Average relative depletions for biotite schist are 5 % for MgO, and 3 % for CaO, whereas SiO_2 has variable but generally lower values. Besides these, increased Au values appear to be closely associated with high contents of S and Ba (Figs. 32 and 33). This is partly related to the increased content of pyrite but also to the presence of barite.

On the basis of the above features, gold in biotite schist appears to be associated with the sulphide component in which it may occur as inclusions (Fig. 34). Commonly, however, it is finer-grained, as microscopically visible gold has been found only rarely. Further evidence supporting the close association of gold with pyrite (and chalcopyrite) in biotite schist is provided by analyses of separated sulphide fractions from samples having high Au contents, with values of Au

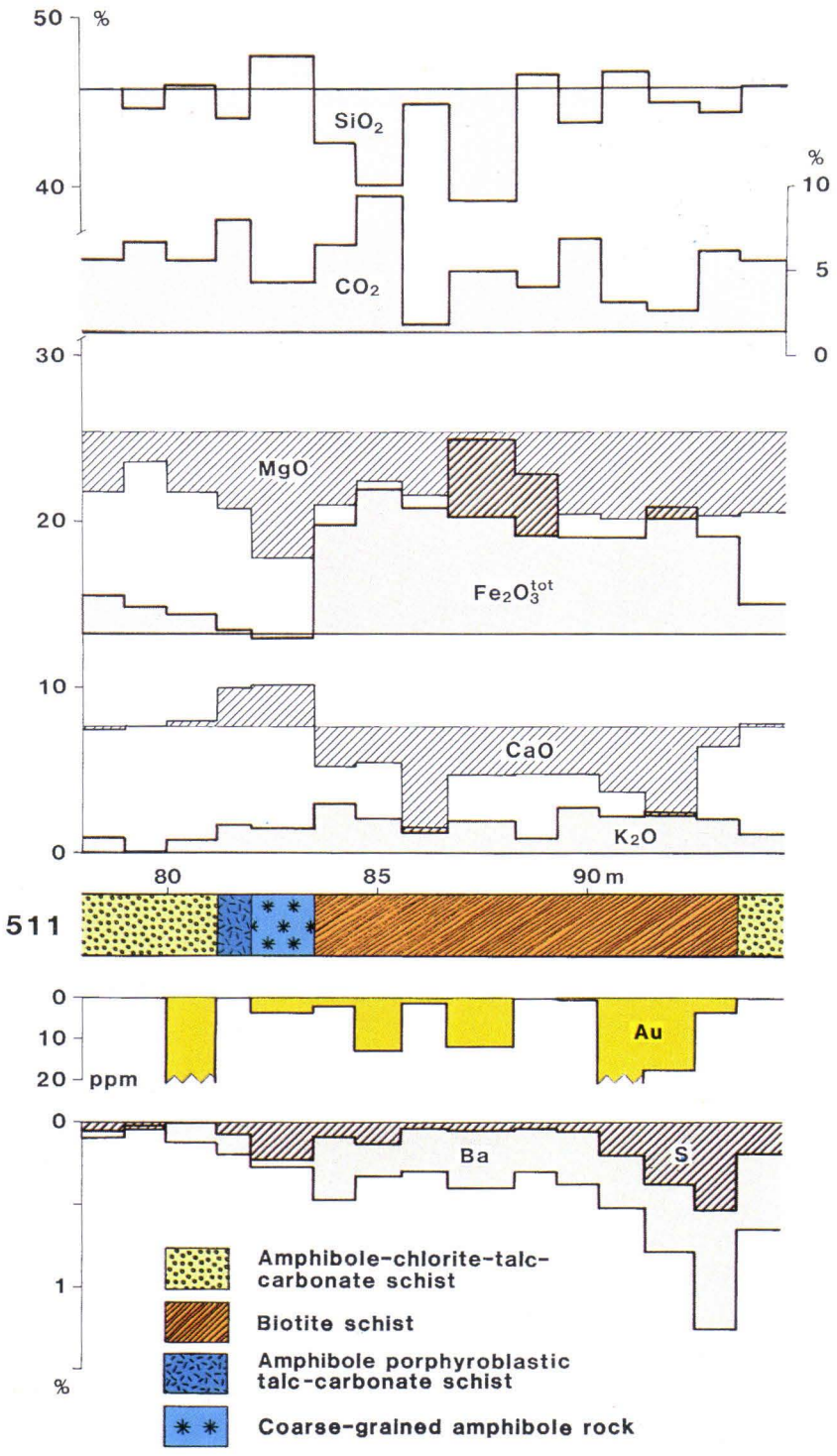

Fig. 31. Selected major and trace element abundances from the highly mineralized section of the drill core 511 over interval between 78.00 and 94.70 m at Pahtavaara. Compositions are recalculated on a volatile-free basis and compared with the average of the four least altered samples from the study area, shown by horizontal lines (cf. Table 1; anal. 1). Note positive correlation between Au and S plus Ba.

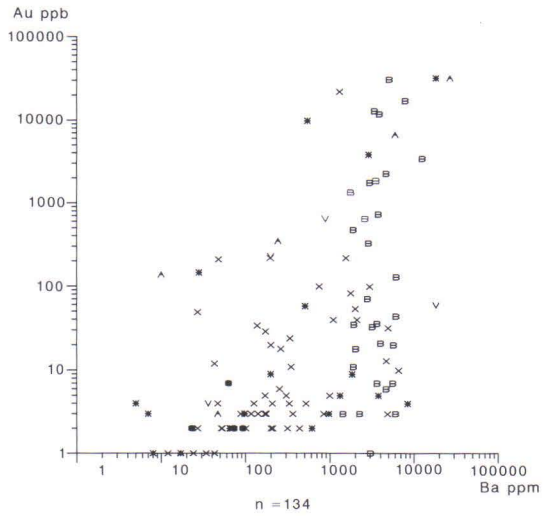

Fig. 32. Relation of Au and Ba contents for variably altered rocks from Pahtavaara gold deposit. Rock symbols as in Figure 17. Note the logarithmic coordinates.

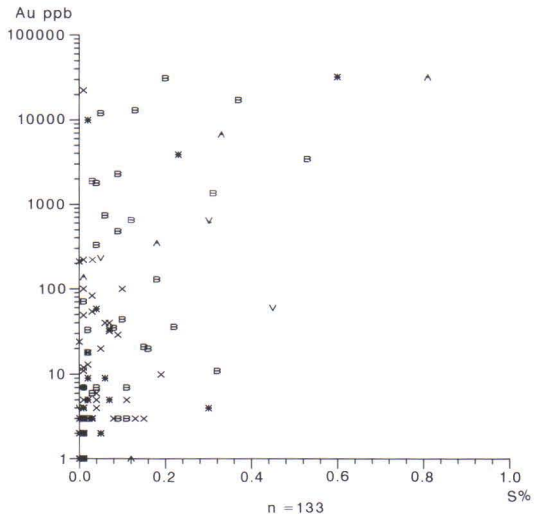

Fig. 33. Relation of Au and S contents for variably altered rocks from Pahtavaara gold deposit. Rock symbols as in Figure 17. Note the logarithmic coordinates for Au.

up to 85 ppm having been determined. This indicates that biotite schist having in excess of 5 % modal pyrite (correlative to ca. 2.5 % of S) would be of economic importance, corresponding to Au grades of 4 ppm. Additionally, Hulkki (1990) has reported high Au values, up to 800 ppm in pyrite and up to 400 ppm in chalcopyrite from individual grains at Pahtavaara. However, since the pyrite and corresponding S content in the more gold-rich samples are generally lower, some of the gold in biotite schist probably occurs in native form. A significant proportion of gold in the biotite schists is also associated with magnetite.

In contrast, gold in coarse-grained amphibole rock occurs in the native state, locally as large aggregates (up to 1 cm in length). Characteristically, these are preferentially associated with the contact areas between amphibole rock and associated quartz ± barite veins (Fig. 35). However, some gold is probably related to pyrite as well. Together these features, and in particular the coarse grain size of gold, suggest that gold in the coarse-grained amphibole rock represents remobilization and second stage of enrichment, an assertion also supported by the purity of coarse gold (Table 9).

Table 9. Average composition of coarse-grained gold from Pahtavaara (5 analyses).

Au (%)	99.02
Ag	0.07
Cu	0.05
Bi	0.25
Te	0.03
Fe	0.01
Hg	0.03
Total	99.46

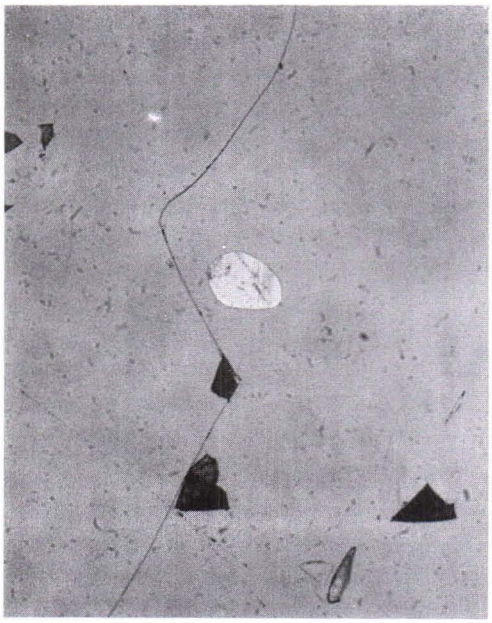

Fig. 34. Gold occurring as inclusion in pyrite from biotite schist. Drill core 508/115.75 m. Field of view is 90 µm. Photographed by K. Kojonen.

Fig. 35. Visible gold (yellow) associated with the contact zone between the quartz-barite vein (white) and coarse-grained amphibole rock (green). Exploration Trench 5; for location, see Figures 3A and 4A. Field of view is 10 cm in width.

Elemental associations

The relationship between gold and other elements associated with the Pahtavaara gold deposit were studied using a correlation matrix for samples having enrichments 10 times or more relative to the estimated background, i.e. > 20 ppb (Table 10). In addition, a varimax rotated factor analysis (Table 11) was carried out in order to specify the interelement ratios indicative of hydrothermal alteration and gold enrichment. Correlation coefficients for samples with more than 20 ppb gold show high positive correlation between Au and Ba at a 0.05 % level of significance (values >0.501, cf. Koch & Link, 1970), and weak correlations with S and SiO_2 at a 5 % level of significance (values 0.264 — 0.366). Gold also has a moderate negative correlation (values 0.366 — 0.501 and 1 % level of significance) with LOI (loss of ignition) and weak negative correlations with CO_2 and MgO.

Table 10 also shows high correlations between Al_2O_3 and TiO_2 (0.88179) which indicates a similar geochemical behaviour (i.e immobility) during hydrothermal alteration. Marked positive correlations also exist between $Fe_2O_3^{tot}$ and K_2O, between Ba and SiO_2, and between CaO and CO_2, and conversely negative correlations of CaO with $Fe_2O_3^{tot}$, Al_2O_3 and TiO_2. The first of the above correlations clearly corresponds lithologically to biotite schist, the second to quartz ± barite veins, and the third to amphibole rock. The negative correlations of $Fe_2O_3^{tot}$, Al_2O_3 and TiO_2 with CaO probably indicate the dilution of these elements by addition of Ca (plus other elements) associated with an overall volume increase during the formation of amphibole rock. It is interesting to note that correlation between $Fe_2O_3^{tot}$ and Ba for gold-enriched samples is insignificant. However, when taking all 134 analyses into consideration, correlations of Ba between K_2O and $Fe_2O_3^{tot}$ are high (at a 0.05 % level of significance) and moderate (at a 1 % level of significance), respectively. This indicates the importance of the barite formation during the ore-forming processes, possibly via the remobilization of Ba from biotite. The high correlation between CaO and CO_2 obviously indicates introduction of Ca during carbonation.

When applying factor analysis to a set of data from various kinds of mineralized rocks, the main interest is in recognizing the elements that characterize both the nature of the hydrothermal alteration and the association of gold with other elements. The model presented in Table 11 with 15 variables and 5 factors explains 78.15 % of the total variance. The first factor has high or moderate negative loadings (in decreasing order) for Ba, Au, K_2O, $Fe_2O_3^{tot}$, S and MnO and low positive loadings for CaO and MgO. This 'gold factor' appears to be lithologically related to biotite schist (high $Fe_2O_3^{tot}$ and K_2O), and is also associated mineralogically with barite and pyrite.

The second, 'immobile element factor', implies mutually similar geochemical behaviour for Al, Ti and Cr during hydrothermal alteration. The third, 'volatile factor', which seems to reflect carbonation, has high positive loadings for LOI and CO_2, high negative loadings for SiO_2, and low positive loadings for CaO and MnO. The fourth, 'amphibole rock factor', is shown by high positive loadings for CaO and Na_2O associated with high negative MgO. P_2O_5 and MnO are related to the fifth factor with a low eigenvalue.

In all, both correlation coefficients and factor analysis show the close association of gold with Ba, K, S, and Fe during hydrothermal alteration and mineralization, consistent with deductions based on mineral paragenesis. However, the relative importance of different stages of alteration for the deposition of gold cannot be determined.

Table 10. Correlation factors for samples with > 20 ppb gold from Pahtavaara (n=47).

	SiO_2	TiO_2	Al_2O_3	Fe_2O_3	MnO	MgO	CaO	Na_2O	K_2O	P_2O_5
SiO_2	1.00									
TiO_2	-0.39	1.00								
Al_2O_3	-0.35	0.88	1.00							
Fe_2O_3	-0.31	0.25	0.26	1.00						
MnO	-0.06	-0.34	-0.51	0.08	1.00					
MgO	-0.64	-0.10	-0.04	0.04	0.14	1.00				
CaO	-0.05	-0.33	-0.45	-0.74	0.13	-0.03	1.00			
Na_2O	0.63	-0.29	-0.27	-0.32	0.05	-0.19	-0.07	1.00		
K_2O	-0.30	0.63	0.59	0.38	-0.07	-0.22	-0.39	-0.42	1.00	
P_2O_5	-0.22	-0.02	-0.27	0.07	0.40	0.31	0.04	0.00	-0.05	1.00
Au	0.30	-0.21	-0.14	0.12	0.08	-0.35	-0.05	-0.03	-0.05	-0.04
S	0.36	-0.23	-0.21	-0.04	0.18	-0.21	-0.02	0.08	-0.19	-0.02
CO_2	-0.70	-0.10	-0.21	-0.21	0.32	0.65	0.52	-0.32	-0.07	0.35
LOI	-0.78	-0.02	-0.09	-0.08	0.22	0.75	0.38	-0.40	-0.08	0.31
Ba	0.50	-0.33	-0.25	0.08	0.33	-0.36	-0.21	0.30	0.02	-0.03
Cr	-0.47	0.20	0.39	0.08	-0.37	0.49	-0.11	-0.19	-0.01	-0.13

	Au	S	CO_2	LOI	Ba	Cr
Au	1.00					
S	0.31	1.00				
CO_2	-0.32	-0.25	1.00			
LOI	-0.37	-0.29	0.96	1.00		
Ba	0.59	0.47	-0.40	-0.48	1.00	
Cr	-0.22	-0.23	0.11	0.22	-0.35	1.00

Table 11. Factor loadings in a 5-factor model, after rectangular varimax rotation (loadings less than 0. 2 excluded). Based on 134 samples from Pahtavaara. Logarithmic values used for Au and Ba.

Variable	FACTORS					Communality
	1	2	3	4	5	
SiO_2			**-0.94**			0.96
TiO_2		**0.88**				0.78
Al_2O_3		**0.90**				0.86
Fe_2O_3	**-0.62**	0.22		-0.54	-0.33	0.84
MnO	-0.43	-0.37	0.24	0.26	**-0.59**	0.79
MgO	0.30			**-0.84**	0.21	0.86
CaO	0.38	-0.28	0.27	**0.74**		0.86
Na_2O				**0.71**		0.54
K_2O	**-0.70**	0.46				0.74
P_2O_5					**-0.81**	0.71
Au	**-0.78**	-0.23				0.68
S	**-0.53**	-0.39			0.27	0.55
CO_2			**0.96**			0.98
LOI			**0.97**			0.97
Ba	**-0.87**			-0.37	0.31	0.75
Cr		**0.61**				
Cumulative percentage of total variance	21.98	41.20	58.76	70.85	78.15	
Eigenvalue	3.52	3.08	2.81	1.94	1.17	
F1	-Ba, -Au, -K_2O, -Fe_2O_3, -S					
F2	Al_2O_3, TiO_2, Cr					
F3	LOI, CO_2, -SiO_2					
F4	MgO, CaO, Na_2O					
F5	-P_2O_5, -MnO					

CHEMICAL MASS BALANCE

Introduction

Mass balance calculations have been widely applied in recent years when determining gains and losses of chemical components accompanying hydrothermal alteration (e.g. Kerrich, 1983; MacLean & Kranidiotis, 1987). These calculations have been carried out according to the procedure of Gresens (1967) and its recent modification by Grant (1986).

Gresens (1967) pointed out that these calculations are often made on a quantitative basis, that is by simply comparing element abundances between unaltered and altered varieties. This kind of examination includes the tacit but often untenable assumption of constant volume. This assumption is particularly unjustified and can result in gross misinterpretation of chemical data, if alteration is accompanied by major changes of chemical components plus volatiles. As this is clearly the case at Pahtavaara it is therefore essential to take volume changes into account. According to Gresens (1967), volume changes for any alteration reaction can be solved by incorporating specific gravity and volume factors into mass balance calculations.

Calculation of volume changes

Determination of volume change is based on the isochemical behaviour of certain elements that are known to be relatively immobile in most geological environments, such as Al, Ti, Hf, Zr, Sc, Y (see Costa et al., 1983; Kerrich, 1983; Kerrich & Fyfe, 1981). Some mobility of these elements has nevertheless been demonstrated by Ludden et al. (1984), and Robert and Brown (1986) in association with Archaean Au-mineralization. The latter authors based their interpretation on the occurrence of Al- and/or Ti-bearing minerals, namely tourmaline, ilmenite and rutile, in gold-rich veins. However, the relative immobility of these elements is generally accepted by most authors (e.g. Costa et al., 1983; Steefel, 1987).

In this study, Al and Ti (expressed in oxides) were found to behave in an immobile manner and therefore are the most suitable elements for determining the degree of hydrothermal alteration. The immobility of these elements is shown by their constant ratios (Fig. 17), in spite of variations in absolute abundances, and by their high positive mutual correlation coefficients (Table 10). Constant elemental ratios also suggest a homogeneous protolith at Pahtavaara.

Immobile elements can also be used to distinguish between different protolith compositions in a heterogeneous geological environment such as at the Macassa (Kerrich & Watson, 1984) and Hollinger mines (Kerrich, 1983) in Canada. In the latter, initially trondhjemitic, basaltic and ultramafic host rocks cluster into three different groups with respect to immobile major and trace elements and can therefore be separated from each other in spite of the pervasive alteration.

As discussed earlier in this study, a homogeneous primary komatiitic composition has been inferred for the Pahtavaara deposit. The mean composition of the four least altered rocks (Table 1; anal. 1) was used as a reference standard against which the compositions of altered rocks were compared in mass balance calculations. These samples were chosen because they have low values of CO_2 (no carbonation), K_2O and Ba (no biotitization), and high MgO abundances. Specific gravity data were available for only about half of the samples (App. 1) and hence

were only used in calculations where available. However, the differences in overall density were relatively small and caused only a minor effect on the results, the maximum deviation in specific gravity between the average of the four least altered samples and the most intensively altered samples being only 4.5 %. Consequently, volume changes as indicated by the volume factor (f_V) between unaltered (A) and altered (B) rocks were determined using the following equation from Gresens (1967) and Grant (1986):

$$(1)\quad f_V = \frac{C(Al_2O_3)^A}{C(Al_2O_3)^B} \times \frac{g^A}{g^B},$$

where g = specific gravity [kg/dm³] and
C = proportion of element [wt. %].

In this study $C(Al_2O_3)^A$ and g^A are the mean of compositions of the four least altered samples (Table 1; anal. 1).

The enrichment factor (F_e), for determining the gains and losses, is defined by Equation 2 as follows:

$$(2)\quad F_e = \frac{X_n}{C^A} + 1, \text{ where}$$

$$(3)\quad X_n = \frac{f_V \times C^B \times g^B}{g^A} - C^A$$

Accordingly, chemical gains and losses of elements are expressed by enrichment factors F_e indicating their relative changes, e.g. an enrichment factor of 1.5 means a 50 % increase compared to the original abundance of an element and a factor of 0.8 corresponds to a 20 % decrease (Figs. 36 and 37).

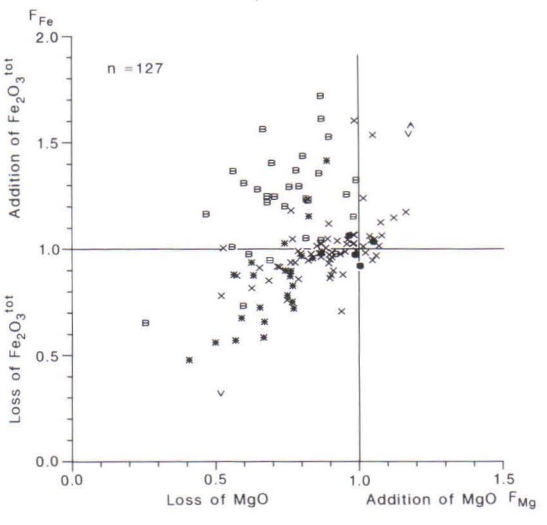

Fig. 36. Additions and losses of MgO and Fe_2O_3 relative to enrichment factors F_{Mg} and F_{Fe} according to mass balance calculations, following the procedure of Gresens (1969). Immobility of Al is assumed. Due to the high enrichment factors of the low-alumina amphibole rocks their results are not shown. For details, see text. Rock symbols as in Figure 17.

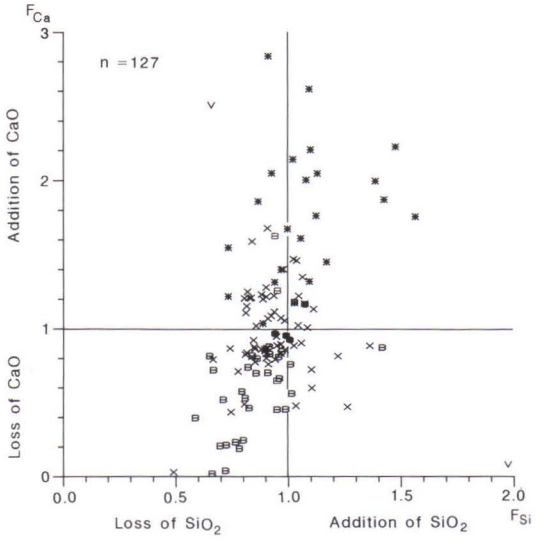

Fig. 37. Additions and losses of SiO_2 and CaO relative to enrichment factors F_{Si} and F_{Ca} according to mass balance calculations, following the procedure of Gresens (1969). Immobility of Al is assumed. Due to the high enrichment factors of the low-alumina amphibole rocks their results are not shown. For details, see text. Rock symbols as in Figure 17.

Chemical gains and losses

Chemical additions and losses of elements are represented relative to the enrichment factor F_e using Equations 1 to 3 and assuming the immobility of aluminum during hydrothermal alteration and a homogeneous primary composition. When considering the results of the mass balance calculations (Figs. 36 — 38) it is important to note that because they are normalized relative to aluminium content (ie. volume factors), the differences between the low-alumina amphibole rocks and other rock types with higher Al contents are emphasized. Geologically high volume factors indicate that the elements in these rocks have been largely mobilized into their present positions. In other words, low-alumina types with high volume factors represent veins or cavity fillings into which the relatively immobile aluminium was transported only in minor amounts.

Mass balance calculations show that biotite schists record volume decrease of approximately 10—30 % (f_V = 0.9 — 0.7; average 0.89), whereas volume changes for amphibole rocks are, while more variable, typically positive. More specifically, volume changes for high-alumina amphibole rock are generally between -20% and +10 % (f_V = 0.8 — 1.1), but ranging up to 550 % (f_V = 5.5) for low-alumina types. Volume change appears to be proportional to the SiO_2 and CO_2 contents to at least some extent, due to the appearance of quartz and/or carbonate veins.

The decrease in volume in biotite schist shows that immobile elements have been relatively enriched by leaching (Fig. 17), whereas the other, more mobile chemical constituents of the altered rocks have been either removed or added to the system, depending on the nature of the hydrothermal fluid and the mobility of elements. In all, leaching predominated over precipitation during the alteration, resulting in the formation of biotite schist. In contrast, the lower proportions of immobile elements in the amphibole rocks have been diluted by the addition of other elements.

Examples of additions and losses of some characteristic major elements included in the hydrothermal alteration are presented in Figures 36 and 37 and summarized in Figure 38. The results for these elements are represented in terms of enrichment factors (e.g. F_e for $Fe_2O_3^{tot}$ is symbolized by F_{Fe}) relative to different rock types in the study area. Accordingly, as shown by Figure 36, Fe for biotite schist displays an increase of up to 70 % (F_{Fe} = 1.7) compared to the four least altered samples but is generally between 20 — 40 % (F_{Fe} = 1.2 — 1.4). In contrast, high-alumina amphibole rock has typically been depleted relative to Fe by 10 to 50 % (X_{Fe} = 0.9 — 0.5). Practically all samples at Pahtavaara, with the exception of the low-alumina amphibole rocks have been depleted in MgO, as shown by low enrichment factors, between 0.5 — 0.9 (Fig. 36).

Enrichment factors for SiO_2 (F_{Si}) and CaO (F_{Ca}) are variable and different rock types plot in different parts of the compositional field. As seen in Figure 37, high-alumina amphibole rock is generally enriched relative to SiO_2 by factors between 1 and 1.5. High F_{Si} indicates saturation relative to silica which is expressed mineralogically by the appearance of quartz. However, some depletion of SiO_2 also occurs in samples that are unusually Al- and Ti-rich.

Amphibole rocks are typically enriched relative to CaO by a factor about 2, whereas biotite schists possess factors from about 0.9 down to zero, indicating extreme loss of CaO during alteration. Of these, the highest F_{Ca} is related to samples with high carbonate contents.

In order to obtain a more comprehensive understanding of the nett gains and losses between different rock types in general, enrichment factors for the averaged compositions in Table 2 were calculated (Fig. 38). The results are expressed relative to the four least altered samples, with the reference composition being indicated by the horizontal line. For comparison, mass bal-

ance factors for one of the above four samples is shown in Figure 38A. When comparing the results it is important to note that elements occurring in large proportions at Pahtavaara show only a minor percentage deviation from the reference composition, in spite of the substantial change in mass. However, major relative gains take place most easily in those elements which were initially present only at effectively negligible concentrations, such as K, Na and Ba.

Weakly altered amphibole-chlorite schist containing variable amounts of talc and carbonate is enriched relative to Ba, Au, K and CO_2 by factors between 5 and 10, whereas additions of S, Na and Mn are lower (Fig. 38B). All of these elements are present in only minor concentrations in the least altered rocks. Therefore minor additions can markedly affect their relative proportions and hence also their enrichment factors. In contrast, several elements which comprise a dominant part of the rock are depleted by a factor of about 0.9. These include Si, Ca and Mg, whereas there has been a slight addition of Fe. Even though the relative changes of these elements in terms of enrichment factors are small, the total differences in whole-rock composition may be significant.

Enrichment factors for the weakly altered amphibole porphyroblastic talc-chlorite schist (Fig. 38D), which represents a transitional type between the least altered amphibole-chlorite schist and the amphibole rock, are generally similar to those for weakly altered amphibole-chlorite schists (Fig. 38B). The only exceptions to this are Ca and P which have been added to the amphibole porphyroblastic talc-carbonate schist.

The major enrichments in the biotite schist shown in Figure 38C are in Au, Ba, K, S and CO_2 all of which are characteristic of alteration patterns in major gold deposits (Colvine et al., 1984; Groves et al., 1987). Iron has been increased by a factor of 1.2, whereas the other dominant components, including Si, Mg and Ca have been depleted by factors of 0.81, 0.75 and 0.65, respectively. Marked depletion also exists relative to Na. Comparable enrichments in Fe appear to be relative rare in the literature, but have been documented from the Crixas gold deposit in Brazil, in association with gains in K and Ba (Thomson, 1986) and also at Yellowknife (Kerrich & Fyfe, 1981).

The high-alumina amphibole rocks have been enriched in Au, Ba, K, S, Na, CO_2, Ca and Si, and conversely, depleted in Mg, Fe and Cr (Fig 38E). When compared to the biotite schist, major differences are the enrichment of Si by factor 1.1, Ca by ca. 1.6, and Na by 4.6, while opposing trends include losses of Fe (F_{Fe} = 0.88). The enrichment factor for K in high-Al amphibole rock is unusually high (F_K = 9.6), but still considerably lower than in biotite schist (F_K = 61). It is interesting to note that the above value for low-Al amphibole rock is only about 1.1.

As shown by textural and mineralogical evidence, hydrothermal alteration resulting in the formation of biotite schist predates the formation of amphibole rock. Accordingly, some amphibole rocks had previously experienced biotite alteration. High K_2O contents in some amphibole rocks may therefore be interpreted as inherited from a biotite schist precursor, and hence, that potassium was not necessarily added at a later stage, during amphibole rock formation. This proposal is also consistent with the highly variable K_2O contents in the amphibole rock.

The high volume factors of the low-alumina amphibole rock (average f_V = 3.1; cf. Appendix 1) indicate that these rocks represent cavity fillings or veins and are enriched relative to a number of elements (Fig. 38F). Only the immobile elements, namely Cr and Ti display lower values than in the weakly altered amphibole-chlorite schist. This suggest that the proportions of these elements have been diluted by other elements added into system. However, the constant ratios between Cr and Ti have remained approximately the same. Other interesting features include the high proportions of S and Ba which probably become increased during the formation of amphibole rock. Mineralogically this is ex-

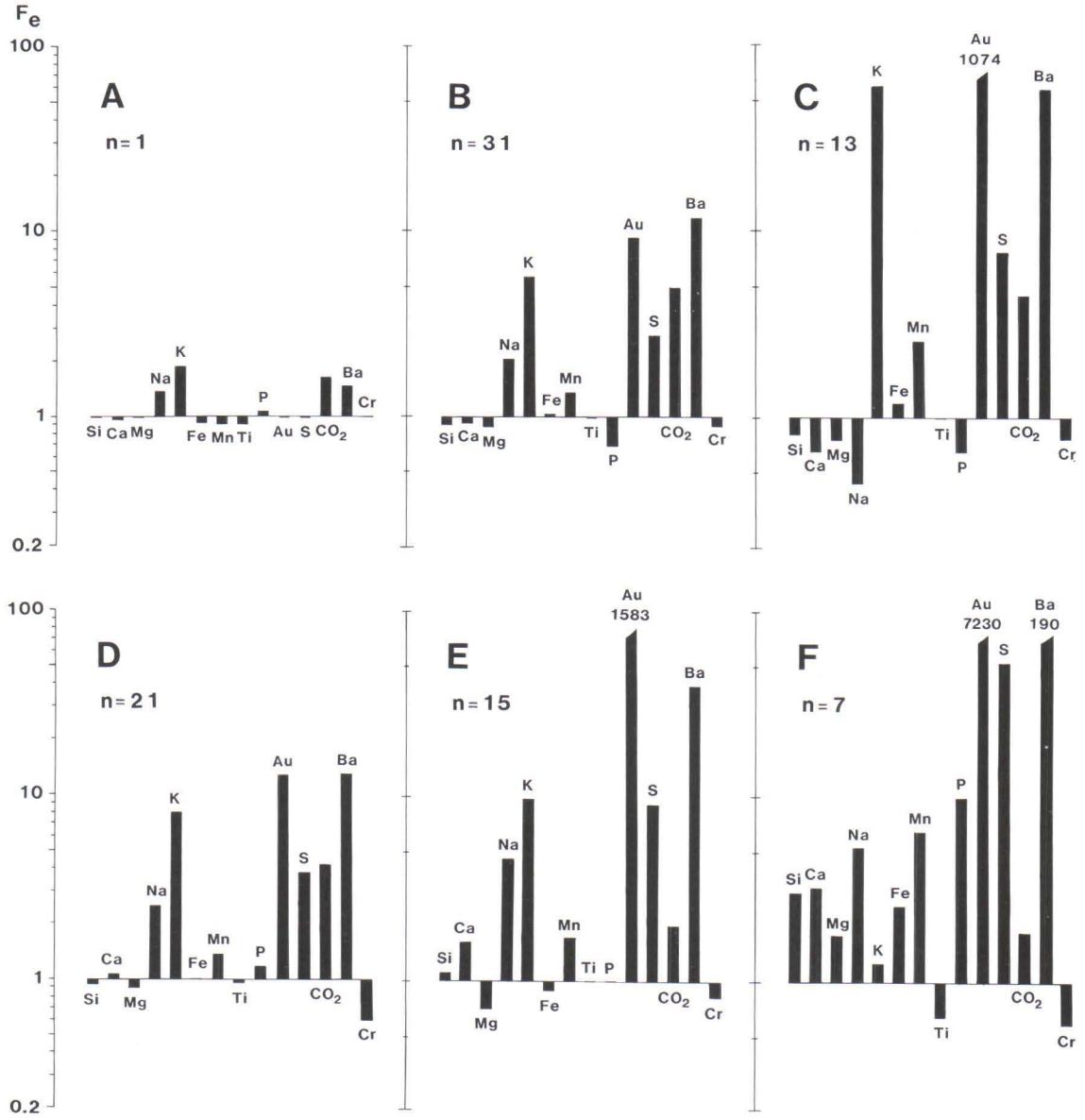

Fig. 38. Average enrichment factors (F_e) for variably altered rock types from Pahtavaara gold deposit, calculated according to the procedure of Gresens (1969). Note the logarithmic coordinates.

A; Example of least altered sample of the amphibole-chlorite schist. Drill core 512/62.60 (App. 1; anal. 133).

B; Weakly talc-carbonate altered amphibole-chlorite schist.

C; Biotite schist.

D; Amphibole porphyroblastic talc-carbonate schist.

E; High-alumina amphibole rock (Al_2O_3 >4 wt. %).

F; Low-alumina amphibole rock (Al_2O_3 <4 wt. %). For further details, see text.

pressed by the common occurrence of barite and pyrite. Furthermore, high enrichment factors of CO_2 in biotite schist compared to amphibole rock indicate that carbonate was removed from the system during the formation of the latter through decarbonation reactions.

DISCUSSION

Komatiites as host rock

Komatiite-associated gold deposits form a minor but important group of greenstone-hosted gold deposits, as described in general above. Examples include those in various parts in South Africa (Houston, 1987; Pearton, 1979; 1982; Viljoen, 1984), Dome mine (Fryer et al., 1979) and Kerr-Addison mine (Kishida & Kerrich, 1987) in Canada, and Harbour Lights, Tower Hill (Skwarnecki, 1987), Mt Percy (Mueller & Groves, 1991) and Marvel Loch (Mueller, 1988) in Western Australia. Besides these, komatiites also occur in close proximity to a number of other important gold deposits including the Detour Lake mine (Marmont, 1986), Duport mines (Smith, 1986) and the Campbell Red Lake and Dickenson mines (MacGeehan & Hodgson, 1982), Madson and Starrant-Olsen deposits in the Red Lake area (Andrews et al., 1986), all in Ontario, the Hunt mine at Kambalda (Neall & Phillips, 1987; Phillips & Groves, 1984), and the Kolar gold deposits in India (Hamilton & Hodgson, 1986).

All the above examples are hosted by Archaean rocks and therefore differ from the rocks of the Sattasvaara komatiites which recent studies have considered to be early Proterozoic in age (e.g. Räsänen et al., 1989). In contrast to other Proterozoic greenstone belts, komatiites which probably indicate the existence of deep-seated, crustal-scale fault-shear systems (Groves et al., 1987) are relatively common rock types in CLGB. They form ribbon-like, and locally extensive occurrences extending from northern Norway (i.e. Karasjok greenstone belt; Often, 1985) to Sattasvaara and Peurasuvanto and to the eastern part of the Lokka reservoir (Räsänen, 1989).

The occurrence of large scale structures in Lapland is shown by distinctive NE — trending ductile shear zones (e.g. Korkiakoski et al., 1988; Ward et al., 1989). Additional evidence for faults having connections down to the mantle is provided by the existence of lamprophyre dikes in northern Kittilä in association with structurally controlled gold deposits (Härkönen & Keinänen, 1989). Together with the occurrence of exposed Archaean basal domes, these features suggest that the CLGB can be interpreted as an intracratonic rift (Korkiakoski et al., 1987; Lanne, 1979).

The importance of komatiites as potential gold-enriched source rocks and in exerting a chemical control of the localization of greenstone-hosted gold deposits has been emphasized by Groves et al. (1985) and Keays (1984). Ultramafic rocks provide favourable chemical environment in that they have the greatest capacity to undergo intense carbonation due to their high total abundance of cations, namely Fe, Mg and Ca, which combine with CO_2 to form carbonates. Hence the original ferro-magnesian mineral content of the rock is a factor controlling the amount of CO_2 that can be added to a rock (i.e. the degree of carbonation) (Kerrich, 1983; Roberts, 1987). Green carbonate assemblages due to Cr-bearing mica (fuchsite) and ferroan dolomite are also characteristic of a number of gold related ultramafic rocks (Colvine at al., 1988; Kishida & Kerrich, 1987). Comparable rocks, termed chromian marbles, have also been described from Kittilä (Pekkala & Puustinen, 1978).

Even though all lithologies are capable of hosting individual gold ore bodies within the green-

stone belt, the most typical lithologies are mafic volcanites, often associated with significant amounts of komatiites (Roberts, 1987). Furthermore, post-volcanic intrusions are very common in mineralized areas, constituting more than 25 % of host rock lithologies, compared to their relative scarcity elsewhere in the greenstone belts (Colvine et al., 1984; Hodgson et al., 1982).

In summary, the common occurrence of komatiites and major, crustal-scale fault-shear systems, combined with the widespread, pervasive nature of hydrothermal alteration, all show that the early Proterozoic CLGB has many similarities to its Archaean equivalents, in spite of its younger age. These features also suggest that ore forming processes have been comparable to each other and, importantly, indicate that there is good potential for the existence of other Proterozoic gold deposits in association with major structural features in the greenstone belts of Lapland. This is already evident from the exploitation of the Saattopora deposit in Kittilä, Viscaria in Sweden and Bidjovagge in Norway, and the existence of numerous other small gold mineralizations in Lapland. Furthermore, Roberts (1987) has claimed that the sparse occurrence of gold deposits in Proterozoic greenstone belts may relate to the lower level of exploration activity in those areas. Accordingly, increased interest for exploration for gold in Proterozoic rocks has taken place for instance in Saskatchewan, Canada (Coombe, 1984; Thomas, 1987). However, the typical shallow water environment indicated during sedimentation and volcanism for the Lapponian rocks of the CLGB, and the similarity to the platform-phase greenstones, as defined Groves and Batt (1984), may not be conductive to the favour the development of giant gold deposits. Additionally, the time interval for the general development for the CLGB appears to be exceptionally long compared to its Archaean counterparts, and may have some negative consequences for ore forming processes.

Hydrothermal alteration

General features

Hydrothermal alteration is a type of metasomatism in which minerals become replaced by others of different composition through the in situ addition and/or removal of chemical components via the direct interaction between rocks and hydrothermal fluid. The final rock composition depends largely upon the degree of interaction between fluid and rock, lithology and the ambient physio-chemical conditions (Colvine et al., 1988; Rose & Burt, 1979).

Alteration types formed as a result of hydrothermal activity can be related and divided into (1) early hydrothermal metamorphism (primary sea-floor alteration according to Kerrich, 1983) during accumulation and burial of a supracrustal sequence and (2) later dynamothermal metamorphism accompanying regional deformation and the emplacement of granitoids. Gold deposits are typically related to the development of deformation zones broadly coeval with the latter type of alteration (Barley & Groves, 1987). In practice, however, primary sea-floor alteration and hydrothermal alteration caused by metamorphic fluid are difficult to separate on the basis of their chemical characteristics. However, some distinction can be made on the basis of the stratiform zonation of the former (Barley & Groves, 1987; Kerrich, 1983) as discussed below in more detail. Evidence for primary sea-floor alteration within the CLGB is seen in stratiform occurrence of albitized, Na and carbonate altered rocks (Lehtonen et al., 1985; Ward et al., 1989; see also Eilu & Idman, 1988; Pankka et al., 1991).

Komatiites in particular are susceptible to early metasomatic changes and hydrothermal metamorphism, because their high heat content which

may result in thermal erosion, partial melting, and assimilation of intercalated lithologies as demonstrated at Kambalda, Western Australia (Groves et al., 1986; Korkiakoski, 1985). Furthermore, the pyroclastic nature of komatiites at Pahtavaara may also have promoted alteration by sea-water due to their presumably high permeability, which may be one of the most important factors in controlling the efficacy of mineralizing fluids during the generation of gold deposits. The above feature, combined with sporadic occurrence of pillow lavas (cf. Saverikko, 1985) also suggests a shallow water depth during the eruption of these lavas as claimed by Often (1985) for pyroclastic komatiites in northern Norway. Again, this may promote the alteration effect since the elevation of water temperature is then relatively easier.

As discussed earlier in more detail, all the altered rocks in the study area are considered to be hydrothermally altered komatiites. To reiterate, evidence for this includes (1) constant ratios between immobile elements, (2) similar low REE patterns close to the chondritic values for all the variably altered rock types, (3) obvious mineralogical and chemical gradations between all the rock types, (4) the local occurrence of less altered blocks within the Pahtavaara alteration zone, and (5) the occurrence of altered rocks as a heterogeneous intercalated association. Furthermore, the elevated Cr_2O_3 contents of biotite and chlorite (generally between 0.5 and 0.8 %) also reflect the high Cr content of the original rock, i.e. komatiitic parentage (cf. Hollinger mine, Timmins; Kerrich, 1983).

The greenschist facies metamorphic grade of the least altered komatiite is indicated by the typical amphibole-chlorite assemblage. Apart from some rare chromites, no primary minerals have been detected at Pahtavaara, and even serpentine, which is indicative of the low-grade alteration (mainly hydration) of ultramafic rock, is absent. Hydrothermal processes at Pahtavaara have been divided into (1) biotitization (potassic alteration), with the coeval formation of talc-carbonate ± pyrite veins and (2) later amphibole overgrowth (calc-silicate alteration) and associated quartz ± barite veins and pods. In the following discussion, these two types of alteration are described separately.

Biotitization

Biotitization or, more generally, potassic alteration, together with the introduction of CO_2, S and H_2O are the most characteristic geochemical features of gold deposits (Colvine et al., 1988). Examples of biotite altered gold deposits in Canada include the Duport mine (Smith, 1986), Madsen and Starrant-Olsen mines (Durocher, 1983) and several other deposits in the Red Lake area (Andrews et al., 1986). Australian deposits are represented for example by the Hunt mine, where basalts have been altered into biotite-rich rocks, (Neal & Phillips, 1987; Phillips & Groves, 1984), and Harbour Lights plus Tower Hill (Skwarnecki, 1987; 1988). Of these, the last two deposits are hosted by altered komatiites, the present mineralogy consisting dominantly of two types (i) phlogopite/Mg-biotite-chlorite-quartz-ankerite-magnetite schist and (ii) fuchsite/sericite-ankerite-quartz ± arsenopyrite schist. The latter type is more mineralized and forms discrete horizons within a broad halo of the former. This suggests that biotitization represents a less favourable and intensive type of alteration with respect to the deposition of gold than does the process leading to the formation of fuchsite.

According to Skwarnecki (1987) biotitization associated with Harbour Lights and Tower Hill mines postdates the peak of metamorphism. In contrast, Houston (1987) is of the opinion that potassic alteration at the Barbrook prospect in the Barberton greenstone belt, South Africa, represents an early stage of hydrothermal metamorphism (i.e. primary sea-floor alteration) during which MgO was depleted and CO_2 and K_2O were enriched in komatiites. Accordingly, early mica formation structurally weakened parts of the volcanic units and these zones became im-

portant for the localization of later mineralization during or after shearing.

At Pahtavaara, the broadly stratiform pattern of the whole alteration zone suggests the existence of early hydrothermal metamorphism. However, as the results of experimental studies of sea-water interaction with ultramafic rocks are inconsistent with the alteration patterns documented from Pahtavaara, this process is considered unlikely. Hajash and Chandler (1981) have shown that Fe, Si, and Ca are depleted and Mg is enriched by sea-water alteration, which is opposite to the trends observed for these elements at Pahtavaara. According to Eilu and Idman (1988) sea-floor alteration of the greenstone complex at Palovaara included enrichment in Na and depletion in K and Mn. Comparable features have also been documented from the Hollinger mine, Timmins, where early alteration of ultramafic rocks by sea-water involved loss of Si, Fe, Mn, Mg, Na and K, with gains of Sr plus volatiles. This differs from the subsequent alteration and emplacement of veins during dynamothermal metamorphism while these rocks experienced massive gains of Au, CO_2, K, Rb and Ba, and minor additions of Fe, Ca and Mn (Kerrich, 1983). As only these latter features correspond to the observed geochemical trends in the study area, it is concluded that biotitization at Pahtavaara does not represent a sea-floor alteration but rather took place during the regional metamorphism. However, the possibility of some kind of the sea-floor alteration can not be totally dismissed.

At Pahtavaara, the coeval nature of talc-carbonate veins and biotitization is indicated by a local gradation from nearly monomineralic biotite to biotite-amphibole-chlorite assemblages with increasing distance from the vein, i.e. further from the influence of fluids (Fig. 10). Further evidence for this is given by the heterogeneous occurrence of the veins, since they crosscut one another as well as biotite schist in very irregular way. This suggests that all the material was relatively plastic, with occasional changes in the location of permeable zones into which hydrothermal fluids were focused. In contrast, however, Barley and Groves (1987) have claimed on the basis of textural evidence from a number of localities in Western Australia that talc-carbonate alteration of ultramafic rocks may predate the peak of regional dynamothermal metamorphism.

Geochemically biotitization and associated talc-carbonate alteration at Pahtavaara include additions of K, CO_2, Fe, S, Ba, Au, Mn, W, Sr and Te and depletions of Mg, Ca, Na, Zn, Co and, to a lesser extent, Si (Figs. 24 and 38). Mineralogically these features are related to the break down of chlorite, the formation of Ba-bearing biotite, intensive carbonation and formation of talc. Biotitization may be simply a consequence of the carbonation of chlorite to Fe-carbonate, as suggested by Kishida and Kerrich (1987).

Possible mineralogical reactions during biotitization and talc-carbonate alteration of ultramafic and mafic rocks include the following (Colvine et al., 1988; Kerrich, 1983):

(4) $2Mg_3Si_2O_5(OH)_4 + 3CO_2 \rightarrow Mg_3Si_4O_{10}(OH)_2 + 3MgCO_3 + 3H_2O$
Serpentine — Talc — Magnesite

(5) $(Mg,Fe)_6Si_4O_{10}(OH)_8 + 6CaCO_3 + 6CO_2 \rightarrow 6(Mg,Fe)Ca(CO_3)_2 + 4SiO_2 + 4H_2O$
Chlorite — Calcite — Ferroan dolomite — Quartz

(6) $(Mg,Fe)_5Al_2Si_3O_{10}(OH)_8 + 3SiO_2 + 1/3Fe_3O_4 + 2H^+ \rightarrow$
Chlorite — Quartz — Magnetite

$2KAl(Mg,Fe)_3Si_3O_{10}(OH)_2 + H_2O + 2H^+$
Biotite

(7) $2Mg_3Si_4O_{10}(OH)_2 + 1/2(Mg,Fe)_5Al_2Si_3O_{10}(OH)_8 + K^+ \rightarrow$
Talc Chlorite

$(Mg,Fe)_7Si_8O_{22}(OH)_2 + KAl(Mg,Fe)_3Si_3O_{10}(OH)_2 + 3H_2O + H^+$
Anthophyllite Biotite

The formation of serpentine is a typical alteration feature of ultramafic rocks (Eckstrand, 1975), commonly being an essentially isochemical process with respect to most elements, only involving substantial addition of H_2O (cf. Donaldson, 1981). The presence of serpentine, which is stable only at low CO_2 contents (Rose & Burt, 1979), indicates relatively low degree of alteration. Accordingly, it is totally absent from the intensively hydrothermally altered area at Pahtavaara (cf. Equation 4). However, it might have been abundant in the Pahtavaara komatiites prior to the intensive alteration, since it is common in weakly altered amphibole-chlorite schists elsewhere within the Sattasvaara komatiites (Saverikko, 1985).

Moreover, the presence of serpentine appears to be related to the original rock composition. For example at Kambalda, antigoritic serpentine is the most characteristic mineral of the magnesian-rich, weakly altered (hydrated) cumulate komatiites but it is absent from less-magnesian spinifex-textured komatiites showing the similar alteration (Lesher, 1983).

Equations 5 and 6 are more typical for mafic rather than in ultramafic compositions, whereas the development of hydrothermal biotite as represented in Equation 7 is associated with higher metamorphic grades and includes a substantial addition of K_2O to the host rock (Colvine et al., 1988; Smith, 1986).

Amphibole growth

In spite of their close resemblance to the Badblaas-type basaltic komatiite described by Viljoen and Viljoen (1969), the amphibole rocks at Pahtavaara are considered to be hydrothermally altered rock type (cf. Viljoen et al., 1983). On the basis of textural evidence (e.g. lack of NE — SW trending areal schistosity) the formation of the amphibole rock postdates biotitization.

Pulkkinen et al. (1986) have argued that coarse-grained amphibole rock (termed tremolite rock) originated from chemogenic carbonate sediments deposited in a subaqueous rift, in the proximity of a volcanic vent area during a hiatus in the komatiitic volcanism. These were then recrystallized during metamorphism, resulting in the formation of tremolite rocks.

However, in this study the above interpretation was found to be unlikely for the following reasons (i) a general lack of carbonate and other sediments in unaltered areas, (ii) similar $Al_2O_3/TiO_2/Cr$ ratios between the amphibole rocks and associated komatiites, (iii) relatively high proportions of the above mentioned immobile elements compared to carbonate sediments (cf. Kishida & Kerrich, 1987; Turekian & Wedepohl, 1961), (iv) high Ni content of amphibole rock, (v) similar low REE contents and patterns to other rock types, and (vi) carbon and oxygen isotope compositions. A komatiitic parentage is therefore affirmed for all the altered rock types at Pahtavaara.

Feasible decarbonation reactions during the formation of amphibole overgrowth are as follows (Colvine et al., 1988; Kerrich, 1983):

(8) $5(Mg,Fe)_3Si_4O_{10}(OH)_2 + 6CaCO_3 + 4SiO_2 \rightarrow 3Ca_2(Mg,Fe)_5Si_8O_{22}(OH)_2 + 6CO_2 + 2H_2O$
Talc Calcite Quartz Tremolite-actinolite

(9) $5Ca(Mg,Fe)(CO_3)_2 + 8SiO_2 + H_2O \rightarrow Ca_2(Mg,Fe)_5Si_8O_{22}(OH)_2 + 3CaCO_3 + 7CO_2$
Ferroan dolomite Quartz Tremolite-actinolite Calcite

Several gold deposits originally hosted by komatiitic rocks are now represented by coarse tremolite rocks, such as the Athens mine in Zimbabwe (Fabiani, 1984), where mineralized lodes typically consist of sulphide-rich quartz and more mineralized tremolite-chlorite schist, complexly interfolded with unmineralized talc-chlorite schist. Due to the lack of any preferred orientation in this 'coarse tremolite ore' it is postulated that the sulphide-rich gold mineralization of the original vein-type deposit become enriched into structural low-pressure sites after tectonism.

Comparable amphibole overgrowth at Pahtavaara is considered to have taken place during a later stage of deformation and metamorphism and to represent decarbonation and calc-silicate alteration of previously carbonated and/or biotitized komatiites. This type of alteration has also geochemical similarities with »replacement skarn gold deposits» described by Mueller (1988) and Mueller and Groves (1991).

Metamorphism and deformation

The metamorphic grade of the host rock to the gold mineralization is an indicator of depth of burial, with the prevailing mineralogical assemblage being dependent on primary composition plus intensity and nature of hydrothermal processes.

The role of metamorphism in mineralizing processes and its relationship to the individual gold deposits are generally poorly studied and therefore poorly understood. However, most greenstone-hosted gold deposits occur in greenschist facies environment (cf. Groves et al., 1985) although mineralizations in higher, amphibolite facies terranes are also relatively common (Mueller & Groves, 1991). Some of the better known examples of the latter include the Madsen and Starrett-Olsen mines in Red Lake area (Andrews et al., 1986; Durocher, 1983), the Musselwhite deposit at Opapimiskan Lake (Hall & Rigg, 1986) in Canada, and the occurrences in the Kolar gold fields of India (Hamilton & Hodgson, 1986).

In addition to that, several other gold mines are surrounded by rocks metamorphosed in amphibolite facies. However, in these cases the mineralization appear to be overprinted by lower retrograde mineral assemblages consistent with greenschist facies temperature — pressure conditions. Examples of these are Detour Lake (Marmont, 1986) and Duport deposits (Smith, 1986) in Ontario, and Victory mine at Kambalda, Western Australia (Clark et al., 1986).

The relationship of biotitization to metamorphism and hydrothermal alteration within the Red Lake greenstone belt in Ontario has been clearly documented by Andrews et al. (1986). There, several gold deposits associated with regional deformation zones are hosted by both greenschist and amphibolite facies domains, the alteration varying systematically along the deformation zones as a function of metamorphic grade. Accordingly, biotite gives way to sericite as the main expression of potassic alteration when going downgrade from amphibolite to the greenschist facies. Furthermore, biotites in the metamorphic and alteration assemblages are

petrographically and compositionally indistinguishable. On the basis of these features Andrews et al. (1986) have concluded that the formation of biotite is a result of both metamorphism and potassic alteration. However, these results are not directly applicable to the Pahtavaara gold deposit as the above mineralogical variation in the Red Lake area is mainly based on mafic volcanic assemblages, although still belonging to the tholeiitic-komatiitic series.

Some effects on alteration mineralogy may also be attributed to the observation that biotite in altered rocks appears to be more characteristic of mafic than ultramafic rocks. For example, the basalts at the Hunt mine, Kambalda, have been intensively biotitized, whereas the overlying komatiites contain biotite only in minor amounts (Neall & Phillips, 1987; Phillips & Groves, 1984).

According to Jolly (1982) the appearance of tremolite-actinolite marks the lower boundary of the greenschist facies for komatiites in the Abitibi greenstone belt in Canada. Likewise, because tremolite-actinolite is the dominant amphibole in the Sattasvaara komatiites and represents the result of regional metamorphism, the metamorphic grade is also considered to be greenschist facies (cf. Tyrväinen, 1983). However, the Pahtavaara gold deposit appears to be at least locally characterized by a locally higher, amphibolite grade metamorphism in comparison to the surrounding regional greenschist facies metamorphism. This is shown by the common occurrence of biotite (and anthophyllite) which is according to Colvine et al. (1988) an indication of higher grade metamorphism (cf. Equation 7). However, biotite may also occur in greenschist facies rocks (Jolly, 1982). Additional evidence for the higher, amphibolite facies metamorphism within the Pahtavaara alteration zone is given by the local occurrence of Ca-plagioclase (anorthite content about 25 %) and the presence of aluminous amphibole (Mg-hornblende) which, according to Jolly (1982), is considered to represent the initiation of amphibolite facies. However, since it is impossible to distinguish between the metamorphic and hydrothermal amphiboles Pahtavaara, their compositions cannot be used in determining the metamorphic grade (cf. Evans, 1982). Furthermore, the Al-content of amphibole is highly variable, as discussed elsewhere, and appears to be related primarily to the availability of Al and also the capacity for different minerals to host it.

Moreover, the primary MgO content of metamorphosed komatiites may also be reflected into composition of amphibole, as at Kambalda, where metamorphosed amphibole is actinolitic in the less-magnesian spinifex-textured komatiites but tremolitic in the more magnesian cumulate komatiites (Lesher, 1983). This may explain why actinolite is more characteristic in weakly altered Pahtavaara komatiites than tremolite, because in terms of MgO content they are comparable to the spinifex-textured komatiites at Kambalda.

In all, the above features indicate that the present mineralogical assemblage at Pahtavaara is a result of the combined effects of metamorphism and hydrothermal alteration, although detailed determinations of metamorphic conditions during the mineralizing event cannot be made. However, the regional metamorphic grade is of greenschist facies, with locally hydrothermal alteration effects corresponding to a higher, probably amphibolite facies metamorphic grade.

According to a number of recent studies, deformation zones containing highly altered rocks played an important, if not fundamental, role in the formation of gold deposits (Colvine et al., 1988; Groves & Phillips, 1987; Groves et al., 1985). Evidence for the structural control of gold mineralizations has also been presented for Finnish Lapland (Härkönen & Keinänen, 1989).

Deformation zones can be divided with increasing depth into brittle, brittle-ductile, and ductile, depending on the presence or absence of fault breccia and the abrupt or gradual offset of marker surfaces (Ramsay, 1980). Of these, the transition to ductile deformation styles at intermediate depths corresponds approximately to the

greenschist — lower amphibolite facies boundary. Furthermore, it is characterized by replacement veins and simple shear zones, whereas brittle and brittle-ductile deformation is characterized by extensional veins (Colvine et al., 1988).

Colvine et al. (1988) have concluded that the komatiite-hosted lower to intermediate level gold deposits are characterized by biotite and anthophyllite with minor talc, tremolite, Cr-mica and chlorite, whereas higher level deposits lack both biotite and anthophyllite. When comparing these features to the observations from Pahtavaara, it appears that biotite schists and associated talc-carbonate veins may have formed at deeper level than the coarse-grained amphibole rocks, and may represent generally ductile deformation at amphibolite facies metamorphic grade. Accordingly, associated talc-carbonate veins represent replacement type of veins.

In contrast, formation of amphibole rock is more consistent with brittle-ductile deformation with extensional structures. This is shown by the occurrence of extensional veins formed at least partially as open space fillings. Chemically this is indicated by the low contents of immobile elements in the veins and the low-alumina amphibole rock.

Unfortunately the determination of bedding planes is generally impossible within the mineralized area due a combination of factors including the primary homogeneous nature of the rocks, alteration, poor exposure, and the lack of intercalated sediments. However, it appears that the alteration zone is roughly parallel to primary bedding and is bounded in the north by the contact zone between pillowed komatiitic lavas and pyroclastic rocks of the same composition. Therefore the ENE — trending alteration zone differs from the regional NE — SW schistosity by about 20 degrees (Fig. 3B).

More detailed examples of the structural features in the study area are given in Figure 4, where both amphibole-chlorite schist and biotite schist show an intensive NE — SW schistosity. In contrast, this feature is not evident in the amphibole rock, which appears to be related to later NNW — SSE structures, possibly resulting from the formation of tectonic cavities into which amphibole growth and associated quartz veins formed.

Model for the enrichment of gold

The major geological and geochemical features associated with the enrichment of gold at Pahtavaara are summarized in Figure 39 and Table 12. Mineralization evidently took place during two geochemically distinct stages and included (1) biotitization and coeval formation of talc-carbonate ± pyrite veins, and (2) amphibole overgrowth in association with quartz ± barite veins and lenses. The first stage of hydrothermal alteration, **biotitization** (potassic alteration), was controlled by the combined effects of (i) high permeability of the original komatiitic tuffs compared to the associated pillow lavas, and (ii) development of the NE-SW regional schistosity. Together these features resulted in the formation of a structurally controlled channelways into which hydrothermal fluids were focused during metamorphism (cf. Colvine et al., 1984; 1988; Groves & Phillips, 1987; Kerrich, 1983). However, the existence of some primary sea-floor alteration during volcanism, as shown by stratiform albitized rocks in other areas of the CLGB (Ward et al., 1989) cannot be totally ruled out at Pahtavaara.

On the basis of metamorphic mineral parageneses and the generation of replacement-type talc-carbonate ± pyrite veins, gold precipitation appears to have taken place during biotitization under greenschist/amphibolite facies conditions during or immediately after the peak of metamorphism. It thus occurred at a relatively deep level accompanied by ductile deformation and

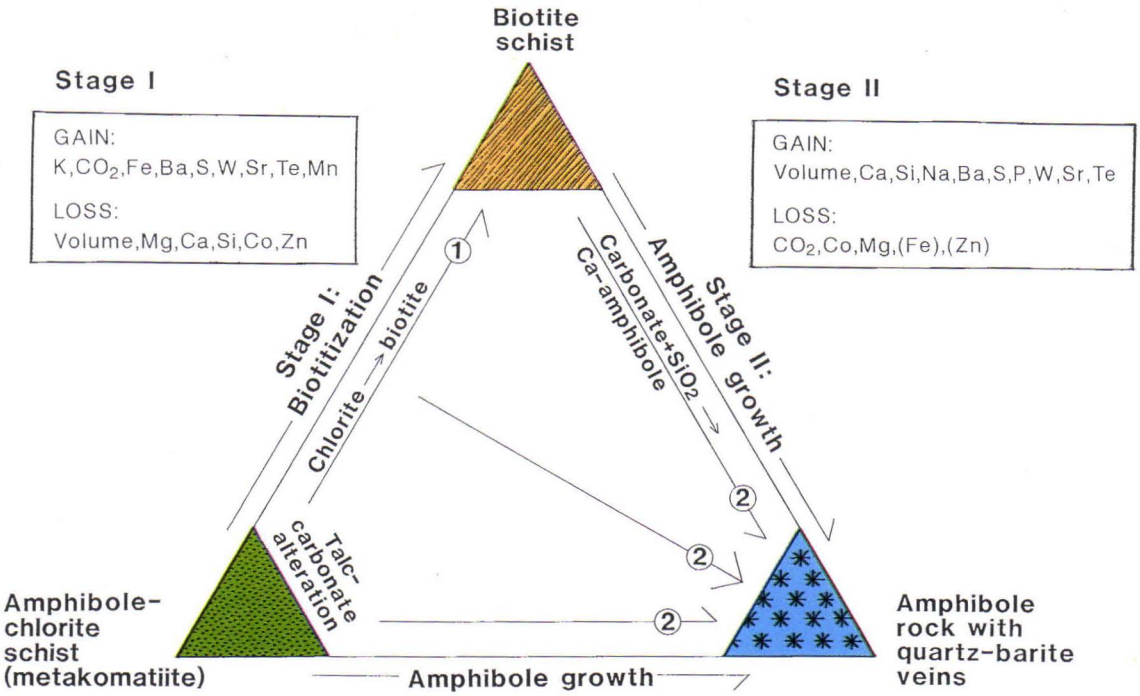

Fig. 39. Schematic diagram of the major chemical and mineralogical changes associated with the different stages of hydrothermal alteration in the Pahtavaara gold deposit. For comparison, see Table 12.

probably largely in response to fluid-wall rock interaction, with synchronous deposition of gold and Fe-sulphides and/or magnetite (cf. Groves et al., 1985). This stage of hydrothermal alteration involved massive introduction of CO_2-H_2O, K and Fe with minor enrichments in Ba, Te, Au, S, W and Sr, and a concomitant depletion of Mg, Ca, Co and, to a lesser extent, Si.

Amphibole overgrowth (calc-silicate alteration) represents the second stage of gold mineralization event. It postdates the biotitization and included mobilization and second stage of enrichment of gold as shown by its pure composition and the large grain size. The mass balance calculations and constant ratios but lowered proportions of immobile elements, together with the structural interpretation have indicated that the formation of quartz and barite-related amphibole rock took place in the structurally controlled zones of dilatation caused by late stage shearing under brittle-ductile deformation. Geochemically the generation of coarse-grained and non-schistose amphibole rock involved addition of Si, Ca, Na, Ba, Te, Au, S, P, W, and Sr and depletion in CO_2, Co and possibly Mg, Fe and Zn.

The amphibole overgrowth probably formed as a result of decarbonation reactions between carbonates formed during the earlier biotitization and related vein formation, and silica supplied by the Si- and Ca-rich hydrothermal fluids. Variations in alteration geochemistry and mineralogy between the two major alteration types is probably related to the evolution of mineralizing fluids and shear zone formation (cf. Barley & Groves, 1987). Accordingly, during the early stage of alteration, resulting in the formation of the biotite schist and coeval replacement-type talc-carbonate veins, deformation was initially ductile and associated with shear zones. A later brittle-ductile stage of deformation resulted in the

Table 12. Summary of major alteration features at the Pahtavaara gold deposit.

FEATURES \ ALTERATION STAGE	STAGE 1: BIOTITIZATION	STAGE 2: AMPHIBOLE GROWTH
Primary host rock	Pyroclastic komatiite (now amphibole-chlorite schist)	Pyroclastic komatiite (partly biotitized)
Altered mineralogy	Biotite-chlorite-magnetite±carbonate ±amphibole±albite±Bi-Se-Te minerals	Amphibole±chlorite±talc±carbonate±biotite± albite±pyrite
Alteration geochemistry	Gain of *K, Fe, CO_2, Ba, S, W, Sr, Te, Mn* Loss of *Mg, Ca, Si, Co, Zn* Constant Al/Ti ratios and REE	Gain of *Ca, Si, Na, Ba, S, P, W, Sr, Te* Loss of *CO_2, Co, Mg, (Fe), (Zn)* Constant Al/Ti ratios and REE
Dominant ore type	Au *(fine, magnetite-pyrite-associated)*	Au *(coarse, native)*
Vein mineralogy	Talc-carbonate±pyrite±albite	Quartz-amphibole±barite±pyrite±albite
Type of veining	Replacement	Extension
Control of mineralization	Primary permeability and shearing	Structurally controlled permeability and fluid flow
Timing	Peak to post-peak of metamorphism and deformation	Retrograde stage of metamorphism
Metamorphism	Greenschist/amphibolite facies	Greenschist facies
Deformation	Ductile	Brittle-ductile
Hydrothermal fluid	Reducing	Oxidizing
Remarks		Decarbonation

generally NNW — trending lenses and extensional quartz ± barite veins, accompanied by remobilization of gold.

Mineralizing fluids responsible for the generation of Archaean gold deposits are very similar in all cratons; according to stable isotope and fluid inclusion data from quartz veins, these fluids typically had low salinity and were CO_2-H_2O-rich, with an estimated trapping temperature being approximately 300 — 350 °C at the depth of 4 — 12 km (Colvine et al., 1988; Ho et al., 1985; Groves & Foster, 1991). Similar fluid compositions may therefore be expected at Pahtavaara even though the relevant physical and chemical properties have not been determined in detail. Although the hydrothermal alteration included at least two recognizeable stages, some estimation of conditions of formation is given by the chlorite geothermometer, using the method of Cathelineau and Nieva (1985) and its later modification by Kranidiotis and MacLean (1987). Preliminary calculations show that the temperature during the formation of chlorite for weakly altered rocks at Pahtavaara was 220 — 240°C, and 260 — 290°C for the altered rocks. However, as biotite is considered to have formed at higher temperature than chlorite, these results give only minimum temperatures for the hydrothermal processes resulting in biotization and gold enrichment.

Further deductions concerning the chemical conditions and changes during the deposition of gold, and the nature of the hydrothermal fluid can be made on the basis of general solubility relations and prevailing mineral parageneses. Accordingly, during the biotitization and talc-carbonate alteration the ore fluid was CO_2-H_2O-rich and slightly reducing, as suggested by the stability fields of existing mineral parageneses, which are analogous to the other potassium-enriched and pyrite-rich gold deposits (cf. Kerrich, 1983). However, the fluid was probably poor in S because of the relative small amounts of pyrite and other sulphides and, conversely, the common occurrence of magnetite. Precipitation of gold may have been caused when the reducing fluid reacted with more oxidized, i.e. previously carbonated rock.

During the later stage of alteration, which resulted into the formation of the amphibole rock, the fluid become poor in CO_2 and silica-saturated, as indicated by the appearance of free quartz. Furthermore, the abundance of sulphate as barite and the local occurrence of haematite suggest that the fluid become more oxidizing during the later stage of hydrothermal alteration (cf. Cameron & Hattori, 1987). This general trend towards more oxidizing fluid during hydrothermal alteration may indicate an increased magmatic influx during the mineralization process (cf. Sillitoe, 1991). The characteristic occurrence of barite may be related to the high Ba content of biotite in the biotite schists from which it was evidently remobilized by reaction with SO_4^{2-} in ore fluid. However, Holland and Malinin (1979) have stated that while precipitation of barite may take place simply by cooling below a temperature of 350 °C, it may be redox controlled as well.

In general, gold mineralization may be related to wider cratonization processes and crustal development, with both magmatic and metamorphic processes having played an important role in the concentration of gold. These processes may have been connected with devolatilization of the lowermost part of the greenstone belt under conditions of granulite facies metamorphism, as has been emphasized by several authors (Cameron, 1988; Groves & Phillips, 1987; Kerrich & Fyfe, 1981). However, it is difficult to discriminate between magmatic and metamorphic processes deep in the crust and both processes are broadly coeval with the emplacement of late tectonic plutons and gold mineralizations in the upper crust (Colvine et al., 1988). The high Ba and K contents together with increased light REE contents of some veins in the Pahtavaara gold deposit suggest the contamination of the mineralizing fluid by sialic Archaean crust (basement gneisses); high values of these elements have been reported from the Möykkelmä dome and as-

sociated komatiites by Räsänen et al. (1989), who interpreted these features as evidence for crustal contamination.

Ore forming processes resulting in the genesis of the Pahtavaara gold deposit occurred late in the development of the Central Lapland Greenstone Belt. They have been interpreted to have taken place broadly during the Svecokarelian orogeny and during the emplacement of granitoid intrusions and remobilization of the Archaean basement gneisses that formed the recent Central Lapland Granitoid Complex at about 1.9 — 1.8 Ga ago (cf. Lehtonen et al., 1989; Silvennoinen, 1985; Skiöld, 1987).

CONCLUSIONS

The Pahtavaara gold deposit provides interesting opportunities for studying hydrothermal alteration processes associated with komatiitic host rocks, and for conducting geochemical analyses pertaining to processes of gold precipitation. This is partly because of the susceptibility of komatiites to alteration and partly due to the homogeneity of the primary composition of the host rock. Many interesting features concerning the nature of the hydrothermal alteration have been recognized, and the following specific conclusions have been made:

1) The Pahtavaara gold deposit is hosted by variably altered pyroclastic komatiites. This is indicated by (i) homogeneous ratios between the immobile elements Al and Ti, (ii) comparable low REE contents and patterns for all the variably altered rock types, (iii) the homogeneity of the bedrock in the weakly altered areas, (iv) the lack of other rock types in the vicinity and the local preservation of weakly altered blocks among intensively altered rocks and (v) the high Cr contents of biotite and chlorite reflecting their ultramafic heritage and (vi) the obvious mineralogical and geochemical gradation between all the rock types in the study area.

2) Hydrothermally altered rocks form a subvertically dipping zone of approximately 100 m × 600 m in size which differs from the surrounding terrain by its high K, Ba and Sr, and low Mg, Co and Zn contents.

3) The weakly altered Sattasvaara metakomatiites contain the regional greenschist facies metamorphism of amphibole-chlorite assemblage, with variable proportions of talc and chlorite. The hydrothermally altered, gold-bearing rock types consist of (i) biotite schist with extensive talc-carbonate ± pyrite veins and (ii) coarse-grained, non-schistose amphibole rock. The latter is closely associated with the quartz ± barite lenses and pods locally carrying visible free gold.

4) Compositionally the weakly altered amphibole-chlorite schists correspond to ultramafic komatiites or Geluk-type komatiites, whereas the amphibole rocks are comparable to the Badblaas-type (basaltic) komatiites as defined by Viljoen and Viljoen (1969). Biotite schists are typified by high Fe, K and Ba, and low Mg contents compared to the weakly altered komatiites.

5) On the basis of mass balance calculations, biotite schists show an average volume decrease of about 10 — 30 %, resulting in the relative enrichment of immobile elements by the leaching more mobile elements. Geochemically the hydrothermal alteration included major additions of K, Fe, CO_2, S, Ba, Te, W and Sr, and depletion in Mg, Ca, Si, Co and Zn. Proportions between the immobile elements Al and Ti have remained the same during the alteration. Several trace elements, commonly associated with gold deposits occur in extremely low quantities at Pahtavaara, including Ag, As, B, Br, Mo and Pb.

6) Coarse-grained amphibole rocks can be divided on the basis of alumina content into high-alumina (>4 wt. % Al_2O_3) and low-alumina (<4 wt. % Al_2O_3) types. The former appears to

be gradational to weakly altered amphibole-chlorite schists, whereas the latter grades into amphibole-rich quartz ± barite veins and is therefore more gold-critical. Mass balance calculations indicate that the latter type display a marked volume increase with enrichments in Ca, Si, Na, Ba, S, P, W and Sr and depletions in CO_2, and to a lesser extent Mg, Zn and Fe.

7) The formation of talc-carbonate ± pyrite veins in biotite schist is broadly coeval with the biotitization and the first stage of gold precipitation. They represent replacement types of veins and formed during ductile deformation in a greenschist/amphibolite facies environment. In contrast, quartz ± barite veins with variable proportions of amphibole are gradational into low-alumina amphibole rocks and represent brittle-ductile deformation and extensional environment.

8) The formation of biotite schist took place broadly during or immediately after the peak of metamorphism and was controlled by the combined effects of high permeability of the original komatiitic tuffs compared to the associated pillow lavas and, secondly, the regional schistosity. Together these features resulted in the formation of a structurally controlled channelways into which hydrothermal fluids were focused. Generation of the amphibole rock clearly postdates the biotitization and occurred during a later stage of metamorphism. Structurally it was controlled by NNE — trending shearing resulting in the formation of zones of dilation and more brittle deformation.

9) Gold displays statistically positive correlations with Ba, S, and Si and negative correlations with MgO and CO_2. Additionally, factor analysis shows high loadings for K, Fe, Au, S and Ba. Gold in biotite schist is associated with pyrite in talc-carbonate veins and also magnetite. In amphibole rock gold forms large aggregates and occurs mainly in the native state in association with quartz ± barite veins and pods.

10) The early Proterozoic Pahtavaara gold deposit is in many respect comparable the late Archaean, structurally controlled and greenstone-hosted gold deposits, in spite of its younger age.

11) Gold enrichment is probably connected to the wider cratonization processes during the Svecokarelian orogeny, and emplacement of extensive granitoid intrusives 1.9 — 1.8 Ga ago, late at greenstone belt development. A close association between the hydrothermal fluids and sialic crust is indicated by high contents of Ba and K both in the Pahtavaara gold deposit and komatiites associated with the basal gneisses in the Archaean Möykkelmä dome.

12) The most sensitive indicators of hydrothermal alteration at Pahtavaara are the high Ba and K contents when compared to unaltered komatiites. These elements combined with structurally favourable zones can be possible used as an exploration guide in comparable areas.

ACKNOWLEDGEMENTS

I am greatly indebted to a number of people, many of them not mentioned here, without whose assistance this work would have been impossible to complete. First of all I would like to thank Eelis Pulkkinen, the leader of the Komatiite Project, whose efforts led to discovery of the Pahtavaara deposit and therefore enabled this study. Continuous support and discussions with Professor Reijo Salminen and Matti Äyräs, who also made it possible to me to concentrate on this study, are greatly acknowledged. Comments and suggestions by Professor Kauko Laajoki on the first version of the manuscript led to several improvements in the text.

This work was supervised by Associate Professor Tauno Piirainen, and Dr Tapio Koljonen and

their advice is gratefully appreciated. The suggestions and contributions of Professors Heikki Papunen and Tauno Piirainen, the official revisors of the manuscript, are acknowledged with gratitude. I express my cordial thanks to Professor Kauko Korpela, then acting Director of the Geological Survey, for approving publication of this paper in the Survey's Bulletin series.

The understanding of the structural geology of the study area benefited from the work carried out together with Dr Peter Sorjonen-Ward, who also revised the language of the manuscript and made a number of useful corrections. Ore mineralogical studies were done by Dr Kari Kojonen and Bo Johanson. Figures were drown by Soili Ahava and photographs of the rock samples were taken by Jarmo Kariniemi. Editorial work was done by Sini Autio. Jarmo Haavikko, Hannu Kairakari, Risto Nikula, Vesa Perttunen and Markku Pänttäjä assisted in the computing. The encouraging discussions and with Professor J.G.S. Govett and Dr William Karvinen and their comments concerning the contents and general conclusions of the research are gratefully acknowledged.

My understanding of the geology of Lapland was greatly increased by discussions with colleagues at the Geological Survey of Finland, Regional Office in Rovaniemi, including Eero Hanski, who also made several corrections on the manuscript, Heikki Juopperi, Matti Lehtonen, Pentti Rastas, Jorma Räsänen and Tuomo Manninen from the Petrological Department, and Heikki Pankka, Veikko Keinänen, Ilkka Härkönen, Seppo Rossi and Erkki Vanhanen from the Exploration Department. Special thanks are due to Antero Karvinen as well as Raimo Manner and Helena Hulkki for co-operation in the field. The assistance of all the staff at the Survey's Geochemical laboratories mentioned in more detail in the chapter on 'Analytical methods' is appreciated. Liisa and Lasse Parkkali are thanked for providing computing facilities while we were on leave in Mozambique. Finally, warmest thanks to my wife Jaana for her patience and support, and our sons Petri, who helped to keep our feet firmly on the ground during the course of study, and to Harri, who arrived just in time to mark its completion.

REFERENCES

Alapieti, T., 1982. The Koillismaa layered igneous complex, Finland — its structure, mineralogy and geochemistry, with emphasis on the distribution of chromium. Geol. Surv. Finland, Bull. 319, 116 p.

Andrews, A.J., Hugon, H., Durocher, M., Corfu, F. & Lavigne, M.J., 1986. The anatomy of a gold-bearing greenstone belt; Red Lake, Northwestern Ontario, Canada. *In* A.J. Macdonald (eds.), Proceedings of Gold '86, an international Symposium on the geology of gold deposits. Toronto, 1986. 3 — 22.

Arndt, N.T., Naldrett, A.J. & Pyke, D.R., 1977. Komatiitic and iron-rich tholeiitic lavas of Munro Township, northeast Ontario. J. Petrol. 18, 319 — 369.

Arndt, N.T. & Nisbet, E.G., 1982. What is komatiite? *In* N.T. Arndt & E.G. Nisbet (eds.), Komatiites. George Allen & Unwin, London, 19 — 27.

Autio, S. (ed.) 1989. Current Research 1988. Geol. Surv. Finland, Spec. Pap. 10. 184 p.

Barbey, P., Convert, J., Moreau, B., Capdevila, R. & Hameurt, J., 1984. Petrogenesis and evolution of the early Proterozoic collisional orogenic belt: the Granulite belt of Lapland and the Belomorides (Fennoscandia). Bull. Geol. Soc. Finland 56, 161 — 188.

Barley, M.E. & Groves D.I., 1987. Hydrothermal alteration of Archaean supracrustal sequences in the central Norseman-Wiluna belt, Western Australia: a brief review. *In* S.E. Ho, & D.I. Groves (eds.), Recent advances in understanding Precambrian gold deposits. Geol. Dep. & Univ. Extension, Univ. Western Australia, Publ. 11, 51 — 66.

Barnes, H.L., 1979. Solubilities of ore minerals. *In* H.L. Barnes (ed.), Geochemistry of hydrothermal ore deposits. Sec. Ed. John Wiley & sons, New York, 404 — 460.

Berger, B.R. & Bagby, W.C., 1991. The geology and origin of Carlin-type gold deposits. *In* R.P. Foster (ed.), Gold metallogeny and exploration. Blackie, Glasgow & London, 210 — 248.

Beswick, A.E., 1982. Some geochemical aspects of alteration, and genetic relations in komatiitic suites. *In* N.T. Arndt & E.G. Nisbet (eds.), Komatiites. George Allen & Unwin, London, 283 — 308.

Björklund, A.J. (ed.), 1991. Gold geochemistry in Finland. J. Geochem. Explor. 39, 255 — 388.

Björlykke, A., Hagen, R. & Söderholm, K., 1987. Bidjovagge copper-gold deposit in Finnmark, Northern Norway. Econ. Geol. 82, 2059 — 2075.

Black, R., 1980. The Precambrian of West Africa. Episodes 4, 3 — 8.

Bolviken, B., Bergstrom, J., Björklund, A. Kontio, M., Lehmuspelto, P., Lindholm, T., Magnusson, J., Ottesen, R.T., Steenfelt, A. & Volden, T., 1986. Geochemical Atlas of northern Fennoscandia, scale 1 : 4 000 000, Geol. Surveys of Finland, Sweden and Norway. 19 p. and 155 maps.

Bowen, K.G. & Whiting, R.G., 1975. Gold in the Tasman geosyncline, Victoria. Australasian Inst. Mining Metall., Mon. 5, 647 — 658.

Boyle, R.W., 1979. The geochemistry of gold and its deposits. Geol. Surv. Canada, Bull. 280. 584 p.

Boyle, R.W., 1984. Gold deposits; their geology, geochemistry and origin. *In* R.P. Foster (ed.), Gold '82: The geology, geochemistry and genesis of Gold deposits. Balkema, Rotterdam, 183 — 190.

Boyle, R.W., 1986. Gold deposits in turbidite sequences: their geology, geochemistry and history of the theories of their origin. *In* J.D. Keppie, R.W. Boyle & S.J. Haynes (eds.), Turbidite-hosted gold deposits. Geol. Assoc. Canada, Spec. Pap. 32, 1 — 13.

Brugmann, G.E., Arndt, N.T., Hofmann, A.W. & Tobschall, H.J. 1987. Noble metal abundances in komatiite suites from Alexona, Ontario, and Gorgona Island, Columbia. Geochim. Cosmochim. Acta 51, 2159 — 2169.

Burk, R., Hodgson, C.J. & Quatermain, R.A. 1986. The geological setting of the Teck-Corona Au-Mo-Ba deposit, Hemlo, Ontario, Canada. *In* A.J. Macdonald (ed.), Proceedings of Gold '86, an international Symposium on the geology of gold deposits. Toronto, 1986, 311 — 326.

Burrows, D.R., Wood, P.C. & Spooner, E.T.C., 1986. Carbon isotope evidence for a magmatic origin for Archaean gold-quartz vein ore deposits. Nature 321, 851 — 854.

Cameron, E.M., 1988. Archean gold: Relation to granulite formation and redox zoning in the crust. Geology 16, 109 — 112.

Cameron, E.M. & Hattori, K., 1985. The Hemlo gold deposits, Ontario: a geochemical and isotopic study. Geochim. Cosmoc. Acta 49, 2041 — 2050.

Cameron, E.M. & Hattori, K., 1987. Archean gold mineralization and oxidized hydrothermal fluids. Econ. Geol. 82, 1177 — 1191.

Campbell, I.H., Lesher, C.M., Coad, P., Franklin, J.M., Gorton, M.P., & Thurston, P.C., 1984. Rare-earth-element mobility in alteration pipes below massive Cu-Zn-sulfide deposits. Chem. Geol. 45, 181 — 202.

Cathelineau, M. & Nieva, D., 1985. A clorite solid solution geothermometer: The Los Azutres (Mexico) geothermal system. Contrib. Mineral. Petrol. 91, 235 — 244.

Cathles, L.M., 1986. The geologic solubility of gold from 200

— 350 °C, and its implications for gold-base metal ratios in vein and stratiform deposits. *In* L.A. Clark (ed.), Gold in the Western Shield. Canadian Instit. Mining Metall., Spec. Vol. 38, 187 — 210.

Clark, M.E., Archibald, N.J. & Hodgson, C.J., 1986. The structural and metamorphic setting of the Victory gold mine, Kambalda, Western Australia. *In* A.J. Macdonald (ed.), Proceedings of Gold '86, an international Symposium on the geology of gold deposits. Toronto 1986. 243 — 254.

Colvine, A.C., Andrews, A.J., Cherry, M.E., Durocher, M,E., Fyon, A.J., Lavigne, M.J., Macdonald, A.J., Marmount, S. Poulsen, K.H., Springer, J.S. & Troop, D.G., 1984. An integrated model for the origin of Archean lode gold deposits. Ontario Geol. Surv. Open File Rep. 5524, 98 p.

Colvine, A.C., Fyon, J.A., Heather, K.B., Marmont, S. Smith, P.M. & Troop, D.G., 1988. Archean lode gold deposits in Ontario. Ontario Geol. Surv. Misc. Pap. 139, 136 p.

Coombe, W., 1984. Gold in Saskatchewan. Saskatchewan Energy and Mines. Saskatchewan Geol. Surv. Open File Rep. 84—1, 134 p.

Costa, U.R., Fyfe, W.S., Kerrich, R. & Nesbitt, H.W., 1980. Archean hydrothermal talc evidence for high ocean temperatures. Chem. Geol. 30, 341 — 349.

Costa, U.R., Barnett, R.L. & Kerrich, R., 1983. The Mattagami Lake mine Archean Zn-Cu sulfide deposit, Quebec: Hydrothermal coprecipitation of talc and sulfides in a sea-floor brine pool — evidence from geochemistry, $^{18}O/^{16}O$, and mineral chemistry. Econ. Geol. 78, 1144 — 1203.

Craig, H., 1961. Isotope variations in meteoric waters. Science 133, 1702 — 1703.

Craig, H., 1957. Isotope standards for carbon and oxygen and correlation factors for mass spectrometric analysis of carbon dioxide. Geochim. Cosmochim. Acta 12, 133 — 149.

Cullers, R.L. & Graf, J.L., 1984. Rare earth elements in igneous rocks of the continental crust: predominantly basic and ultrabasic rocks. *In* P. Henderson (ed.), Rare earth element geochemistry. Developments in geochemistry 2. Elsevier, Amsterdam, 237 — 274.

Davies, J.F., Whitehead, R.E.S., Cameron, R.A. & Duff, D., 1982. Regional and local patterns of CO_2-K-Rb-As alteration: a guide to gold in the Timmins area. *In* R.W. Hodder & W. Petruk (eds.), Geology of Canadian gold deposits. Canadian Inst. Mining. Metall. Spec. 24, 130 — 143.

Deer, W.A., Howie, R.A. & Zussman, J., 1967. Rock forming minerals 3, Sheet silicates. Sixth impression. W. Glowes and Sons Ltd, London and Beccles. 270 p.

Donaldson, M.J., 1981. Redistribution of ore elements during serpentinization and talc-carbonate alteration of some Archean dunites, Western Australia. Econ. Geol. 76, 1698 — 1713.

Drummond, S.E. & Ohmoto, H., 1985. Chemical evolution and mineral deposition in boiling hydrothermal systems. Econ. Geol. 80, 126 — 147.

Durocher, M.E., 1983. The nature of hydrothermal alteration associated with the Madsen and Starratt-Olsen gold deposits, Red Lake area. *In* A.C. Colvine (ed.), The geology of gold in Ontario. Ontario Geol. Surv. Misc. Pap. 110, 123 — 140.

Eckstrand, O.R., 1975. The Dumont serpentinite: a model for control of nickeliferous opaque mineral assemblages by alteration products in ultramafic rocks. Econ. Geol. 70, 183 — 201.

Eilu, P. & Idman, H., 1988. Hydrothermal alteration in the lower part of an early Proterozoic greenstone complex at Palovaara, Enontekiö, northwestern Finland. Geol. Soc. Finland, Bull. 60, 115 — 127.

Elo, S., Lanne, E., Ruotoistenmäki, T. & Sindre, A., 1989. Interpretation of gravity anomalies along the POLAR profile in the northern Baltic Shield. Tectonophysics 162, 135 — 150.

Evans, B.W., 1982. Amphiboles in metamorphosed ultramafic rocks. *In* D.R. Veblen & P.H. Ribbe (eds.), Amphiboles: Petrology and experimental phase relations. Miner. Soc. America. Reviews in Mineralogy 9B, 98 — 112.

Fabiani, W.M.B., 1984. Archaean gold-copper mineralization in the Athens Mine, Mvuma, Zimbabwe. *In* R.P. Foster (ed.), Gold '82: The geology, geochemistry and genesis of Gold deposits. Balkema, Rotterdam, 449 — 468.

Finlow-Bates, T. & Stumpfl, E.F., 1981. The behaviour of so-called immobile elements in hydrothermally altered rocks associated with volcanogenic submarine-exhalative ore deposits. Mineralium Deposita 16, 319 — 328.

Floyd, P.A. & Winchester, J.A., 1978. Identification and discrimination of altered and metamorphosed volcanic rocks using immobile elements. Chem. Geol. 21, 291 — 306.

Foster, R.P., 1990. Gold mineralization: recent advances in predictive metallogeny. Terra Nova 2, 215 — 225.

Front, K., Vaarma, M., Rantala, E. & Luukkonen, A., 1989. Keski-Lapin varhaisproterotsooiset Nattas-tyypin graniittikompleksit, niiden kivilajit, geokemia ja mineralisaatiot. Summary: Early Proterozoic Nattanen-type granite complexes in central Finnish Lapland: rock types, geochemistry and mineralization. Geol. Surv. Finland, Rep. Invest. 85, 77 p.

Fryer, B.J. & Hutchinson, R.W., 1976. Generation of metal deposits on the sea floor. Canadian J. Earth Sci. 13, 126 — 135.

Fryer, B.J., Kerrich, R., Hutchinson, R.W., Pierce, M.G. & Rogers, D.S., 1979. Archaean precious-metal hydrothermal systems, Dome mine, Abitibi greenstone belt. I. Patterns of alteration and metal distribution. Canadian J. Earth Sci. 16, 421 — 439.

Fyfe, W.S., 1986. The transport and deposition of gold. *In* L.A. Clark (ed.), Gold in the Western Shield. Canadian Instit. Mining Metall., Spec. 38, 156 — 167.

Fyfe, W.S. & Kerrich, R., 1984. Gold: Natural concentration processes. *In* R.P. Foster (ed.), Gold '82: The geology, geochemistry and genesis of gold deposits. Balkema, Rotterdam, 99 — 127.

Fyon, J.A. & Crocket, J.H., 1982. Gold exploration in the Timmins district using field and lithogeochemical characteristics of carbonate alteration zone. *In* R.W. Hodder & W. Petruk (eds.), Geology of Canadian gold deposits.

Canadian Inst. Mining. Metall. Spec. 24, 113 — 129.

Fyon, J.A., Crocket, J.H. & Schwartz, H.P., 1983. Magnesite abundance as a guide to gold mineralization associated with ultramafic flows, Timmins area. J. Geochem. Explor. 18, 245 — 266.

Gaál, G., 1986. 2200 million years of crustal evolution: the Baltic Shield. Geol. Soc. Finland, Bull. 58, 149 — 168.

Gaál, G., Berthelsen, A., Gorbatschev, R., Kesola, R., Lehtonen, M.I., Marker, M. & Raase, P., 1989. Structure and composition of the Precambrian crust along the POLAR profile in the northern Baltic Shield. Tectonophysics 162, 1 — 25.

Gaál, G., Mikkola, A. & Söderholm, B., 1978. Evolution of the Archean crust in Finland. Prec. Res. 6, 199 — 215.

Gibbs, A.K. & Barron, C.N., 1983. The Guiana shield reviewed. Episodes 1983, 7 — 14.

Golding, S.D. & Wilson, A.F., 1983. Geochemical and stable isotope studies of the No. 4 lode, Kalgoorlie, Western Australia. Econ. Geol. 78, 438 — 450.

Grant, J.A., 1986. The isocon diagram — A simple solution to Gresens' equation for metasomatic alteration. Econ. Geol. 81, 1976 — 1982.

Graves, M.C. & Zentilli, M., 1982. A review of the geology of gold in Nova Scotia. Canadian Instit. Mining Metall. Spec. Pap. 24, 233 — 242.

Gresens, R.L., 1967. Composition-volume relationships of metasomatism. Chem. Geol. 2, 47 — 65.

Gresham, J.J. & Loftus-Hills, G.D., 1981. The geology of the Kambalda nickel field, Western Australia. Econ. Geol. 76, 1373 — 1416.

Groves, D.I. & Batt, W.D., 1984. Spatial and temporal variations of Archaean metallogenic associations in terms of evolution of granitoid-greenstone terrains with particular emphasis on the Western Australian Shield. *In* A. Kröner, G.N. Hanson & A.M. Goodwin (eds.), Archaean geochemistry. Springer, Berlin, 73 — 98.

Groves, D.I. & Foster, R.P., 1991. Archean lode gold deposits. *In* R.P. Foster (ed.), Gold metallogeny and exploration. Blackie, Glasgow. 63 — 103.

Groves, D.I., Korkiakoski, E.A., McNaughton, N.J., Lesher, C.M. & Cowden, A., 1986. Thermal erosion by komatiites at Kambalda, Western Australia and the genesis of nickel ores. Nature 319, 136 — 139.

Groves, D.I. & Phillips, G.N., 1987. The genesis and tectonic control on Archaean gold deposits of Western Australian shield — a metamorphic replacement model. Ore Geol. Rev. 2, 287 — 322.

Groves, D.I., Phillips, G.N., Ho, S.E. & Houston, S.M., 1985. The nature, genesis and regional controls of gold mineralization in Archaean greenstone belts of the Western Australian shield: a brief review. Trans. geol. Soc. S. Africa 88, 135 — 148.

Groves, D.I., Phillips, G.N., Ho, S.E., Houston, S.M. & Standing, C., 1987. Craton-scale distribution of Archean greenstone gold deposits: predictive capacity of metamorphic model. Econ. Geol. 82, 2045 — 2058.

Hajash, A. & Chandler, G.W., 1981. An experimental investigation of high-temperature interactions between seawater and rhyolite, andesite, basalt and peridotite. Contrib. Mineral. Petrol. 78, 240 — 254.

Hall, R.S. & Rigg, D.M., 1986. Geology of the West Anticline Zone, Musselwhite prospect, Opapimiskan Lake, Ontario, Canada. *In* A.J. Macdonald (ed.), Proceedings of Gold '86, an international Symposium on the geology of gold deposits. Toronto, 1986, 124 — 136.

Hamilton, J.V. & Hodgson C.J., 1986. Mineralization and structure of the Kolar gold field, India. *In* A.J. Macdonald (ed.), Proceedings of Gold '86, an international Symposium on the geology of gold deposits. Toronto, 1986, 270 — 283.

Hanson, G.N., 1989. An approach to trace element modelling using a simple igneous system as an example. *In* B.R. Lipin & G.A. McKay (eds.), Geochemistry and mineralogy of rare earth elements. Mineral. Soc. America. Reviews in Mineralogy 21, 79 — 97.

Härkönen, I., 1984. The gold-bearing conglomerates of Kaarestunturi, central Finnish Lapland. *In* R.P. Foster (ed.), Gold '82: The geology, geochemistry and genesis of gold deposits. Balkema, Rotterdam, 239 — 247.

Härkönen, I. & Keinänen, V., 1989. Exploration of structurally controlled gold deposits in the Central Lapland Greenstone Belt. Geol. Surv. Finland, Spec. Pap. 10, 79 — 82.

Hawthorne, F.C., 1981. Crystal chemistry of the amphiboles. *In* D.R. Veblen (ed.), Amphiboles and other hydrous pyriboles — mineralogy. Mineral. Soc. America. Reviews in Mineralogy 9A, 1 — 102.

Henley, R.W., 1973. Solubility of gold in hydrothermal chloride solutions. Chem. Geol. 11, 73 — 87.

Ho, S.E., Groves, D.I. & Phillips, G.N., 1985. Fluid inclusions as indicators of the nature and source of ore fluids and ore depositional conditions for Archaean gold deposits of the Yilgarn Block, Western Australia. Trans. geol. Soc. S. Africa 88, 149 — 158.

Hodgson, C.J., 1989. Uses (and abuses) of the ore deposit models in mineral exploration. *In* G.D. Garland (ed.), Proceedings of exploration '87. Ontarion Geol. Surv., Spec. 3, 31 — 45.

Hodgson, C.J., Chapman, R.S.G. & MacGeehan, P.J., 1982. Application of exploration criteria for gold deposits in the Superior Province of the Canadian Shield to gold exploration in the Cordillera. *In* A.A. Levinson (ed.), Precious metals in the Cordillera. Assoc. Explor. Geochemists, Toronto, 173 — 206.

Holland, H.D. & Malinin, S.D., 1979. The solubility and occurrence of non-ore minerals. *In* H.L. Barnes (ed.), Geochemistry of hydrothermal ore deposits. Sec. Ed. John Wiley & sons, New York, 461 — 508.

Houston, S.M., 1987. Competency contrasts and chemical controls as guides to gold mineralization: an example from the Barberton Mountain Land. *In* S.E. Ho, & D.I. Groves (eds.), Recent advances in understanding Precambrian gold deposits. Geol. Dep. & Univ. Extension, Univ. Western Australia, Publ. 11, 147 — 160.

Huhma, H., 1986. Sm-Nd, U-Pb and Pb-Pb isotopic evidence for the origin of the Early Proterozoic Svecokarelian crust in Finland. Geol. Surv. Finland, Bull. 337, 48 p.

Hulkki, H., 1990. Sodankylän Sattasvaaran komatiittikompleksin Au-kriittinen muuttumisvyöhyke. Unpubl. M.Sc. thesis. Univ. Helsinki. 190 p.

Humphris, S.E., 1984. The mobility of rare earth elements in the crust. *In* P. Henderson (ed.), Rare earth element geochemistry. Developments in geochemistry 2. Elsevier, Amsterdam, 317 — 342.

Hutchinson, R.W., 1987. Metallogeny of Precambrian gold deposits: space and time relationships. Econ. Geol. 82, 1993 — 2007.

Hutchinson, R.W. & Burlington, J.L., 1984. Some broad characteristics of greenstone belt gold lodes. *In* R.P. Foster (ed.), Gold '82: The geology, geochemistry and genesis of gold deposits. Balkema, Rotterdam, 339 — 371.

Jensen , L.S., 1976. A new cation plot for classifying subalkalic volcanic rocks. Ontario Division of Mines, Misc. Pap. 66, 22 p.

Jolly, W.T., 1982. Progressive metamorphism of komatiites and related Archaean lavas of the Abitibi area, Canada. *In* N.T. Arndt & E.G. Nisbet (eds.), Komatiites. George Allen & Unwin. London, 247 — 266.

Juopperi, H. & Räsänen, J., 1989. Savukosken vulkaniittitutkimukset. *In* T. Manninen (ed.), Tulivuorenkivet Kolarista Kuusamoon, Lapin vulkaniittiprojektin ekskursio ja esitelmäseminaari 5.-10.6.1989. Geologian tutkimuskeskus, Opas 23, 40 — 53.

Kaivosoja, J. & Koivumaa, S., 1984. Hierarkinen standarditietorakenne (HST). Ohjelmien käyttöohje. Oulun yliopisto. Kuhmon ja Kittilän malmiprojekti. Rap. 18 B, 59 p.

Karvinen, W.O., 1982. Geology and evolution of gold deposits, Timmins area, Ontario. *In* R.W. Hodder & W. Petruk (eds.), Geology of Canadian gold deposits. Proceedings of the CIM gold symposium, September 1980. Canadian Inst. Min. Metall. Spec. 24, 101 — 112.

Keays, R.R., 1984. Archaean gold deposits and their source rocks: the upper mantle connection. *In* R.P. Foster (ed.), Gold '82: The geology, geochemistry and genesis of gold deposits. Balkema, Rotterdam, 17 — 51.

Keinänen, V., 1987. Vein-type gold occurrence in Soretiavuoma carbonate rocks, Finnish Lapland. Gold '87, Program and Abstracts. Univ. Turku. Dep. Geol. Publ. 19, p. 8.

Keppie, J.D., 1976. Structural model for the saddle reef and associated gold veins in the Meguma Group, Nova Scotia. Canadian Inst. Mining Metall. Bull. 69, 103 — 116.

Kerrich, R., 1983. Geochemistry of gold deposits of the Abitibi greenstone belt. Canadian Instit. Mininig Metall. Spec. Pap. 27, 75 p.

Kerrich, R. & Fryer, B.J., 1979. Archean precious metal hydrothermal systems; Dome Mine, Abitibi greenstone belt; II REE and oxygen isotope relations. Canadian Jour. Earth Sci. 16, 440 — 458.

Kerrich, R. & Fyfe, W.S., 1981. The gold-carbonate association: source of CO_2, and CO_2 fixation reactions in Archean lode deposits. Chem. Geol. 33, 265 — 294.

Kerrich, R. & Hodder, R.W., 1982. Archean lode gold and base metal deposits: evidence for metal separation into independent hydrothermal systems. *In* R.W. Hodder & W. Petruk (eds.), Geology of Canadian gold deposits. Proceedings of the CIM gold symposium, September 1980. Canadian Inst. Mining. Metall. Spec. Vol. 24, 144—160.

Kerrich, R. & Watson, G.P., 1984. The Macassa mine Archean lode gold deposit, Kirkland Lake, Ontario: Geology, patterns of alteration, and hydrothermal regimes. Econ. Geol. 79, 1104 — 1130.

Ketola, M., 1989. The role of geophysics and geochemistry in sulphide and precious metal exploration in the light of some recent ore discoveries in Finland. *In* G.D. Garland (ed.), Proceedings of exploration '87. Ontarion Geol. Surv., Spec. 3, 837 — 854.

Kishida, A. & Kerrich, R., 1987. Hydrothermal alteration zoning and gold concentration at the Kerr-Addison Archean Lode Gold deposit, Kirkland Lake, Ontario. Econ. Geol. 82, 649 — 690.

Koch, G.S. & Link, R.F., 1970. Statistical analysis of geochemical data. Wiley & Sons, New York. 374 p.

Kojonen, K. & Johanson, B., 1989. Pahtavaaran Au-malmiaiheen malmimineraaleista. Geologian tutkimuskeskus. Raportti M 40/3714/-88/1/41.2, Sodankylä, Pahtavaara. 2 p.

Koljonen, T. (ed.). The Geochemical Atlas of Finland, part 2: Till. Geol. Surv. Finland, Espoo, (in prep.).

Kontas, E., 1981. Rapid determination of gold by flameless atomic absorption spectrometry in the ppb and ppm ranges without organic solvent extraction. Atomic Spectr. 2, 59 — 61.

Kontas, E., Niskavaara, H. & Virtasalo, J., 1986. Flameless atomic absorption determination of gold and palladium in geological reference samples. Geostand. Newsletters 10, 169 — 171.

Kontoniemi, O., 1989. The Osikonmäki gold occurrence at Rantasalmi, southeastern Finland. Geol. Surv. Finland, Spec. Pap. 10, 107 — 110.

Korkiakoski, E.A, 1987. Mineralogical and geochemical alteration of the komatiite-associated Pahtavaara gold prospect, northern Finland. Program and abstracts. Gold '87. Univ. Turku, Dep. Geol. Publ. 19, 4 p.

Korkiakoski, E.A., 1985. The nature of spinifex-textured Fe-Ni-Cu sulphide ores at Kambalda, Western Australia: Evidence for a magmatic origin and thermal erosion by komatiites. Unpubl. Phil. Lic. thesis. Univ. Oulu. 112 p. Also reported at the Geol. Dep., Univ. Western Australia.

Korkiakoski, E.A., Karvinen, A. & Pulkkinen, E., 1989. Geochemistry and hydrothermal alteration of the Pahtavaara gold mineralization, Finnish Lapland. Geol. Surv. Finland, Spec. Pap. 10, 83 — 89.

Korkiakoski, E.A., Pulkkinen, E., Hulkki, H. & Manner, R., 1987. Mineralogical and geochemical alteration associated with the gold prospect in the early Proterozoic Sattasvaara Komatiite Complex; Northern Finland. IGCP 217. Abstracts. Proterozoic geochemistry. Lund, June 3 — 6, 1987. 52 p.

Korkiakoski, E.A., Pulkkinen, E. & Ward, P., 1988. Geochemical alteration, regional setting and structural control of the lower Proterozoic Pahtavaara Au-prospect. Bicentennial Gold 88, Extended abstract, Poster Programme 1, Geol. Soc. Australia, Abstracts Ser. 23, 190 — 192.

Kranidiotis, P. & MacLean, W.H., 1987. Systematics of chlorite alteration at the Phelp Dodge massive sulfide deposit, Matagami, Quebec. Econ. Geol. 82, 1898 — 1911.

Krill. A.G., Bergh, S., Lindahl, I., Mearns, E.W., Often,

M., Olerud, S., Olesen, O., Sandstad, J.S., Siedlecka, A. & Solli, A., 1985. Rb-Sr, U-Pb and Sm-Nd isotopic dates from Precambrian rocks of Finnmark. Norges Geol. Unders., Bull. 403, 37 — 54.

Kristiansson, K. & Malmqvist, L., 1987. Trace elements in the geogas and their relation to bedrock composition. Geoexploration 24, 517 — 534.

Kuhns, R.J., 1986. Alteration styles and trace element dispersion associated with the Golden Giant deposits, Hemlo, Ontario, Canada. *In* A.J. Macdonald (ed.), Proceedings of Gold '86, an international Symposium on the geology of gold deposits. Toronto, 1986, 340 — 354.

Lanne, E., 1979. Vuotoksen ja Kittilän alueiden geofysikaalisesta tulkinnasta. English summary: On the interpretation of geophysical data from Vuotos and Kittilä areas, northern Finland. Geol. Surv. Finland, Rep. Invest. 25, 1 — 38.

Lauerma, R., 1982. On the ages of some granitoid and schist complexes in northern Finland. Geol. Soc. Finland, Bull. 54, 85 — 100.

Leake, B.E., 1978. Nomenclature of amphiboles. Canadian Mineral. 16, 501 — 520.

Lehtonen, M., Manninen, T., Rastas, P. Väänänen, J., Roos, S.I. & Pelkonen, R., 1984. Geological map of Central Lapland, Northern Finland. Scale 1 : 200 000. Geol. Surv. Finland, Espoo.

Lehtonen, M., Manninen, T., Rastas, P. Väänänen, J., Roos, S.I. & Pelkonen, R., 1985. Keski-Lapin geologisen kartan selitys. Summary: Explanation to the geological map of Central Lapland. Geol. Surv. Finland, Rep. Invest. 71, 55 p.

Lehtonen, M. & Rastas, P., 1988. Aluetutkimukset: Keski-Lappi. *In* T. Manninen, E. Hanski & R. Kesola (eds.), Lapin vulkaniittiprojekti, vuosikertomus 1987. Geologian tutkimuskeskus, K/1988/1, 4 — 15.

Lehtonen, M., Rastas, P. & Räsänen, J., 1989. Keski-Lapin vulkaniittitutkimukset. *In* T. Manninen (ed.), Tulivuorenkivet Kolarista Kuusamoon, Lapin vulkaniittiprojektin ekskursio ja esitelmäseminaari 5.-10.6.1989. Geologian tutkimuskeskus, Opas 23, 9 — 39.

Lesher, C.M., 1983. Localization and genesis of komatiite-associated Fe-Ni-Cu sulphide mineralization at Kambalda, Western Australia. Unpubl. Ph.D. thesis. Univ. West. Australia. 318 p.

Lesher, C.M., Goodwin, A.M., Campbell, I.H. & Gorton, M.P., 1985. Trace-element geochemistry of ore-associated and barren, felsic metavolcanic rock in the Superior Province, Canada. Canadian J. Earth Sci. 23, 222 — 237.

Ludden, J.N., Daigneault, R., Robert, F. & Taylor, R.P., 1984. Trace element mobility with Archean Au lode deposits. Econ. Geol. 77, 1131 — 1141.

MacGeehan, P.J. & Hodgson, C.J., 1982. Environments of gold mineralization in the Campbell Red Lake and Dickenson Mines, Red Lake district. *In* R.W. Hodder & W. Petruk (eds.), Geology of Canadian gold deposits. Canadian Inst. Min. Metall. Spec. 24, 184 — 207.

MacLean, W.H. & Kranidiotis, P., 1987. Immobile elements as monitor of mass transfer in hydrothermal alteration: Phelps Dodge massive sulphide deposit, Matagam, Quebec. Econ. Geol. 82, 951 — 962.

Mäkelä, K., 1980. Geochemistry and origin of Haveri and Kiipu, Proterozoic strata-bound volcanogenic gold-copper and zinc mineralizations from southwestern Finland. Geol. Surv. Finland, Bull. 310, 79 p.

Mäkelä, M., Sandberg, E. & Rantala, O., 1987. Vein-type gold occurrences associated with the granitoids of central Pohjanmaa, Finland. Gold '87, Program and abstracts. Univ. Turku. Dep. Geol. Publ. 19, p. 28.

Makkonen, H. & Ekdahl, E., 1988. Petrology and structure of the early Proterozoic Pirilä gold deposit in southeastern Finland. Geol Soc. Finland, Bull. 60, 55 — 66.

Malmqvist, L., 1988. Geogas survey at the Pahtavaara gold prospect in northern Finland. SEMTECH. Unpubl. report. 10 p.

Malmqvist, L. & Kristiansson, K., 1984. Experimental evidence for an ascending microflow of geogas in the ground. Earth Plan. Sci. Lett. 70, 407 — 416.

Manninen, T., 1991. Sallan alueen vulkaniitit. Summary: Volcanic rocks in the Salla area, northeastern Finland. Geol. Surv. Finland, Rep. Invest. 104, 97 p.

Marmont, S., 1986. The geological setting of the Detour Lake gold mine, Ontario, Canada. *In* A.J. Macdonald (ed.), Proceedings of Gold '86, an international Symposium on the geology of gold deposits. Toronto, 1986, 81 — 96.

Mason, R. & Melnik, N., 1986. The anatomy of an Archean gold system — the McIntyre-Hollinger Complex at Timmins, Ontario, Canada. *In* A.J. Macdonald (ed.), Proceedings of Gold '86, an international Symposium on the geology of gold deposits. Toronto, 1986, 40 — 55.

Mikkola, E., 1941. Kivilajikartan selitys, B7-C7-D7, Muonio — Sodankylä — Tuntsajoki. English summary: Explanation to the map of rocks. The General geological map of Finland 1 : 400 000, 286 p.

Mueller, A.G., 1988. Archaean gold-silver deposits with prominent calc-silicate alteration in the Southern Gross greenstone belt, Western Australia: analogues of Phanerozoic skarn deposits. *In* S.E. Ho and D.I. Groves (eds.), Advances in understanding Precambrian gold deposits II. Geol. Dept. & Univ. Ext., Univ. Western Australia, Publ. 12, 141 — 163.

Mueller, A.G. & Groves, D.I., 1991. The classification of Western Australian greenstone-hosted gold deposits according to wallrock-alteration mineral assemblages. Ore Geol. Rev. 6, 291 — 331.

Mutanen, T., 1976. Komatiites and komatiite provinces in Finland. Geologi 28, 49 — 56.

Mutanen, T., 1989. Koitelainen intrusion and Keivitsa-Satovaara Complex. Excursion guide. 5th International Platinum Symposium. Geol. Surv. Finland. Guide 28, 49 p.

Neall, F.B. & Phillips, G.N., 1987. Fluid-wall rock interaction in an Archean hydrothermal gold deposit: a thermodynamic model for the Hunt Mine, Kambalda. Econ. Geol. 82, 1679 — 1694.

Nesbitt, R.W., Sun, S.-S. & Purvis, A.C., 1979. Komatiites: geochemistry and genesis. Canadian Miner. 17, 165 — 186.

Nikula, R., 1988. The palaeosedimentary environments of the metasediments at Virttiövaara and Värttiövaara, Sodankylä. *In* K. Laajoki & J. Paakkola (eds.), Sedimen-

tology of the Precambrian formations in eastern and northern Finland. Geol. Surv. Finland, Spec. Pap. 5, 177 — 188.

Nisbet, E.G., Arndt, N.T., Bickle, M.J., Cameron, W.E., Chauvel, C., Cheadle, M., Hegner, E., Kyser, T.K., Martin, A., Renner, R. & Roedder, E., 1987. Uniquely fresh 2.7 Ga komatiites from the Belingwe greenstone belt, Zimbabwe. Geology 15, 1147 — 1150.

Nurmi, P.A., Hartikainen, A., Damsten, M. & Rasilainen, K., 1988. Geochemical exploration for Archean gold deposits in the Ilomantsi greenstone belt, eastern Finland. Bicentennial Gold 88, Extended abstract, Poster Programme 1. Geol. Soc. Australian, Abstracts Ser. 23, 559 — 561.

Nurmi, P.A., Hartikainen, A., Damsten, M. & Rasilainen, K., 1989. Sampling strategies and pathfinder elements in till and rock geochemical gold exploration, Hattu schist belt, Ilomantsi, eastern Finland. Geol. Surv. Finland, Spec. Pap. 10, 53 — 58.

Nurmi, P.A., Lestinen, P. & Niskavaara, H., 1991. Geochemical characteristics of mesothermal gold deposits in the Fennoscandian Shield, and a comparison with selected Canadian and Australian deposits. Geol. Surv. Finland, Bull. 351, 101 p.

Nurmi, P.A. & Ward, P.A., 1989. Gold exploration, Hattu schist belt, Ilomantsi, eastern Finland. Geol. Surv. Finland, Spec. Pap. 10, 45 — 48.

Often, M., 1985. The early Proterozoic Karasjok greenstone belt, Norway: A preliminary description of lithology, stratigraphy and mineralization. Norges Geol. Unders. Bull. 403, 75 — 88.

Ohmoto, H. & Rye, R.O., 1979. Isotopes of sulphur and carbon. *In* H.L. Barnes (ed.), Geochemistry of hydrothermal ore deposits. New York. John Wiley, 509 — 567.

Ollila, H., Saikkonen, R., Moisio, J. & Kojonen, K., 1990. Oriveden Kutemajärven kultaesiintymä. English summary: The gold deposit in Kutemajärvi, Orivesi. Vuoriteollisuus-Besgshanteringen 1, 26 — 30.

Paakkola, J., 1971. The volcanic complex and associated manganiferous iron formations of the Porkonen — Pahtavaara area in Finnish Lapland. Bull. Comm. geol. Finlande 247, 83 p.

Pankka, H., 1988. Gold-bearing sulphide deposits in the Kuusamo early Proterozoic volcano-sedimentary belt, northeastern Finland. Bicentennial Gold 88, Extended abstract. Poster Programme 1. Geol. Soc. Australian, Abstract Ser. 23, 165 — 167.

Pankka, H.S. & Bornhorst, T.J. in press. Hydrothermal alteration and alteration mineralogy of the Kuusamo Au-Co-U deposits in northeastern Finland.

Pankka, H., Puustinen, K. & Vanhanen, E., 1991. Kuusamon liuskealueen kulta-koboltti-uraaniesiintymät. Summary: Au-Co-U deposits in the Kuusamo volcano-sedimentary belt, Finland. Geol. Surv. Finland, Rep. Invest. 101, 53 p.

Pankka, H.S. & Vanhanen, E., 1989. Aulacogen related epigenetic Au-Co-U deposits in northeastern Finland. Geol. Surv. Finland, Spec. Pap. 10, 91 — 94.

Papunen, H., Idman, H., Ilvonen, E., Neuvonen, K.J., Pihlaja, P. & Talvitie, J., 1977. Lapin ultramafiiteista. English summary: The ultramafics of Lapland. Geol. Surv. Finland, Rep. Invest. 23, 87 p.

Pearton, T.N., 1979. A geochemical investigation of the carbonate and associated rocks of the Monarch antimony mine, Murchinson Range, North-Eastern Transvaal. Geol. Soc. S. Africa, Spec. Publ. 5, 159 — 166.

Pearton, T.N., 1982. Gold and antimony mineralization in altered komatiites of the Murchinson greenstone belt, South Africa. *In* N.T. Arndt & E.G. Nisbet (eds.), Komatiites. George Allen & Unwin, London, 459 — 475.

Pearton, T.N., 1984. The role of carbonate alteration in Archaean gold mineralization (abstract). *In* R.P. Foster (ed.), Gold '82: The geology, geochemistry and genesis of gold deposits. Balkema, Rotterdam, p. 687.

Pekkala, Y. & Puustinen, K., 1978. The chromian marbles of Kittilä, Finnish Lapland. Geol. Soc. Finland, Bull. 50, 15 — 29.

Pekkarinen, L., 1988. The Hattuvaara gold occurrence, Ilomantsi; a case history. *In* V. Lappalainen & H. Papunen (eds.), Tutkimuksia geologian alalta. Annales Universitatis Turkuensis. Turun yliopiston julkaisuja, sarja C 67, 79 — 87.

Phillips, N.G. & Groves, D.I., 1983. The nature of Archaean gold-bearing fluids as deduced from gold deposits of Western Australia. Jour. Geol. Soc. Australia 30, 25 — 39.

Phillips, N.G. & Groves, D.I., 1984. Fluid access and fluid-wall rock interaction in the genesis of the Archaean gold-quartz vein deposits at Hunt mine, Kambalda, Western Australia *In* R.P. Foster (ed.), Gold '82: The geology, geochemistry and genesis of gold deposits. Balkema, Rotterdam, p. 390 — 416.

Piirainen, T. 1988. The geology of the Archaean greenstone — granitoid terrain in Kuhmo, eastern Finland. Geol. Surv. Finland, Spec. Pap. 4, 39 — 51.

Pulkkinen, E., 1987. Biogeochemical and geobotanical exploration for gold in the Central Lapland greenstone belt. Gold '87, Program and abstracts. Univ. Turku. Dep. Geol. Publ. 19, p. 5.

Pulkkinen, E., 1983. Sattasen karttalehtialueen geokemiallisen kartoituksen tulokset. Geokemiallisten karttojen selitykset, Lehti 3714. English summary: The results of the geochemical survey in the Sattanen map-sheet area. Explanatory notes to geochemical maps, Sheet 3714. Geol. Surv. Finland, 67 p.

Pulkkinen, E., Ollila, J., Manner, R. & Koljonen, T., 1986. Geochemical exploration for gold in the Sattasvaara komatiite complex, Finnish Lapland. *In* Prospecting in areas of glaciated terrain, 1986. Inst. Min. Metall. London, 129 — 137.

Pulkkinen, E., Räisänen, M-L. & Ukonmaanaho, L., 1989. Geobotanical and biochemical exploration for gold in the Sattasvaara volcanic complex Finnish Lapland. J. Geochem. Explor. 32, 223 — 230.

Ramsay, J.G., 1980. Shear zone geometry: a review. J. Struct. Geol. 2, 83 — 99.

Räsänen, J., 1983. Keski-Lapin liuskealueen komatiiteista. English summary. Geologi 35, 25 — 29.

Räsänen, J., 1989. Komatiitit. *In* T. Manninen & R. Kesola (eds.), Lapin vulkaniittiprojekti, Vuosikertomus 1988. Geologian tutkimuskeskus, Rap. K/20.3/1989/1, 33 — 34.

Räsänen, J., Hanski, E. & Lehtonen, M., 1989. Komatiites, low-Ti basalts and andesites in the Möykkelmä area, Central Finnish Lapland. Geol. Surv. Finland, Rep. Invest. 88, 41 p.

Rastas, P., 1980. Stratigraphy of the Kittilä area. *In* A. Silvennoinen (ed.), Jatulian geology in the eastern part of the Baltic Shield. Proceedings of a Symposium held in Finland 21st — 26th August, 1979. The Committee for Scientific and Technical Co-operation between Finland and the Soviet Union, Rovaniemi, 145 — 151.

Robert, F. & Brown, A.C., 1986. Archean gold-bearing quartz veins at the Sigma mine, Abitibi greenstone belt, Quebec: II. Vein paragenesis and hydrothermal alteration. Econ. Geol. 81, 593 — 616.

Roberts, R.G., 1987. Ore depositional models 11. Archean lode gold deposits. Geosc. Canada 14, 37 — 52.

Roedder, E., 1984. Fluid-inclusion evidence bearing on the environments of gold deposition. *In* R.P. Foster (ed.), Gold '82: The geology, geochemistry and genesis of gold deposits. Balkema, Rotterdam, 129 — 165.

Romberger, S.B., 1986. The solution chemistry of gold applied to the origin of hydrothermal deposits. *In* L.A. Clark (ed.), Gold in the Western Shield. Canadian Instit. Mining Metall., Spec. Vol. 38, 168 — 186.

Romberger, S.B., 1988. Geochemistry of gold in hydrothermal deposits. U.S. Geol. Surv., Bull. 1857, A9 — A25.

Rose, A.W. & Burt, D.M., 1979. Hydrothermal alteration. *In* H.L. Barnes (ed.), Geochemistry of hydrothermal ore deposits. Sec. Ed. John Wiley & Sons. New York, 173 — 235.

Rosenbaum, J. & Sheppard, S.M.S., 1986. An isotopic study of siderites, dolomites and ankerites at high temperature. Geochim. Cosmochim. Acta 50, 1147 — 1150.

Rouhunkoski, P. & Isokangas, P., 1974. The copper-gold vein deposit of Kivimaa at Tervola, N-Finland. Geol. Soc. Finland, Bull. 46, 29 — 36.

Saverikko, M., 1983. Explosive komatiitic volcanism in Finnish Lapland. Geologi 2, 21 — 23.

Saverikko, M., 1985. The pyroclastic komatiite complex at Sattasvaara in northern Finland. Geol. Soc. Finland, Bull. 57, 55 — 87.

Saverikko, M., 1990. Komatiitic explosive volcanism and its tectonic setting in Finland, the Fennoscandian (Baltic) Shield. Geol. Soc. Finland, Bull. 62, 3 — 38.

Seward, T.M., 1979. Hydrothermal transport and deposition of gold. Univ. Western Australia, Geol. Dept. Ext. Serv., Publ. 3, 45 — 55.

Seward, T.M., 1984. The transport and deposition of gold in hydrothermal systems. *In* R.P. Foster (ed.), Gold '82: The geology, geochemistry and genesis of gold deposits. Balkema, Rotterdam, 239 — 247.

Sillitoe, R.H., 1991. Intrusion-related gold deposits. *In* R.P. Foster (ed.), Gold metallogeny and exploration. Blackie, Glasgow, 165 — 209.

Silvennoinen, A., 1985. On the Proterozoic stratigraphy of Northern Finland. Geol. Surv. Finland, Bull. 331, 107 — 116.

Silvennoinen, A., Honkamo, M., Juopperi, H., Lehtonen, M., Mielikäinen, P., Perttunen, V., Rastas, P., Räsänen, J. & Väänänen, J., 1980. Main features of the stratigraphy of North Finland. *In* A. Silvennoinen (ed.), Jatulian geology in the eastern part of the Baltic Shield. Proceedings of a Symposium held in Finland 21st — 26th August, 1979. The Committee for Scientific and Technical Co-operation between Finland and the Soviet Union, Rovaniemi, 153 — 162.

Simonen, A., 1980. The Precambrian in Finland. Geol. Surv. Finland, Bull. 304, 58 p.

Skiöld, T., 1987. Aspects of the Proterozoic geochronology of northern Sweden. Prec. Res. 35, 161 — 167.

Skwarnecki, M.S., 1987. Controls on Archaean gold mineralization in the Leonora district, Western Australia. *In* S.E. Ho & D.I. Groves (eds.), Recent advances in understanding Precambrian gold deposits. Geol. Dep. & Univ. Extension, Univ. Western Australia, Publ. 11, 109 — 135.

Skwarnecki, M.S., 1988. Alteration and deformation in a shear zone hosting gold mineralization at Harbour Lights, Leonora, Western Australia. *In* S.E. Ho & D.I. Groves (eds.), Advances in understanding Precambrian gold deposits, II. Geol. Dep. & Univ. Ext., Univ. Western Australia, Publ. 12, 111 — 129.

Smith, P.M., 1986. Duport, a structurally controlled gold deposit in Northwestern Ontario, Canada. *In* Proceedings of Gold '86, an international Symposium on the geology of gold deposits. Toronto, 1986, 197 — 212.

Steefel, C.I., 1987. The Johnson River prospect, Alaska: Gold-rich sea-floor mineralization from the Jurassic. Econ. Geol. 82, 894 — 914.

Sun, S.-S. & Nesbitt, R.W., 1978. Petrogenesis of Archaean ultrabasic and basic volcanics: evidence from rare earth elements. Contr. Mineral. Petrol. 65, 301 — 325.

Tamminen, E. Saattoporan kultamalmi. Unpubl. Phil. Lic. thesis. Univ. Oulu (in prep).

Thomas, D.J., 1987. Gold deposits of the La Ronge Domain, Field trip guidebook, trip 4. Geol. Ass. Canada and Miner. Ass. Canada. Joint annual meeting. Saskatoon, Saskatchewan, May 22 — 23, 70 p.

Thomson, M.L., 1986. Petrology of the Crixas gold deposit, Brazil: Evidence for gold associated with hydrothermal alteration, subsequent to metamorphism. *In* A.J. Macdonald (ed.), Proceedings of Gold '86, an international Symposium on the geology of gold deposits. Toronto, 1986, 284 — 296.

Turekian, K.K. & Wedepohl, K.H., 1961. Distribution of the elements in some major units of the earth's crust. Geol. Soc. America, Bull. 7, 175 — 192.

Tyrväinen, A., 1983. Sodankylän ja Sattasen kartta-alueiden kallioperä. Kallioperäkarttojen selitykset — Explanation to the maps of Pre-Quaternary rocks. Lehdet — Sheets 3713, 3714. Summary: Pre-Quaternary rocks of the Sodankylä and Sattanen map-sheet areas. Geological Survey of Finland, 59 p.

Tyrväinen, A., 1979. Geological map of Finland 1 : 100 000. Pre-Quaternary rocks. Sheet 3714 Sodankylä. Geological Survey of Finland.

Väänänen, J., 1989. Kolarin alueen vulkaniitit. Summary: Volcanic rocks of the Kolari area, western Finnish Lapland. Geol. Surv. Finland, Rep. Invest. 86, 79 p.

Vance, R.K. & Condie, K.C., 1987. Geochemistry of footwall alteration associated with the Early Proterozoic

United Verde massive sulphide deposit, Jerome, Arizona. Econ. Geol. 82, 571 — 586.

Viljoen, M.J., 1984. Archaean gold mineralization and komatiites in southern Africa. *In* R.P. Foster (ed.), Gold '82: The geology, geochemistry and genesis of gold deposits. Balkema, Rotterdam, 595 — 627.

Viljoen, M.J. & Viljoen, R.P., 1969. The geology and geochemistry of the lower ultramafic unit of the Onverwacht Group and a proposed new glass of igneous rocks. Geol. Soc. S. Africa, Spec. Publ. 2, 55 — 86.

Viljoen, M.J., Viljoen, R.P. & Pearton, T.N., 1982. The nature and distribution of Archaean komatiite volcanics in South Africa. *In* N.T. Arndt & E.G. Nisbet (eds.), Komatiites. George Allen & Unwin, London, 53 — 79.

Viljoen, M.J., Viljoen, R.P., Smith, H.S. & Erlank, A.J., 1983. Geological, textural and geochemical features of komatiitic flows from the Komati Formation. Geol. Soc. S. Africa, Spec. Publ. 9, 1 — 20.

Ward, P., Härkönen, I., Nurmi, P. & Pankka, H., 1989. Structural studies in the Lapland greenstone belt, northern Finland and their application to gold mineralization. Geol. Surv. Finland, Spec. Pap. 10, 71 — 77.

Wood, P.C., Burrows, D.R., Thomas, A.V. & Spooner, E.T.C., 1986. The Hollinger-McIntyre Au-quartz vein system, Timmins, Ontario, Canada: geologic characteristics, fluid properties and light stable isotope geochemistry. *In* A.J. Macdonald (ed.), Proceedings of Gold '86, an international Symposium on the geology of gold deposits. Toronto, 1986, 56 — 80.

Wood, D.A., Gibson, I.L. & Thompson, R.N., 1976. Element mobility during zeolite facies metamorphism of the Tertiary basalts of Eastern Iceland. Contrib. Mineral. Petrol. 55, 241 — 254.

Wyman, D.A., Kerrich, R. & Fryer, B.J., 1986. Gold mineralization overprinting iron formations at the Agnico-Eagle deposit, Quebec, Canada: mineralogical, microstructural and geochemical evidence. *In* A.J. Macdonald (ed.), Proceedings of Gold '86, an international Symposium on the geology of gold deposits. Toronto, 1986, 108 — 123.

APPENDIX 1:

Recalculated whole rock compositions with detailed mineral assemblages and associated rock classification symbols for the samples from the Pahtavaara gold deposit. Samples 1—8 are from outcrops and 9—134 from drill cores. Data is arranged according to the drill core number and depth.

Rock symbols:

- ● = Amphibole-chlorite schist (four least altered samples)
- ○ = Amphibole-chlorite schist with talc-carbonate alteration
- X = Amphibole porphyroblastic talc-carbonate schist
- B = Biotite schist
- * = High-alumina (>4 wt. %' Al_2O_3) amphibole rock
- A = Low-alumina (< wt. % Al_2O_3) amphibole rock
- V = Vein

Note: In Figures within the text rock symbols '○' and 'X' of weakly altered rock types are combined for simplicity and shown by symbol 'X'. Al/Ti ratio in oxide.

Mineral abbreviations:

- AB = Albite
- AF = Coarse-grained amphibole
- AM = Fine-grained amphibole
- BA = Barite
- BT = Biotite
- CB = Carbonate
- CL = Chlorite
- MG = Magnetite
- QU = Quartz
- TC = Talc
- V: = Minor vein

Others:

- D = Density [kg/dm^3]
- f_V = Volume factor

APPENDIX 1.

	1	2	3	4	5	6	7	8
SiO_2 (%)	45.01	53.62	52.98	44.52	45.22	47.34	47.37	44.61
TiO_2	0.92	0.25	0.35	0.98	0.69	0.65	0.61	0.75
Al_2O_3	8.74	3.09	4.87	9.61	6.72	6.34	7.04	7.22
$Fe_2O_3^{tot}$	15.50	14.83	13.97	15.19	13.43	12.50	10.08	14.32
MnO	0.30	0.46	0.46	0.23	0.38	0.18	0.30	0.34
MgO	19.40	16.52	16.69	19.31	22.59	24.15	25.52	22.19
CaO	8.81	10.19	9.97	8.85	10.93	8.60	8.80	10.09
Na_2O	1.19	0.95	0.65	1.15	0.00	0.19	0.20	0.36
K_2O	0.07	0.04	0.00	0.07	0.00	0.01	0.01	0.06
P_2O_5	0.06	0.05	0.07	0.07	0.05	0.04	0.06	0.06
Total	100.00	100.00	100.00	100.00	100.00	100.00	100.00	100.00
Au (ppb)	2	33000	33000	2	146	2	2	12
Te	1	n.d.	n.d.	1	n.d.	6	2	6
S (%)	0.01	0.81	0.60	0.01	1.57	0.01	0.01	0.01
CO_2	2.08	2.00	0.25	0.04	6.19	0.03	1.22	4.96
Ba (ppm)	27	26800	18300	53	28	23	70	43
Cr	1830	1290	1000	1600	1970	1780	2920	2260
Ni	1100	640	n.d.	1100	n.d.	1300	920	930
V	320	190	n.d.	310	n.d.	190	160	230
Co	71	n.d.	n.d.	77	n.d.	71	69	63
Zn	90	30	n.d.	83	n.d.	81	100	25
Sc	27.7	n.d.	n.d.	29.2	n.d.	22.2	23.9	22.8
W	20	n.d.	n.d.	13	n.d.	10	11	11
Sr	10	350	n.d.	10	n.d.	10	10	23
Al/Ti	9.53	12.38	13.88	9.80	9.68	9.82	11.47	9.57
D (kg/dm^3)	3.00	n.d.	n.d.	3.00	n.d.	2.96	2.86	2.94
f_v	0.74	2.13	1.35	0.67	0.98	1.03	0.96	0.91

SAMPLE	MINERALOGY	ROCK SYMBOL			
1 = 050/0.0	AM-CL-(CB)	○	5 = 054/0.0	AF-CB	*
2 = 051/0.0	AF V:AB-QU-AM-BA-CB	A	6 = 055/0.0	AM-CL	●
3 = 052/0.0	AF-(AB-BA)	*	7 = 057/0.0	AM-CL	○
4 = 053/0.0	AM-CL	○	8 = 061/0.0	AM-CL-TC-CB	○

APPENDIX 1 (continued).

	9	10	11	12	13	14	15	16
SiO_2 (%)	45.44	44.49	47.22	47.76	49.46	50.63	47.51	51.72
TiO_2	0.82	0.70	0.75	0.84	0.68	0.78	0.67	0.70
Al_2O_3	7.24	6.80	7.24	7.74	6.45	6.66	6.86	6.63
$Fe_2O_3^{tot}$	15.03	14.65	13.73	14.66	13.39	11.15	10.44	8.83
MnO	0.21	0.23	0.26	0.24	0.21	0.22	0.29	0.27
MgO	24.26	25.31	21.29	18.68	24.39	19.77	20.31	17.16
CaO	7.00	7.65	9.39	9.32	5.43	10.23	13.37	13.60
Na_2O	0.00	0.12	0.00	0.69	0.00	0.55	0.48	1.09
K_2O	0.00	0.02	0.00	0.00	0.00	0.00	0.00	0.00
P_2O_5	0.00	0.04	0.12	0.06	0.00	0.00	0.08	0.00
Total	100.00	100.00	100.00	100.00	100.00	100.00	100.00	100.00
Au (ppb)	0	2	0	0	0	0	0	4
Te	n.d.	1	n.d.	n.d.	n.d.	n.d.	n.d.	n.d.
S (%)	0.01	0.01	0.03	0.01	0.06	0.01	0.02	0.01
CO_2	0.6	0.96	2.27	0.41	0.7	0.7	5.02	1.82
Ba (ppm)	4	73	238	4	5	4	4	5
Cr	2810	2630	2450	3140	2440	2190	1790	2510
Ni	n.d.	1300	n.d.	n.d.	n.d.	n.d.	n.d.	n.d.
V	n.d.	220	n.d.	n.d.	n.d.	n.d.	n.d.	n.d.
Co	n.d.	81	n.d.	n.d.	n.d.	n.d.	n.d.	n.d.
Zn	n.d.	93	n.d.	n.d.	n.d.	n.d.	n.d.	n.d.
Sc	n.d.	24.0	n.d.	n.d.	n.d.	n.d.	n.d.	n.d.
W	n.d.	8	n.d.	n.d.	n.d.	n.d.	n.d.	n.d.
Sr	n.d.	10	n.d.	n.d.	n.d.	n.d.	n.d.	n.d.
Al/Ti	8.85	9.71	9.62	9.21	9.48	8.59	10.21	9.53
D (kg/dm^3)	n.d.	n.d.	n.d.	n.d.	n.d.	n.d.	n.d.	n.d.
f_V	0.91	0.97	0.91	0.85	1.02	0.99	0.96	0.99

SAMPLE	MINERALOGY	ROCK SYMBOL			
9 = 230/33.25	CL-AM	O	13 = 232/34.2	CL-AF-TC	X
10 = 230/44.5	CL-AM	●	14 = 236/5.8	AF	*
11 = 232/6.75	AF-TC-(CB)	X	15 = 236/17.8	AF-CB	*
12 = 232/17.45	AF-CL	*	16 = 239/6.9	AF-(AB)	*

APPENDIX 1 (continued).

	17	18	19	20	21	22	23	24
SiO_2 (%)	48.31	38.91	48.14	52.54	44.18	47.74	51.49	41.30
TiO_2	0.61	1.27	0.59	1.00	0.88	0.70	1.04	0.93
Al_2O_3	6.36	8.51	6.31	5.99	5.86	7.09	5.44	7.11
$Fe_2O_3^{tot}$	7.52	5.50	9.21	12.31	18.22	14.02	12.66	14.95
MnO	0.33	0.44	0.29	0.09	0.23	0.20	0.13	0.33
MgO	16.41	17.00	18.81	24.72	23.69	22.81	23.57	25.33
CaO	19.39	24.82	16.22	3.28	6.88	7.39	5.60	10.01
Na_2O	1.06	3.55	0.43	0.00	0.00	0.00	0.00	0.00
K_2O	0.00	0.00	0.00	0.00	0.00	0.00	0.00	0.00
P_2O_5	0.00	0.00	0.00	0.08	0.06	0.04	0.06	0.05
Total	100.00	100.00	100.00	100.00	100.00	100.00	100.00	100.00
Au (ppb)	1	4	3	0	1	1	0	0
Te	n.d.	n.d.	n.d.	n.d.	n.d.	n.d.	n.d.	n.d.
S (%)	0.01	0.01	0.03	0.03	0.01	0.01	0.01	0.01
CO_2	6.18	21.5	6.21	0.41	6.14	1.43	0.52	9.02
Ba (ppm)	8	36	7	7	12	43	4	8
Cr	2530	1180	2170	2000	3760	2600	1720	2130
Ni	n.d.	n.d.	n.d.	n.d.	n.d.	n.d.	n.d.	n.d.
V	n.d.	n.d.	n.d.	n.d.	n.d.	n.d.	n.d.	n.d.
Co	n.d.	n.d.	n.d.	n.d.	n.d.	n.d.	n.d.	n.d.
Zn	n.d.	n.d.	n.d.	n.d.	n.d.	n.d.	n.d.	n.d.
Sc	n.d.	n.d.	n.d.	n.d.	n.d.	n.d.	n.d.	n.d.
W	n.d.	n.d.	n.d.	n.d.	n.d.	n.d.	n.d.	n.d.
Sr	n.d.	n.d.	n.d.	n.d.	n.d.	n.d.	n.d.	n.d.
Al/Ti	10.47	6.69	10.71	5.99	6.65	10.11	5.24	7.67
D (kg/dm^3)	n.d.	n.d.	n.d.	n.d.	n.d.	n.d.	n.d.	n.d.
f_v	1.03	0.77	1.04	1.10	1.12	0.93	1.21	0.93

SAMPLE	MINERALOGY	ROCK SYMBOL			
17 = 239/8.1	AF-CB-(AB)	*	21 = 242/13.0	CL-AM-TC-CB	○
18 = 239/11.05	CB-AB-AF	V	22 = 246/10.0	CL-AM	○
19 = 240/7.95	AF-CB	*	23 = 248/8.95	CL-AM-TC	○
20 = 242/9.8	AF-TC-CL	X	24 = 248/16.6	AM-CB-CL	○

APPENDIX 1 (continued).

	25	26	27	28	29	30	31	32
SiO_2 (%)	48.41	48.03	46.23	41.24	44.64	50.79	43.61	40.26
TiO_2	0.88	0.97	0.63	1.22	0.89	1.07	0.17	1.03
Al_2O_3	5.71	6.25	6.48	7.63	9.20	6.93	1.20	6.36
$Fe_2O_3^{tot}$	13.58	15.71	13.68	19.10	18.82	12.34	7.43	11.54
MnO	0.11	0.13	0.23	0.20	0.32	0.36	0.46	0.42
MgO	25.63	24.48	26.05	24.25	19.81	15.09	17.90	18.72
CaO	5.41	4.35	6.69	6.31	2.20	12.98	28.92	21.02
Na_2O	0.20	0.00	0.00	0.00	0.00	0.40	0.00	0.41
K_2O	0.02	0.00	0.00	0.00	4.13	0.00	0.29	0.19
P_2O_5	0.05	0.07	0.00	0.05	0.00	0.05	0.00	0.05
Total	100.00	100.00	100.00	100.00	100.00	100.00	100.00	100.00
Au (ppb)	2	0	0	1	7	0	138	1
Te	1	n.d.	n.d.	n.d.	n.d.	n.d.	n.d.	n.d.
S (%)	0.01	0.01	0.01	0.01	0.11	0.02	0.01	0.01
CO_2	1.98	1.33	5.17	6.24	3.03	3.14	16.4	13.9
Ba (ppm)	67	3	7	34	3656	61	10	17
Cr	2320	2320	1610	3052	3050	1590	1010	2140
Ni	1400	n.d.	n.d.	n.d.	n.d.	n.d.	n.d.	n.d.
V	200	n.d.	n.d.	n.d.	n.d.	n.d.	n.d.	n.d.
Co	86	n.d.	n.d.	n.d.	n.d.	n.d.	n.d.	n.d.
Zn	110	n.d.	n.d.	n.d.	n.d.	n.d.	n.d.	n.d.
Sc	24.6	n.d.	n.d.	n.d.	n.d.	n.d.	n.d.	n.d.
W	9	n.d.	n.d.	n.d.	n.d.	n.d.	n.d.	n.d.
Sr	12	n.d.	n.d.	n.d.	n.d.	n.d.	n.d.	n.d.
Al/Ti	6.51	6.43	10.23	6.28	10.35	6.50	7.07	6.16
D (kg/dm^3)	n.d.	n.d.	n.d.	n.d.	n.d.	n.d.	n.d.	n.d.
f_v	1.15	1.05	1.01	0.86	0.71	0.95	5.46	1.03

SAMPLE	MINERALOGY	ROCK SYMBOL			
25 = 248/16.75	AM-CL-TC	O	29 = 250/6.5	BT-CL-TC-(CB)	B
26 = 248/27.0	AM-CL-TC	O	30 = 250/20.0	AF-(CB)	*
27 = 248/38.85	CL-AM-CB	O	31 = 250/21.9	AF V:CB-AF	A
28 = 249/8.3	TC-AM-CL-CB	O	32 = 250/22.5	AF-CB	*

APPENDIX 1 (continued).

	33	34	35	36	37	38	39	40
SiO_2 (%)	54.70	40.15	42.36	42.23	54.03	42.67	44.94	45.91
TiO_2	0.43	1.12	0.77	0.92	0.32	0.63	0.58	0.92
Al_2O_3	5.33	8.64	7.95	9.17	3.76	6.77	6.90	9.11
$Fe_2O_3^{tot}$	9.69	17.08	20.83	24.34	12.06	13.90	12.30	21.49
MnO	0.30	0.48	0.55	0.37	0.33	0.45	0.31	0.20
MgO	15.29	20.57	23.23	21.22	17.15	22.27	25.14	16.42
CaO	13.83	7.24	2.14	0.20	11.95	13.22	9.83	2.24
Na_2O	0.44	0.00	0.00	0.00	0.27	0.00	0.00	0.82
K_2O	0.00	4.71	2.16	1.50	0.06	0.09	0.00	2.81
P_2O_5	0.00	0.00	0.00	0.05	0.06	0.00	0.00	0.08
Total	100.00	100.00	100.00	100.00	100.00	100.00	100.00	100.00
Au (ppb)	0	0	3	20	350	5	1	1
Te	n.d.	n.d.	n.d.	n.d.	n.d.	n.d.	n.d.	n.d.
S (%)	0.01	0.01	0.11	0.16	0.18	0.04	0.01	0.01
CO_2	3.57	9.84	6.16	0.04	1.25	10.9	9.58	0.09
Ba (ppm)	19	4572	2260	5736	243	304	24	3037
Cr	270	3000	2440	2700	910	1980	1390	3830
Ni	n.d.	n.d.	n.d.	n.d.	n.d.	n.d.	n.d.	n.d.
V	n.d.	n.d.	n.d.	n.d.	n.d.	n.d.	n.d.	n.d.
Co	n.d.	n.d.	n.d.	n.d.	n.d.	n.d.	n.d.	n.d.
Zn	n.d.	n.d.	n.d.	n.d.	n.d.	n.d.	n.d.	n.d.
Sc	n.d.	n.d.	n.d.	n.d.	n.d.	n.d.	n.d.	n.d.
W	n.d.	n.d.	n.d.	n.d.	n.d.	n.d.	n.d.	n.d.
Sr	n.d.	n.d.	n.d.	n.d.	n.d.	n.d.	n.d.	n.d.
Al/Ti	12.47	7.70	10.27	10.00	11.93	10.79	11.84	9.89
D (kg/dm^3)	n.d.	n.d.	n.d.	n.d.	n.d.	n.d.	n.d.	n.d.
f_v	1.24	0.76	0.83	0.72	1.75	0.97	0.95	0.72

SAMPLE	MINERALOGY	ROCK SYMBOL			
33 = 250/24.4	AF-CL-(CB)	*	37 = 252/21.0	AF-TC-(AB)	A
34 = 251/15.9	BT-CB-TC V:CB-TC	B	38 = 253/9.6	AF-CB-(BT)	X
35 = 251/23.7	BT-CL-CB-TC	B	39 = 253/13.1	CL-TC V:CB-AM	O
36 = 252/10.5	TC-CL-BT	B	40 = 254/9.15	BT-CL-AM V:QU-TC-AF	B

APPENDIX 1 (continued).

	41	42	43	44	45	46	47	48
SiO_2 (%)	55.58	53.88	56.20	16.68	43.88	43.53	46.11	44.08
TiO_2	0.18	0.06	0.11	0.08	0.64	0.78	0.68	0.69
Al_2O_3	2.77	2.90	2.49	0.62	7.63	8.68	8.13	7.39
$Fe_2O_3^{tot}$	13.38	19.90	11.50	18.65	18.57	24.03	13.45	14.16
MnO	0.53	0.85	0.46	1.02	0.49	0.17	0.25	0.34
MgO	19.02	18.19	17.99	26.95	21.84	18.83	19.67	23.49
CaO	8.39	3.21	11.19	35.76	4.11	0.39	10.91	8.78
Na_2O	0.08	0.18	0.00	0.00	0.00	0.00	0.80	1.07
K_2O	0.00	0.00	0.00	0.25	2.82	3.54	0.00	0.00
P_2O_5	0.07	0.85	0.06	0.00	0.03	0.05	0.00	0.00
Total	100.00	100.00	100.00	100.00	100.00	100.00	100.00	100.00
Au (ppb)	1	3	0	2	6	21	49	0
Te	n.d.	n.d.	n.d.	n.d.	n.d.	n.d.	n.d.	n.d.
S (%)	0.12	0.03	0.01	0.06	0.03	0.15	0.01	0.05
CO_2	0.58	0.06	0.53	34.4	5.59	0.35	6.88	12.1
Ba (ppm)	17	47	63	81	4692	4036	27	100
Cr	500	300	80	10	1940	2730	1760	1950
Ni	n.d.	n.d.	n.d.	n.d.	n.d.	n.d.	n.d.	n.d.
V	n.d.	n.d.	n.d.	n.d.	n.d.	n.d.	n.d.	n.d.
Co	n.d.	n.d.	n.d.	n.d.	n.d.	n.d.	n.d.	n.d.
Zn	n.d.	n.d.	n.d.	n.d.	n.d.	n.d.	n.d.	n.d.
Sc	n.d.	n.d.	n.d.	n.d.	n.d.	n.d.	n.d.	n.d.
W	n.d.	n.d.	n.d.	n.d.	n.d.	n.d.	n.d.	n.d.
Sr	n.d.	n.d.	n.d.	n.d.	n.d.	n.d.	n.d.	n.d.
Al/Ti	15.71	46.17	21.82	8.00	11.95	11.19	12.00	10.79
D (kg/dm^3)	n.d.	n.d.	n.d.	n.d.	n.d.	n.d.	n.d.	n.d.
f_v	2.38	2.27	2.65	10.60	0.86	0.76	0.81	0.89

SAMPLE	MINERALOGY	ROCK SYMBOL			
41 = 254/13.4	AF	A	45 = 255/2.45	BT-CL-TC-CB	B
42 = 254/16.2	AF-(QU)	A	46 = 255/9.3	BT-TC-(MG)	B
43 = 254/17.5	AF-(QU)	A	47 = 256/2.6	AM-CB-(MG)	O
44 = 254/24.3	CB-TC-CL-(BT)	V	48 = 256/16.5	CL-CB-TC-(AB)	O

APPENDIX 1 (continued).

	49	50	51	52	53	54	55	56
SiO_2 (%)	38.81	47.40	47.46	57.49	41.58	47.26	48.47	44.40
TiO_2	0.62	0.58	0.70	0.07	0.88	0.86	0.65	0.61
Al_2O_3	11.38	6.42	8.47	1.37	9.18	6.67	7.53	6.21
$Fe_2O_3^{tot}$	23.15	12.79	13.04	9.77	13.63	9.78	8.54	17.07
MnO	0.94	0.29	0.15	0.39	0.29	0.36	0.32	0.67
MgO	23.15	22.44	24.51	18.52	21.18	16.86	14.53	20.64
CaO	0.40	10.08	4.82	12.39	8.70	16.64	17.97	8.54
Na_2O	0.94	0.00	0.15	0.00	0.00	1.33	1.64	0.38
K_2O	0.62	0.00	0.70	0.00	4.55	0.17	0.28	1.42
P_2O_5	0.00	0.00	0.00	0.00	0.00	0.08	0.07	0.06
Total	100.00	100.00	100.00	100.00	100.00	100.00	100.00	100.00
Au (ppb)	13	0	0	0	33	9	2	11
Te	n.d.	n.d.	n.d.	n.d.	n.d.	9	11	33
S (%)	0.02	0.02	0.01	0.01	0.02	0.02	0.05	0.32
CO_2	16.5	7.52	0.32	0.4	8.5	6.16	6.59	6.45
Ba (ppm)	4700	73	32	41	3211	199	612	1900
Cr	2170	1730	2320	140	2960	2360	2320	2060
Ni	n.d.	n.d.	n.d.	n.d.	n.d.	980	650	1500
V	n.d.	n.d.	n.d.	n.d.	n.d.	200	180	190
Co	n.d.	n.d.	n.d.	n.d.	n.d.	40	31	67
Zn	n.d.	n.d.	n.d.	n.d.	n.d.	41	29	28
Sc	n.d.	n.d.	n.d.	n.d.	n.d.	25.5	26.6	23.4
W	n.d.	n.d.	n.d.	n.d.	n.d.	57	54	43
Sr	n.d.	n.d.	n.d.	n.d.	n.d.	140	217	70
Al/Ti	18.37	11.14	12.03	18.86	10.39	7.76	11.51	10.13
D (kg/dm^3)	n.d.	n.d.	n.d.	n.d.	n.d.	2.92	2.91	3.03
f_v	0.58	1.03	0.78	4.79	0.72	0.99	0.88	1.03

SAMPLE	MINERALOGY	ROCK SYMBOL			
49 = 256/23.3	CB-CL-(AB-BT-BA)	O	53 = 262/33.0	BT-CL V:CB-TC-AM	B
50 = 256/33.55	TC-AM-CB-CL	O	54 = 506/9.0	AF-CB-(AB)	*
51 = 257/15.3	CL-AM-TC	O	55 = 506/16.6	AF-QU-CB-AB	*
52 = 262/18.0	AF	A	56 = 506/29.2	AF-BT-CB-TC	B

APPENDIX 1 (continued).

	57	58	59	60	61	62	63	64
SiO_2 (%)	44.65	44.72	35.80	41.90	51.94	43.29	47.74	45.28
TiO_2	0.60	0.70	0.34	0.75	0.44	0.84	0.67	0.80
Al_2O_3	7.01	6.71	1.38	7.42	5.39	6.84	6.09	7.52
$Fe_2O_3^{tot}$	14.92	17.61	18.09	14.73	10.45	18.97	10.75	10.29
MnO	0.51	0.39	0.65	0.34	0.33	0.61	0.35	0.31
MgO	22.04	20.49	31.11	24.66	17.45	20.61	17.85	17.16
CaO	7.17	6.31	11.76	9.57	12.54	5.58	14.52	16.27
Na_2O	0.28	0.31	0.10	0.38	1.17	0.22	0.81	0.93
K_2O	2.76	2.70	0.25	0.19	0.25	2.99	1.17	1.37
P_2O_5	0.07	0.05	0.52	0.06	0.03	0.05	0.05	0.07
Total	100.00	100.00	100.00	100.00	100.00	100.00	100.00	100.00
Au (ppb)	18	130	230	34	3	44	4	9
Te	12	22	9	7	5	28	6	12
S (%)	0.02	0.18	0.05	0.07	0.01	0.1	0.3	0.06
CO_2	6.28	3.40	18.8	7.46	1.81	4.64	5.05	6.33
Ba (ppm)	2030	6200	199	138	972	6130	8430	1840
Cr	2270	2220	1530	2350	2070	1630	1280	2010
Ni	1400	1200	1100	1200	910	1100	790	870
V	180	170	40	160	170	170	190	220
Co	64	63	65	88	45	63	43	43
Zn	24	25	26	29	21	22	19	20
Sc	24.5	24.1	9.50	27.6	25.7	27.0	23.5	30.4
W	150	24	13	39	56	15	29	37
Sr	49	73	93	54	53	51	256	149
Al/Ti	11.70	9.53	4.08	9.85	12.29	8.14	9.13	9.43
D (kg/dm^3)	2.98	3.03	2.99	2.96	3.05	2.98	3.01	2.99
f_v	0.93	0.95	4.69	0.88	1.17	0.95	1.05	0.86

SAMPLE	MINERALOGY	ROCK SYMBOL			
57 = 506/33.5	BT-CL-CB	B	61 = 506/70.6	AF-(BT-AB)	*
58 = 506/47.4	BT V:AF-TC-CB	B	62 = 506/76.6	BT-TC-(CL)	B
59 = 506/53.8	TC-CB	V	63 = 506/80.6	AF-QU-CB-(BT-AB-BA)	*
60 = 506/59.8	CL-TC-AF-CB	X	64 = 506/88.8	AF-CB-AB-(BT)	*

APPENDIX 1 (continued).

	65	66	67	68	69	70	71	72
SiO_2 (%)	48.10	48.44	45.63	48.18	44.33	46.12	44.20	44.14
TiO_2	1.79	0.92	0.70	0.65	0.65	0.54	0.62	0.63
Al_2O_3	11.76	9.52	7.28	6.75	6.90	6.49	6.08	6.60
$Fe_2O_3^{tot}$	15.55	9.20	13.52	14.03	13.63	11.53	13.86	16.82
MnO	0.29	0.26	0.36	0.25	0.24	0.31	0.40	0.32
MgO	11.66	14.99	20.12	19.27	24.86	22.61	25.24	24.39
CaO	5.41	13.48	10.84	9.22	8.73	11.10	8.65	5.09
Na_2O	0.74	1.76	1.24	1.45	0.58	0.67	0.83	0.33
K_2O	4.55	1.37	0.23	0.16	0.03	0.60	0.07	1.64
P_2O_5	0.16	0.06	0.05	0.05	0.05	0.05	0.05	0.05
Total	100.00	100.00	100.00	100.00	100.00	100.00	100.00	100.00
Au (ppb)	480	5	5	58	4	83	5	3
Te	61	19	8	9	0	12	12	20
S (%)	0.09	0.02	0.01	0.04	0.01	0.03	0.11	0.02
CO_2	1.35	3.79	4.10	2.21	6.09	6.78	10.8	6.54
Ba (ppm)	1900	1320	996	510	330	1770	171	1430
Cr	120	2640	2280	2590	2270	2110	1980	2610
Ni	510	900	960	1300	1500	1200	1300	1400
V	410	230	160	190	170	160	140	160
Co	54	34	58	70	92	72	52	46
Zn	31	26	30	43	61	35	12	20
Sc	37.9	28.5	27.3	26.6	23.9	24.2	17.5	20.3
W	64	39	29	25	16	33	11	10
Sr	23	164	84	78	69	65	124	45
Al/Ti	6.59	10.38	10.34	10.33	10.56	11.96	9.87	10.45
D (kg/dm^3)	2.97	2.96	3.05	3.02	2.90	2.95	2.93	2.99
f_V	0.55	0.69	0.87	0.95	0.97	1.01	1.08	0.98

SAMPLE	MINERALOGY	ROCK TYPES			
65 = 506/98.8	BT-QU-TC V:AF-QU	B	69 = 506/122.4	AM-TC-CL-CB-(AB)	O
66 = 506/107.8	AF-CB-(AB-BT)	*	70 = 507/10.4	AF-CB-(AB-BT)	X
67 = 506/113.8	AF-(CB-AB-BT)	X	71 = 507/22.0	TC-CL-CB-(AB)	O
68 = 506/119.6	AF-(CB-TC-CL-AB)	*	72 = 507/31.3	BT-TC-CB V:TC-CB	B

APPENDIX 1 (continued).

	73	74	75	76	77	78	79	80
SiO_2 (%)	44.72	44.84	45.74	44.17	46.64	43.31	43.75	45.68
TiO_2	0.63	0.63	0.59	0.63	0.55	0.69	0.63	0.69
Al_2O_3	6.77	6.35	6.67	7.44	6.43	6.30	7.01	6.79
$Fe_2O_3^{tot}$	13.88	17.04	14.41	15.48	12.79	21.92	14.81	13.65
MnO	0.13	0.46	0.15	0.14	0.20	0.32	0.31	0.24
MgO	26.49	24.25	25.31	24.85	25.36	21.06	25.95	25.94
CaO	6.98	4.14	6.66	6.71	7.66	3.33	6.94	6.58
Na_2O	0.33	0.54	0.39	0.49	0.30	0.20	0.31	0.30
K_2O	0.03	1.69	0.03	0.05	0.03	2.83	0.24	0.09
P_2O_5	0.05	0.06	0.03	0.05	0.03	0.03	0.05	0.05
Total	100.00	100.00	100.00	100.00	100.00	100.00	100.00	100.00
Au (ppb)	3	36	3	3	3	3	11	3
Te	9	84	24	4	1	25	8	1
S (%)	0.03	0.22	0.13	0.02	0.02	0.09	0.01	0.03
CO_2	7.05	7.66	4.47	3.42	3.39	3.61	6.84	4.68
Ba (ppm)	847	3650	170	176	88	6060	347	117
Cr	2410	1860	2150	2510	2110	2710	2240	2430
Ni	1400	1300	1300	1400	1200	1300	1500	1300
V	170	150	140	170	180	180	160	160
Co	65	66	71	72	68	44	60	68
Zn	21	17	37	44	67	38	34	42
Sc	19.9	19.6	19.5	23.4	20.8	18.4	18.9	19.5
W	9	12	10	9	8	11	13	8
Sr	68	218	47	26	10	37	58	23
Al/Ti	10.73	10.09	11.31	11.77	11.66	9.16	11.09	9.87
D (kg/dm^3)	2.92	2.95	2.92	2.93	2.93	3.04	2.93	2.93
f_v	0.98	1.03	0.99	0.88	1.03	1.01	0.94	0.97

SAMPLE	MINERALOGY	ROCK TYPES			
73 = 507/38.3	TC-CL-CB-AM	O	77 = 507/76.0	TC-CL-AM V:CB-TC	O
74 = 507/52.5	BT-CL-CB V:TC-CB-AB	B	78 = 508/16.9	BT-CL V:TC-CB	B
75 = 507/60.7	CL-TC-AF V:CB-TC-AF	X	79 = 508/23.7	AM-TC-CB	O
76 = 507/66.0	TC-CL-AF-CB-(AB)	X	80 = 508/40.6	AF-TC-(CB)	X

APPENDIX 1 (continued).

	81	82	83	84	85	86	87	88
SiO_2 (%)	43.61	44.30	44.57	59.22	46.67	42.27	42.50	43.66
TiO_2	0.67	0.72	0.70	0.19	0.63	0.80	0.72	0.69
Al_2O_3	7.41	6.72	7.27	4.31	6.26	8.15	7.43	6.21
$Fe_2O_3^{tot}$	14.00	14.54	14.17	13.45	12.98	19.51	15.68	19.22
MnO	0.28	0.29	0.25	0.43	0.34	0.22	0.27	0.31
MgO	25.59	25.41	24.34	19.52	23.12	24.00	24.89	21.46
CaO	7.96	7.42	7.28	0.41	8.53	4.13	6.39	5.49
Na_2O	0.36	0.49	0.96	2.16	0.65	0.44	0.35	0.54
K_2O	0.08	0.06	0.43	0.24	0.79	0.45	1.73	2.36
P_2O_5	0.05	0.06	0.03	0.07	0.03	0.03	0.05	0.05
Total	100.00	100.00	100.00	100.00	100.00	100.00	100.00	100.00
Au (ppb)	3	2	4	60	3	100	35	7
Te	16	13	17	13	26	18	16	21
S (%)	0.01	0.01	0.01	0.45	0.08	0.01	0.08	0.04
CO_2	7.27	7.57	7.91	0.34	5.23	4.28	7.48	4.85
Ba (ppm)	141	101	520	18300	4880	750	1930	5610
Cr	2240	2340	2370	530	1990	2970	2340	2000
Ni	1300	1400	1300	1000	1300	1500	1500	1300
V	160	170	150	64	150	170	170	130
Co	68	85	60	29	43	75	57	55
Zn	41	26	14	14	12	26	23	25
Sc	21.3	12.2	21.7	16.8	18.4	23.1	22.6	26.9
W	18	12	15	34	20	3	3	13
Sr	50	35	75	462	108	23	48	49
Al/Ti	11.14	9.32	10.43	23.00	9.90	10.24	10.38	8.95
D (kg/dm^3)	2.94	2.95	2.94	2.97	2.98	2.99	2.96	3.04
f_v	0.89	0.97	0.90	1.51	1.04	0.79	0.88	1.02

SAMPLE	MINERALOGY	ROCK SYMBOL			
81 = 508/50.5	CL-AM-CB-TC	O	85 = 508/80.8	AF-TC-CB-(BT-CL-BA)	X
82 = 508/60.0	AM-TC-CB-CL	O	86 = 508/87.1	TC-CL-BT V:CB-TC-AF	X
83 = 508/66.1	AM-CB-TC-(BT-AB)	O	87 = 508/91.6	BT-TC-CB V:TC-CB-AM	B
84 = 508/72.9	AF-TC-(AB-BA)	V	88 = 508/100.0	BT-TC-(CB-CL)	B

APPENDIX 1 (continued).

	89	90	91	92	93	94	95	96
SiO_2 (%)	43.31	43.64	40.76	43.87	44.43	54.34	45.13	44.00
TiO_2	0.70	0.69	0.65	0.67	0.59	0.17	0.62	0.51
Al_2O_3	7.30	6.95	6.99	6.91	6.18	1.88	7.13	6.11
$Fe_2O_3^{tot}$	14.85	13.70	13.86	15.68	20.07	12.25	12.47	13.13
MnO	0.38	0.29	0.40	0.51	0.46	0.42	4	0.31
MgO	24.91	24.06	23.41	23.86	23.46	18.52	24.72	24.42
CaO	7.35	9.85	12.93	6.12	3.44	11.22	8.88	10.38
Na_2O	0.50	0.69	0.78	0.96	0.98	1.13	0.73	0.91
K_2O	0.65	0.07	0.17	1.37	0.34	0.04	0.05	0.20
P_2O_5	0.05	0.06	0.05	0.05	0.05	0.02	0.05	0.03
Total	100.00	100.00	100.00	100.00	100.00	100.00	100.00	100.00
Au (ppb)	54	6	29	32	100	6800	3	4
Te	16	21	32	70	53	58	4	2
S (%)	0.03	0.04	0.09	0.07	0.1	0.33	0.15	0.04
CO_2	6.51	7.73	10.5	8.38	5.39	2.11	7.13	9.36
Ba (ppm)	2010	253	173	4950	2990	5980	364	208
Cr	2180	2510	2460	2380	2090	670	1780	2950
Ni	1400	1300	1300	1300	1100	660	1200	1300
V	160	160	140	150	130	80	150	150
Co	70	88	71	62	66	70	95	78
Zn	22	19	12	15	17	17	45	69
Sc	30.3	27.1	29.5	29.1	22.5	14.6	29.4	25.3
W	12	15	27	19	9	31	12	20
Sr	83	67	126	178	155	217	52	55
Al/Ti	10.48	10.07	10.71	10.37	10.54	10.76	11.44	12.05
D (kg/dm^3)	2.97	2.95	2.97	2.95	2.99	3.06	2.92	2.95
f_v	0.89	0.94	0.93	0.95	1.05	3.35	0.93	1.07

SAMPLE	MINERALOGY	ROCK SYMBOL			
89 = 508/101.0	TC-CL-AM-CB	O	93 = 508/114.0	TC-CL-CB-(BT-AB-BA)	O
90 = 508/104.5	TC-CB-CL-AM	O	94 = 508/114.6	AF-(CB-AB-BA)	A
91 = 508/109.3	TC-CB-CL	O	95 = 508/124.5	TC-AF-CB-(AB)	X
92 = 508/112.9	TC-CL-CB-AF-(BT-BA)	X	96 = 508/129.8	TC-AF-CB-(AB)	X

APPENDIX 1 (continued).

	97	98	99	100	101	102	103	104
SiO_2 (%)	45.54	44.54	44.30	45.91	43.28	44.02	47.91	44.11
TiO_2	0.54	0.66	0.69	0.70	0.72	1.15	0.83	0.63
Al_2O_3	7.25	7.07	6.47	6.24	7.60	8.65	6.39	7.20
$Fe_2O_3^{tot}$	13.19	14.15	13.74	13.46	13.21	9.98	10.13	14.44
MnO	0.14	0.22	0.23	0.15	0.31	0.36	0.32	0.42
MgO	25.47	25.97	26.35	26.01	23.12	19.04	18.51	21.88
CaO	6.76	7.16	7.95	6.57	11.06	15.57	14.92	10.32
Na_2O	1.07	0.13	0.17	0.21	0.62	0.93	0.79	0.51
K_2O	0.02	0.03	0.03	0.70	0.03	0.18	0.15	0.44
P_2O_5	0.03	0.06	0.06	0.05	0.07	0.11	0.05	0.06
Total	100.00	100.00	100.00	100.00	100.00	100.00	100.00	100.00
Au (ppb)	4	4	2	2	210	2	3	2
Te	3	2	1	1	1	8	7	14
S (%)	0.01	0.01	0.05	0.01	0.01	0.01	0.01	0.01
CO_2	7.07	3.04	5.84	5.57	7.29	7.06	4.93	7.67
Ba (ppm)	126	47	52	314	48	65	98	210
Cr	2930	2680	2500	2060	2740	2960	2140	2940
Ni	1400	1400	1500	1600	1400	960	980	1100
V	150	200	190	210	220	190	180	170
Co	95	110	100	100	60	47	40	50
Zn	80	120	110	120	66	60	31	36
Sc	26.9	29.5	27.7	29.9	28.0	22.9	24.5	22.2
W	10	13	9	12	12	62	48	27
Sr	34	11	25	25	43	137	60	51
Al/Ti	13.45	10.67	9.34	8.90	10.59	7.50	7.72	11.39
D (kg/dm^3)	2.89	2.93	2.94	2.91	2.98	3.01	3.02	3.01
$f_{V'}$	0.92	0.93	1.02	1.06	0.85	0.74	1.00	0.89

SAMPLE	MINERALOGY	ROCK SYMBOL			
97 = 508/136.7	TC-CB-CL-(AM-AB)	O	101 = 509/51.6	TC-CL-AF-CB-(MG)	X
98 = 509/16.7	AM-CL-(CB)	O	102 = 509/57.3	AF-CB-(CL-AB)	*
99 = 509/36.4	AM-CL-CB	O	103 = 509/61.3	AF-(CB-AB)	*
100 = 509/40.6	AM-TC-CL-CB-(BT)	O	104 = 509/64.8	AF-CB-(CL-BT)	X

APPENDIX 1 (continued).

	105	106	107	108	109	110	111	112
SiO_2 (%)	44.07	43.14	45.94	41.52	42.13	52.24	44.70	45.83
TiO_2	0.69	0.62	0.67	0.72	0.55	0.39	0.78	0.73
Al_2O_3	6.91	6.35	6.94	7.15	6.38	3.60	7.68	7.35
$Fe_2O_3^{tot}$	13.65	12.48	17.26	15.17	14.89	20.31	14.76	15.59
MnO	0.38	0.31	0.24	0.33	0.36	0.32	0.30	0.35
MgO	24.52	26.00	21.94	24.43	24.22	19.10	20.53	21.77
CaO	6.66	10.37	5.27	10.05	9.34	2.80	7.30	7.38
Na_2O	0.25	0.43	0.14	0.13	0.34	1.19	0.50	0.00
K_2O	2.81	0.24	1.60	0.51	1.78	0.00	3.38	0.94
P_2O_5	0.05	0.05	0.00	0.00	0.00	0.05	0.05	0.06
Total	100.00	100.00	100.00	100.00	100.00	100.00	100.00	100.00
Au (ppb)	71	24	1360	220	650	650	1870	40
Te	18	15	n.d.	n.d.	n.d.	n.d.	n.d.	n.d.
S (%)	0.01	0.01	0.31	0.03	0.12	0.30	0.03	0.06
CO_2	8.60	9.09	4.39	9.48	11.45	3.77	5.89	5.65
Ba (ppm)	2810	337	1800	200	2700	900	3600	1100
Cr	2270	2240	2300	2800	2300	1500	1800	2100
Ni	1100	1100	n.d.	n.d.	n.d.	n.d.	n.d.	n.d.
V	94	150	235.5	244.3	200.2	198.1	256.0	n.d.
Co	59	60	90	86	77	59	70	n.d.
Zn	23	25	42	274	33	20	22	n.d.
Sc	21.9	21.4	24.0	23.8	19.9	14.4	23.9	n.d.
W	10	12	n.d.	n.d.	n.d.	n.d.	n.d.	n.d.
Sr	99	53	49.4	119.0	111.8	56.8	83.3	n.d.
Al/Ti	9.95	10.28	10.39	9.98	11.60	9.31	9.82	10.04
D (kg/dm^3)	2.94	2.94	n.d.	n.d.	n.d.	n.d.	n.d.	n.d.
f_v	0.95	1.03	0.95	0.92	1.03	1.83	0.86	0.90

SAMPLE	MINERALOGY	ROCK SYMBOL			
105 = 509/70.9	BT-TC-CB	B	109 = 509/102.3	BT-AM-CB-TC	B
106 = 509/78.2	TC-CL-CB-AF-(BT)	X	110 = 509/112.1	AF-QU-AB-(CB)	V
107 = 509/88.8	BT-CL	B	111 = 509/116.4	BT-TC-CB-(AM)	B
108 = 509/95.0	CL-TC-CB-AF-(BT)	X	112 = 511/79.0	TC-CL-AM-CB-(BT)	O

APPENDIX 1 (continued).

	113	114	115	116	117	118	119	120
SiO_2 (%)	44.67	46.03	43.97	47.76	42.59	40.06	44.86	39.00
TiO_2	0.73	0.76	0.75	0.71	0.71	0.71	0.73	0.74
Al_2O_3	7.87	7.79	7.85	7.31	7.71	6.71	8.24	7.88
$Fe_2O_3^{tot}$	14.92	14.44	13.55	12.97	19.47	21.91	20.85	24.94
MnO	0.27	0.23	0.28	0.27	0.36	0.44	0.27	0.39
MgO	23.60	21.76	20.77	17.85	21.00	22.52	21.61	20.25
CaO	7.66	7.95	11.02	11.18	5.16	5.46	1.81	4.75
Na_2O	0.00	0.17	0.00	0.32	0.00	0.00	0.00	0.00
K_2O	0.19	0.82	1.78	1.56	2.97	2.13	1.60	2.02
P_2O_5	0.08	0.05	0.05	0.07	0.05	0.05	0.03	0.04
Total	100.00	100.00	100.00	100.00	100.00	100.00	100.00	100.00
Au (ppb)	20	22500	40	3900	2300	13200	1790	12100
Te	n.d.	n.d.	n.d.	n.d.	n.d.	n.d.	n.d.	n.d.
S (%)	0.05	0.01	0.07	0.23	0.09	0.13	0.04	0.05
CO_2	6.78	5.63	8.03	4.33	6.64	9.42	1.83	4.96
Ba (ppm)	200	1300	2100	2900	4700	3400	3000	3900
Cr	2200	2100	1900	1800	1800	1800	2300	1900
Ni	n.d.	n.d.	n.d.	n.d.	n.d.	n.d.	n.d.	n.d.
V	n.d.	n.d.	n.d.	n.d.	n.d.	n.d.	n.d.	n.d.
Co	n.d.	n.d.	n.d.	n.d.	n.d.	n.d.	n.d.	n.d.
Zn	n.d.	n.d.	n.d.	n.d.	n.d.	n.d.	n.d.	n.d.
Sc	n.d.	n.d.	n.d.	n.d.	n.d.	n.d.	n.d.	n.d.
W	n.d.	n.d.	n.d.	n.d.	n.d.	n.d.	n.d.	n.d.
Sr	n.d.	n.d.	n.d.	n.d.	n.d.	n.d.	n.d.	n.d.
Al/Ti	10.76	10.31	10.47	10.30	10.84	9.44	11.28	10.71
D (kg/dm^3)	n.d.	n.d.	n.d.	n.d.	n.d.	n.d.	n.d.	n.d.
f_v	0.84	0.84	0.84	0.90	0.85	0.98	0.80	0.83

SAMPLE	MINERALOGY	ROCK SYMBOL			
113 = 511/80.0	TC-AM-CB-CL	O	117 = 511/84.5	BT-TC-AF-CB	B
114 = 511/81.2	TC-CL-AM-CB-(BT)	O	118 = 511/85.6	BT-TC-CB-CL V:CB-AF	B
115 = 511/82.0	TC-AF-CB-(BT)	O	119 = 511/86.7	TC-BT-CB-AM-CL	B
116 = 511/83.5	AF-CB-(BT)	*	120 = 511/88.3	BT-TC-CB V:CB-TC-AF	B

APPENDIX 1 (continued).

	121	122	123	124	125	126	127	128
SiO_2 (%)	46.63	43.73	46.75	44.90	44.29	45.96	52.04	45.06
TiO_2	0.62	0.73	0.66	0.72	0.59	0.76	0.45	0.71
Al_2O_3	4.73	7.77	7.07	8.06	6.55	8.15	5.26	6.87
$Fe_2O_3^{tot}$	22.84	19.19	20.11	20.91	19.09	15.05	12.29	14.31
MnO	0.43	0.51	0.28	0.41	0.50	0.38	0.43	0.28
MgO	19.03	20.40	19.00	20.13	20.34	20.57	16.73	26.02
CaO	4.81	4.79	3.72	2.29	6.45	7.83	11.46	6.33
Na_2O	0.00	0.00	0.00	0.00	0.00	0.05	0.84	0.25
K_2O	0.91	2.83	2.37	2.54	2.14	1.20	0.45	0.12
P_2O_5	0.00	0.05	0.03	0.04	0.06	0.05	0.04	0.05
Total	100.00	100.00	100.00	100.00	100.00	100.00	100.00	100.00
Au (ppb)	330	740	31500	17600	3500	10	10000	220
Te	n.d.	n.d.	n.d.	n.d.	n.d.	n.d.	9	19
S (%)	0.04	0.06	0.20	0.37	0.53	0.19	0.02	0.01
CO_2	4.03	6.88	3.14	2.67	6.12	5.50	0.67	5.03
Ba (ppm)	2900	3800	5100	7900	12600	6600	541	1550
Cr	800	1300	1400	1900	1400	2100	1890	2510
Ni	n.d.	n.d.	n.d.	n.d.	n.d.	n.d.	1100	1300
V	n.d.	n.d.	n.d.	n.d.	n.d.	n.d.	160	180
Co	n.d.	n.d.	n.d.	n.d.	n.d.	n.d.	37	66
Zn	n.d.	n.d.	n.d.	n.d.	n.d.	n.d.	22	12
Sc	n.d.	n.d.	n.d.	n.d.	n.d.	n.d.	18.9	22.6
W	n.d.	n.d.	n.d.	n.d.	n.d.	n.d.	24	18
Sr	n.d.	n.d.	n.d.	n.d.	n.d.	n.d.	21	37
Al/Ti	7.63	10.58	10.76	11.19	11.19	10.72	11.57	9.68
D (kg/dm^3)	n.d.	n.d.	n.d.	n.d.	n.d.	n.d.	3.08	2.87
f_v	1.39	0.85	0.93	0.82	1.00	0.81	1.19	0.98

SAMPLE	MINERALOGY	ROCK SYMBOL			
121 = 511/89.3	TC-AM-BT-CB-CL	B	125 = 511/93.6	BT-TC-AF-CB	B
122 = 511/90.3	BT-TC-CB-CL	B	126 = 511/94.7	TC-AM-CB-CL-BT	O
123 = 511/91.4	BT-AM-TC-CB-CL	B	127 = 512/13.0	AF-(BT-CB-QU)	*
124 = 511/92.6	BT-AM-CB V:TC-AF-QU	B	128 = 512/28.9	TC-AM-CL	O

APPENDIX 1 (continued).

	129	130	131	132	133	134
SiO_2 (%)	49.94	43.77	47.30	45.02	46.20	45.46
TiO_2	0.48	0.58	0.53	0.64	0.60	0.66
Al_2O_3	6.14	7.50	6.12	7.16	6.71	6.49
$Fe_2O_3^{tot}$	12.03	14.44	11.74	13.94	12.50	13.59
MnO	0.38	0.15	0.12	0.13	0.18	0.21
MgO	18.95	26.03	24.72	25.00	25.98	26.32
CaO	10.37	7.08	8.07	6.94	7.45	6.99
Na_2O	0.92	0.39	0.93	0.35	0.25	0.17
K_2O	0.75	0.02	0.43	0.79	0.08	0.05
P_2O_5	0.04	0.03	0.03	0.04	0.05	0.04
Total	100.00	100.00	100.00	100.00	100.00	100.00
Au (ppb)	5	2	18	2	2	7
Te	14	1	0	0	0	0
S (%)	0.07	0.01	0.02	0.01	0.01	0.01
CO_2	2.24	6.38	7.20	4.67	2.22	2.15
Ba (ppm)	3780	201	262	436	93	63
Cr	1760	3120	2410	2890	2380	2620
Ni	1100	1400	1200	1100	1100	1200
V	170	200	150	190	180	200
Co	43	82	81	89	80	79
Zn	21	59	59	63	59	64
Sc	20.4	23.3	19.7	23.9	22.9	23.1
W	25	10	10	9	6	11
Sr	96	29	34	16	10	22
Al/Ti	12.82	12.94	11.53	11.16	11.22	9.79
D (kg/dm^3)	3.02	2.90	2.91	2.93	2.92	2.93
f_v	1.04	0.89	1.09	0.92	0.99	1.02

SAMPLE	MINERALOGY	ROCK SYMBOL			
129 = 512/35.8	AF-(BT-AB-BA)	*	132 = 512/50.0	CL-AM-(BT-AB)	○
130 = 512/42.8	TC-CB-CL-AF-(AB)	X	133 = 512/62.6	AM-CL	●
131 = 512/47.6	TC-AF-CB-(AB-BT)	X	134 = 512/76.0	CL-AM	●

Tätä julkaisua myy

GEOLOGIAN
TUTKIMUSKESKUS (GTK)
Julkaisumyynti
02150 Espoo
☎ 90-46931
Teleksi: 123 185 geolo sf
Telekopio: 90-462 205

GTK, Väli-Suomen
aluetoimisto
Kirjasto
PL 1237
70701 Kuopio
☎ 971-205 111
Telekopio: 971-205 215

GTK, Pohjois-Suomen
aluetoimisto
Kirjasto
PL 77
96101 Rovaniemi
☎ 960-297 219
Teleksi: 37 295 geolo sf
Telekopio: 960-297 289

Denna publikation säljes av

GEOLOGISKA
FORSKNINGSCENTRALEN (GFC)
Publikationsförsäljning
02150 Esbo
☎ 90-46931
Telex: 123 185 geolo sf
Telefax: 90-462 205

GFC, Mellersta Finlands
distriktsbyrå
Biblioteket
PB 1237
70701 Kuopio
☎ 971-205 111
Telefax: 971-205 215

GFC, Norra Finlands
distriktsbyrå
Biblioteket
PB 77
96101 Rovaniemi
☎ 960-297 219
Telex: 37 295 geolo sf
Telefax: 960-297 289

This publication can be obtained
from
GEOLOGICAL SURVEY
OF FINLAND (GSF)
Publication sales
SF-02150 Espoo, Finland
☎ 90-46931
Telex: 123 185 geolo sf
Telefax: 90-462 205

GSF, Regional office of
Mid-Finland
Library
P.O. Box 1237
SF-70701 Kuopio, Finland
☎ 971-205 111
Telefax: 971-205 215

GSF, Regional office of
Northern Finland
Library
P.O. Box 77
SF-96101 Rovaniemi, Finland
☎ 960-297 219
Telex: 37 295 geolo sf
Telefax: 960-297 289

ISBN 951-690-455-6
ISSN 0367-522X